Chapter 1

Introduction

1.1. Problem Statement

Although significant advances have been made in medical techniques that reconstruct tissue damaged as a result of trauma or degenerative disease, damage to bone is still treated with bone grafting or by inserting metallic or ceramic implants. In the United States, over 500,000 bone grafting procedures occur each year, with over 2.2 million occurring worldwide[1]. Approximately 90% of these grafts are autografts (from the patient) or allografts (from another human donor) in the United States[2]. Both of these options have significant drawbacks such as donor site morbidity and pathogen transmission, respectively[3]. While metallic and ceramic implants typically avoid the drawbacks of autografts and allografts, their material properties often do not match those of the native bone which can lead to later revision surgery due to additional bone damage caused by the implant[4].

Bone Tissue Engineering offers an alternative to these traditional treatments[5]. One of the most common approaches to tissue engineering involves growing cells on a three-dimensional biodegradable scaffold[6]. Since most cell types are anchorage dependent[7], the scaffold plays a pivotal role in the tissue development as it provides a

support structure as the new bone develops and degrades as the tissue matures[8]. Through emulating the natural cellular support structure in bone tissue or extracellular matrix (ECM), the scaffold may better facilitate the accelerated tissue formation for which tissue engineering strives[8]. The ECM of bone is complex, containing organic (proteins) and inorganic (apatitic crystals) features at multiple size scales[9]. However during early embryonic development, type I collagen is the principle component of the bone ECM[10]. As the tissue matures, the cells secret other proteins and eventually modulate the mineralization of the matrix to create the complex ECM of mature bone.

Type I collagen is composed of three collagen polypeptide chains wound together to form a ropelike superhelix that assembles into the fibers ranging in size from 50 to 500nm[11]. The fibrillar structure of collagen has been shown to have important effects on cellular attachment, proliferation and differentiation in tissue culture[11-13]. Emulating this structure alone may have a positive effect on tissue formation compared to more traditional scaffolds, since cells have been shown to respond differently to surface features of varying scale lengths[14]. Using phase separation, synthetic three dimensional nanofibers of the same size scale of natural type I collagen can be generated[15-19]. Previous work with these materials indicate that they enhance the osteogenic differentiation of progenitor cells[17, 20], illustrating that mimicking the ECM of bone at this level has biological effect.

Embryonic stem cells possess the ability to differentiate to any cell type within the human body[21]. This has spurred interest in their use in tissue engineering and cell replacement therapies. However, current attempts to differentiate the cells to a desired lineage yield a heterogeneous cell population. These low yield protocols often focus on

the addition of biologically active factors such as ascorbic acid and dexamethasone to drive cellular differentiation toward bone and ignore the contributions of the ECM during development[22-25]. Through providing similar signals to those of the ECM in these protocols, the cellular population of the desired lineage may be enhanced and more efficient protocols for controlled differentiation may be developed.

1.2 Hypothesis

Nanofibers may be advantageous in the controlled osteogenic differentiation of embryonic stem cells. Therefore, it is hypothesized that mimicking the natural extracellular matrix in terms of size scale (nanofibers) will facilitate the directed differentiation of embryonic stem cells and the development of bone tissue throughout tissue engineering scaffolds.

1.3 Specific Aims

1. Analyze the effects of nanofibrous architecture on mouse embryonic stem cell differentiation. Thin poly(L-lactic acid) matrices with nanofibrous architecture and flat (solid) films will be used as a model to study the effects of scaffold wall architecture on the differentiation of mouse embryonic stem cells to the osteoblastic lineage as a prelude to their use as a cell source for bone tissue engineering.
2. Evaluate effects of embryoid body formation and growth factors on mouse embryonic stem cell differentiation to the osteoblastic lineage on the nanofibrous architecture. By emulating the early stages of development with the formation of

embryoid bodies, growth factors and nanofibrous architecture, the effects of these cues on enhancing osteogenesis in both two dimensional and three dimensional culture will be assessed independently and in combination in vitro compared to more traditional flat (solid) films and solid-walled scaffolds.

3. Assess effects of nanofibrous architecture on human embryonic stem cell differentiation. The culture system will be optimized for human embryonic stem cells and then the effects of nanofibrous architecture will be studied in two and three dimensional culture in vitro as a prelude to their use in vivo.

1.4 Significance

Embryonic stem cells represent a potentially unlimited cell source for tissue engineering applications[21]. Mesenchymal stem cells are not immortal. Their proliferation and differentiation capacity are affected by donor age and culture time[26, 27], but are currently used in many tissue engineering applications due to their multiple lineage potential. Embryonic stem cells provide greater differentiation potential and a reduced need to characterize new batches of cells for clinical use since single cell lines can be maintained for long periods of time. However, there are several obstacles to the use of human embryonic stem cells clinically. They include contamination from animal products[28], the tumorgencity of the undifferentiated cells[21], and the heterogeneous cell population generated by current differentiation protocols[29].

Synthetic poly(L-lactic acid) nanofibers have structural similarities to type I collagen and could increase the desired cell lineage within the differentiating cell population. Additionally, this synthetic system allows for batch to batch consistency,

tailored mechanical properties, biodegradability and eliminates the potential of pathogen transmission and immune-rejection which cannot always be done when natural collagen is used.

Enhancing the yield of the desired cell type from embryonic stem cell differentiation protocols is one of the many steps necessary to produce usable tissue from these cells. Although this work is preliminary, as is the study of embryonic stem cells as a cell source in tissue engineering, it could lead to the development of differentiation systems for these cells which yield a pure population of the desired cell type facilitating their use clinically.

1.5 Dissertation Overview

The following chapter, Chapter 2, provides a general literature review of the current state of tissue engineering with nanofibrous scaffolds. Emphasis is placed on the three major methods of fabrication for nanofibrous scaffolds (electrospinning, self assembly and phase separation) as well as the biological effects of such scaffolds in tissue engineering with particular emphasis on osteogenic differentiation. This work is accepted for publication in Soft Matter[30].

Chapter 3 begins the main work of the thesis with an examination of the differentiation of mouse embryonic stem cells on two-dimensional materials with nanofibrous and flat (solid) architectures. Here undifferentiated cells are seeded directly on to the materials and the differentiation is observed. Additionally, integrin expression and activation are examined as a potential contributor to the differences in differentiation on the various architectures. This work will be submitted for publication in Tissue

Engineering.

In Chapter 4, the mouse embryonic stem cells were pre-differentiated prior to seeding on the materials through the formation of embryoid bodies. After disassociating the embryoid bodies and seeding them on to the materials, the effects of two and three dimensional culture and the addition of various biological factors are examined on the differentiation of mouse embryonic stem cells on the nanofibrous and flat (solid) architectures. This work will be submitted to Biomaterials for publication.

Using the knowledge gained from the studies of mouse embryonic stem cells, Chapter 5 examines the differentiation of human embryonic stem cells in two and three dimensional culture on the nanofibrous and flat (solid) architecture. First, a new differentiation procedure will be designed to yield osteogenic progenitor cells for culture on the different architectures, and then the osteogenic differentiation of the cells will be examined similar to previous studies with mouse embryonic stem cells. This work will be submitted to Biomaterials for publication.

Chapter 6 summarizes the thesis work and discusses possible future directions for this work to take.

1.6 References

1. Giannoudia, P.V., H. Dinopoulos, and E. Tsiridis. Bone substitues: An update. Injury, 2005. **36**: p. S20-S27.

2. Betz, R.R. Limitations of autograft and allograft: new synthetic solutions. Orthopedics, 2002. **25**: p. s561-s570.

3. Liu, X. and P.X. Ma. Polymeric Scaffolds for Bone Tissue Engineering. Annals of Biomedical Engineering, 2004. **32**(3): p. 477-486.

4. Christenson, E.M., K.S. Anseth, J.J.J.P. vanden Beucken, C.K. Chan, B. Ercan, J.A. Janson, C.T. Laurencin, W.J. Li, R. Murugan, L.S. Nair, S. Ramakrishna, R.S. Tuan, T.H. Webster, and A.G. Mikos. Nanobiomaterial Applications in Orthopedics. Inc. J Orthop Res, 2007. **25**: p. 11-22.

5. Langer, R. and J. Vacanti. Tissue Engineering. Science, 1993. **260**: p. 920-926.

6. Ma, P.X. Scaffolds for tissue fabrication. Materials Today, 2004. **7**: p. 30-40.

7. Stupack, D.G. Integrins as a distinct subtype of dependence receptors. Cell Death Differ, 2005. **12**: p. 1021-1030.

8. Ma, P.X. Biomimetic materials for tissue engineering. Adv Drug Deliv Rev, 2008. **60**: p. 184-198.

9. McKee, M.D., W.N. Addison, and M.T. Kaartinen. Hierarchies of extracellular matrix and mineral organization in bone of the craniofacial complex and skeleton. Cells Tissues Organs, 2005. **181**: p. 176-188.

10. Kadler, K. Matrix loading: assembly of extracellular matrix collagen fibrils during embryogenesis. Birth Defects Res C Embryo Today, 2004. **72**: p. 1-11.

11. Elsdale, T. and J. Bard. Collagen substrata for studies on cell behavior. J cell biology, 1972. **54**: p. 626-637.

12. Strom, S.C. and G. Michalopoulos. Collagen as a substrate for cell growth and differenitaion. Methods Enzymol, 1982. **82**: p. 544-555.

13. Grinnell, F. and M.H. Bennett. Ultrastructural studes of cell--collagen interactions. Methods Enzymol, 1982. **82**: p. 535-544.

14. Flemming, R.G., C.J. Murphy, G.R. Abrams, S.L. Goodman, and P.F. Nealey. Effects of synthetic micro- and nano-structured surfaces on cell behavior. Biomaterials, 1999. **20**: p. 573-588.

15. Ma, P.X. and R. Zhang. Synthetic nano-scale fibrous extraellular matrix. Biomed Mater Res, 1999. **46**: p. 60-72.

16. Chen, V. and P.X. Ma. Nano-fibrous poly(L-lactic acid) scaffolds with interconnected spherical macropores. Biomaterials, 2004. **25**: p. 2065-2073.

17. Chen, V.J., L.A. Smith, and P.X. Ma. Bone regeneration on computer-designed nano-fibrous scaffolds. Biomaterials, 2006. **27**: p. 3973-3979.

18. Zhang, R. and P.X. Ma. Synthetic nano-fibrillar extracellar matrices with predesigned macroporous architectures. J Biomedi Mater Res, 2000. **52**: p. 430-438.

19. Woo, K.M., V.J. Chen, and P.X. Ma. Nano-fibrous scaffolding architecture selectively enhances protein adsorption contributing to cell attachement. J Biomed Mater Res, 2003. **67A**: p. 531-537.

20. Woo, K.M., J.H. Jun, V.J. Chen, J. Seo, J.H. Baek, H.M. Ryoo, G.S. Kim, M.J. Somerman, and P.X. Ma. Nano-fibrous scaffolding promotes osteoblast differentiation and biomeneralization. Biomaterials, 2007. **28**: p. 335-343.

21. Thomson, J.A., J. Itskovitiz-Eldor, S.S. Shapiro, M.S. Waknitz, J.J. Swiergiel, V.S. Marshall, and J.M. Jones. Embryonic stem cell lines derived from human blastocysts. Science, 1998. **282**: p. 1145-1147.

22. Sottile, V., A. Thomson, and J. McWhir. In vitro Osteogenic Differentiaiton of Human ES Cells. Cloning and Stem Cells, 2003. **5**: p. 149-155.

23. Cao, T., B.C. Heng, C.P. Ye, H. Liu, W.S. Toh, P. Robson, P. Li, Y.H. Hong, and L.W. Stanton. Osteogenic differentiation within intact human embryoid bodies result in a marked increased in osteocalcin secretion after 12 days of in vitro culture, and formation of morpholoigcally distinct nodule-like structures. Tissue and Cell, 2005. **37**: p. 325-334.

24. Karp, J.M., L.S. Ferreira, A. Khademhosseini, A.H. Kwon, J. Yeh, and R.S. Langer. Cultivation of human embryonic stem cells without the embroid body step enhances osteogenesis in vitro. Stem Cells, 2006. **24**: p. 835-843.

25. Buttery, L., S. Bourne, J. Xynos, H. Wood, F. Hughes, S. HUghes, V. Episkopou, and J. Polak. Differentiation of Osteoblasts and in vitro bone formation of murine embryonic stem cells. Tissue engineering, 2001. **7**: p. 89-99.

26. Muraglia, A., R. Cancedda, and R. Quarto. Clonal mesenchymal progenitors from human bone marrow differentiate in vitro according to a hierarchical model. J Cell Sci, 2000. **113**: p. 1161-1166.

27. Fehrer, C. and G. Lepperdinger. Mesenchymal stem cell aging. Exp Gerontol, 2005. **40**: p. 926-930.

28. Martin, M.J., A. Muotri, R. Gage, and A. Varki. Human embryonic stem cells express an immunogenic nonhuman sialic acid. Nat Med, 2005. **11**: p. 228-232.

29. Ameen, C., R. Strehl, P. Bjorquist, A. Lindahl, J. Hyllner, and P. Sartipy. Human embryonic stem cells: Current technologies and emerging industrial applications. Crit Rev Oncol Hematol, 2008. **65**: p. 54-80.

30. Smith, L., X. Liu, and P.X. Ma. Tissue engineering with nano-fibrous scaffolds. Soft Matter, 2008. **In Press**.

Chapter 2

Literature Review

2.1 Introduction

Organ failure (heart, kidney, liver, lungs, pancreas, etc) or tissue loss (bone, ligaments, corneas, arteries, veins, skin, etc) accounts for around half of the medical spending in the U.S. leading to roughly 8 million surgical procedures and 40–90 million hospital days per year required for treatment of these ailments[1]. In 2005, there were 27,527 organ transplantation procedures in the United States, while approximately 90,000 patients remained on waiting lists waiting for organs[2]. Many of those left on the waiting list will die before an organ becomes available. In addition to organ transplants, there were approximately 1.5 million transplantations of human tissue in 2004. This number has doubled over the past 10 years[3, 4]. As the need for organs and tissue continues to increase and surpass the supply, the interdisciplinary field of tissue engineering has emerged to help meet these needs. Tissue engineering aims to develop biological substitutes which restore, maintain or improve tissue function through the application of engineering principles and the life sciences[5, 6].

There are three basic approaches to tissue engineering[5, 6]: use of isolated cells or cell substitutes to replace the cells that supply a needed function; delivery of tissue-inducing substances such as growth factors to a targeted location; and growing cells in a three-dimensional scaffold. For small, well-contained defects the first two approaches may be suitable. However, to produce larger blocks of tissue with predesigned shapes only the third approach, using a scaffold to direct cell growth, is sufficient. As such, both cells and materials play an important role in de novo tissue development.

Traditionally, there are several important factors to consider when designing a scaffold for tissue engineering applications, including scaffold morphologies (porosity, pore size and interpore connectivity), mechanical properties and degradation[7]. Recent development has focused on designing biomimetic scaffolds to elicit favorable biological effects. It has been indicated that the architecture of natural extracellular matrix (ECM) plays an important role in regulating cellular behavior[8-10]. For example, type I collagen has a nanofibrous structure[11] and is the base attachment structure for cells in many tissues[12]. As ECM matures, other proteins and bio-molecules are either adsorbed from the serum or secreted from the cells joining type I collagen to form the tissues native ECM. In bone, type I collagen composes 95% of the organic ECM which is strengthened by the cellular deposition of hydroxyapatite[13] to form the mature ECM of bone. It is this maturation process which nanofibrous and surface modified tissue engineering scaffolds attempt to mimic in order to create replacement tissues.

As you progress through this review, cell sourcing for tissue engineering then methods of nanofibrous scaffold fabrication and methods of surface modification will be

addressed followed by the biological effects of nanofibrous architecture on bone formation.

2.2 Cell Sources for Tissue Engineering

Since its inception, a variety of cells have been used in tissue engineering. Currently due to their ability to produce multiple cell types and self renew[14], stem cells have gained popularity as a cell source for tissue engineering. Stem cells can be isolated from multiple sources including adult tissue[15-20], umbilical cord blood[17], amniotic fluid[21] and embryos[22]. Of the adult tissue stem cells, hematopoietic stem cells have been used clinically for years to restore the hematopoietic system[23] and mesenchymal stem cells are currently being investigated in clinical trials for the treatment of multiple conditions[24-28] due to their multiple lineage potentials[18, 29] and ability to illicit a reduced immune response[30-33]. However, mesenchymal stem cells are not immortal and their ability to proliferate and differentiate are affected by donor age and culture time[34, 35].

In contrast, embryonic stem cells, isolated from the inner cell mass of blastocysts[22], appear to have long term self renewal charateristics providing a potentially unlimited source of cells for tissue engineering and are capable of differentiating into all the cell types in the human body. Recent evidence indicates that embryonic stem cells and embryonic stem cell derived cells may be less immunogenic than adult cells[36] and with the use of somatic cell nuclear transfer embryonic stem cells may become autologous. However, embryonic stem cells cultured with animal products have been found to carry immunogenic non-human surface markers[37]. This

contamination from animal products, the potential tumorgenicity of the undifferentiated cells, and the heterogeneous cell population generated by current differentiation protocols all must be resolved before embryonic stem cells are used clinically as a cell source for tissue engineering. However, it is important to note that the study of these cells is still in its infancy and these obstacles will most likely be overcome in time with further studies.

2.3 Nanofibrous Scaffold Fabrication

While a large number of scaffolding fabrication methods have been developed, the techniques of controlling the architecture of scaffold at nano-scale level, which is required to emulate the size scale of collagen, are still limited. Only three techniques have been developed in the fabrication of nanofibrous scaffolds for use in tissue engineering: electrospinning, self-assembly, and phase separation.

2.3.1 Electrospinning

The electrospinning process has long been utilized to fabricate industrial products before it was recently applied to produce nanofibrous structures for use in tissue engineering [38, 39]. The principle of electrospinning is to use an electric field to draw a polymer solution from an orifice to a collector, producing polymer fibers with diameters in the range of nanometers to micrometers[38, 40]. Due to the simplicity and the ability to produce nanofibers from various materials of this method, electrospinning has attracted considerable attention for use in tissue engineering. A variety of synthetic and natural biomaterials, including poly(L-lactic acid) (PLLA), poly(lactic-co-glycolic acid) (PLGA), poly(caprolactone) (PCL), polyethylene terephthalate (PET), poly(ethylene oxide) (PEO),

poly(vinyl alcohol) (PVA), collagen, gelatin, chitosan, silk protein and fibrinogen have been used to form nanofibrous scaffolds for tissue engineering[39, 41-52]. The fiber diameters can simply be controlled by altering the concentration of the polymer solution, that is, solutions made of higher concentrations produce larger diameter fibers. In addition, fiber alignment can be controlled by rotating the grounded target. While the simplicity of electrospinning makes it a very active research field, significant challenges include the difficulties to create three-dimensional (3-D) scaffolds with well-defined pore architecture and complex geometries.

2.3.2 Molecular Self-Assembly

Molecular self-assembly is a useful approach for fabricating supramolecular architectures[53] and can be defined as a spontaneous process to form structurally ordered and stable arrangement through a number of non-covalent interactions, such as hydrogen bonds, van der Waals interactions, electrostatic interactions, and hydrophobic interactions[54, 55]. Found throughout biology, self-assembly of biomolecules, such as peptides and proteins, to well-defined architectures perform a variety of functions[55]. A good example is the self-assembly of collagen molecules to collagen fibrils, and subsequent side-by-side packing in parallel bundles to form large collagen fibers with diameter ranged from 50 to 500 nm[56]. Inspired by nature, several groups have designed and synthesized polypeptides or oligopeptides molecules to self-assemble into nanofibrous structures under suitable conditions[53, 57-59]. The formation of nanofibers by molecular self-assembly is a “bottom-up” strategy and usually the fiber diameter is much smaller than those produced by using electrospinning[57]. While molecular self-

assembly is a fairly new technique for the formation of nano-scale scaffolds, it has not been determined how to control the pore size and pore structures, which are important to allow for cell incorporation, migration and proliferation. The mechanical strength of self-assembled scaffolds also must be addressed before they can be used in tissue engineering applications.

2.3.3 Thermally Induced Phase Separation

Thermally induced phase separation (TIPS) has been used for several years to fabricate synthetic porous scaffolds for tissue engineering[60-62]. In this process, the temperature of a polymer solution is controlled to induce a phase separation into two phases, a polymer-rich phase and a polymer-lean phase. After removal of the solvent by extraction, evaporation, or sublimation, the polymer-rich phase solidifies and forms a polymer foam. By varying the types of polymer and solvent, polymer concentration, and phase-separation temperature, different pore morphology and structures can be achieved. To mimic the fibrous structure of natural type I collagen, a novel TIPS technique has recently been developed to fabricate nanofibrous matrices by using synthetic biodegradable polymers[63]. For example, a solution of PLLA dissolved in THF is thermally induced following a series of processes to phase separate. The solvent is exchanged with water and then freeze-dried to yield nanofibrous PLLA matrices. The fibers formed in this manner have diameters ranging from 50-500 nm, and have a porosity as high as 98% (Figure 2.1).

By combining this TIPS with other processing techniques (such as particulate leaching or solid free-form fabrication), scaffolds with complex 3-D structures and well-

defined pore morphologies can be produced[64, 65]. For example, a solution of PLLA in THF was dripped onto a sugar fiber assembly in a mold and then cooled to a preset gelation temperature. After phase separation, the gel-sugar composite was immersed in distilled water to extract the solvent and leach the sugar from the composite. The sample was freeze-dried, resulting in a 3-D nanofibrous matrix with macropores left behind from the leached sugar fibers[64]. To further control the interconnectivity between pores in the scaffold, a novel technique to generate interconnected spherical pore network has been combined with TIPS to fabricate nanofibrous scaffolds with interconnected spherical macropores (Figure 2.2)[66-68]. The combined technique advantageously controls macropore shape and size by sugar spheres, interpore opening size by assembly conditions (time and temperature of heat treatment), and pore wall morphology by phase-separation parameters.

2.4 Surface Modification of Nanofibrous Scaffolds

Although a variety of synthetic biodegradable polymers have been used as tissue engineering scaffolding materials, one disadvantage of these materials is their lack of biological recognition sites. The surface of the scaffold fabricated with these synthetic biomaterials can be modified to obtain more desirable characteristics to positively enhance cell-scaffold interactions[69].

Several approaches have been developed to modify the scaffold surface[70-73]. For example, low pressure ammonia plasma treatment has been used for the modification of poly(3-hydroxybutyrate) (PHB) thin film[73]. The introduction of amine functions was used in order to permit subsequent protein immobilization. The plasma treatment of PHB

induced a durable conversion of hydrophobic material into hydrophilic but did not cause significant changes in the morphology of the analyzed thin films. Such surface modification work, however, is limited to 2-D film surfaces or very thin 3-D constructs. Our lab has recently developed several techniques to effectively modify the surface of 3-D scaffolds[66, 74, 75]. For example, an electrostatic layer-by-layer self-assembly technique has been used to modify nanofibrous PLLA (NF-PLLA) scaffolds with gelatin[66]. The NF-PLLA scaffold was first fabricated and activated in an aqueous poly(diallyldimethylammonium chloride) (PDAC) solution to obtain positive charges on the scaffold surface. The scaffold was then immersed in a solution of negatively charged gelatin, so that gelatin molecules were self-assembled onto the activated scaffold surface. By alternately immersing the scaffold into the solutions of positively charged PDAC and negatively charged gelatin, polyelectrolyte multilayers containing gelatin molecules were deposited on the NF-PLLA surfaces. This technique provides a means to create polycation-polyanion polyelectrolyte complexes one molecular layer at a time, thereby allowing for an unprecedented level of control over the composition and surface functionality of materials. The layer-by-layer self-assembly method can be used for any complex 3-D geometry as long as the pores are interconnected.

2.5 Effect of Nanofibrous Scaffold on Cell Behavior and Tissue Development

Although limited data are available, effect of nanofibrous scaffolds on cellular behavior and tissue formation have been observed with numerous cell types[76]. For example, nanofibrous scaffolding has recently been shown to facilitate recovery from

spinal cord injury in mice[77]. However, discussion will principally focus on the cellular effects of nanofibrous scaffolding in bone tissue engineering.

Briefly, bone formation begins when precusor cells migrate from the neural crest (craniofacial skeleton), paraxial mesoderm(axial skeleton) or the lateral plate mesoderm (limbs) to the sites for bone formation and form mesenchymal condensation[78]. Cell-cell and cell-matrix interactions within the mesenchymal condensation initiates further differentiation of the pre-osteoblasts[78]. The pre-osteoblasts secrete bone ECM proteins, terminally differentiate and mineralize the ECM[79]. Once bone is initially formed, it is maintained and repaired by the cells within the tissue (osteoblasts, osteoclasts and osteocytes) and meschenchymal stem cells which differentiate to replenish lost cell types[80]. In vitro messenchymal stem cells have been found to differentiate to osteoblasts in the presence of differentiation factors such as ascorbic acid, β-glycerophosphate and dexamethasone[81] through the bone morphogen protein, transforming growth factor beta and Wnt signaling pathways[82]. Embryonic stem cells have been found to differentiate to osteoblasts in the presence of differentiation factors such as ascorbic acid, β-glycerophosphate, 1α,25-OH vitamin D3 and dexamethasone in approximately 4 weeks[81]. Embryonic stem cells may also first differentiate to meschymal stem and then toward bone[83, 84]. However, regardless of the method used to derive osteoblasts from embryonic stem cells little is understood about the roles the differentiation factors and other cytokines are playing in the early differentiation process.

2.5.1 Attachment and Proliferation

Several cells types, including osteoblasts[85, 86], fibroblasts[87, 88], rat kidney cells[87], smooth muscle cells[89], neural stem cells[90] and embryonic stem cells[91], have shown increased attachment on various nanofibers compared to their corresponding control materials. Additionally, a recent study found that branched nanofibers improve fibroblast attachment compared to linear nanofibers[92].

Integrins are a large family of heterodimeric transmembrane proteins which mediate cell attachment to ECM. Several studies using different cell types have noted differences in integrin expression on nanofibrous materials compared to control[86, 87, 93, 94]. Increased expression of α_2, α_V, β_1, and β_3 integrins has been seen in osteoblasts on nanofibrous scaffolds compared to comparable solid-walled scaffolds[86]. A previous study with these same scaffolds found that several integrin-binding protein components of the ECM (fibronectin, vitronectin and laminin) were adsorbed selectively at a higher level on nanofibrous scaffolds compared to the solid-walled scaffolds[85], which may contribute to the increased integrin expression by creating a more adhesive surface on nanofibrous scaffolds compared to solid-walled scaffolds. Notably, the up regulation of α_2 and β_1 integrins, which are associated with type I collagen binding, were maintained in cells grown on nanofibrous scaffolds compared to solid-walled scaffolds after cellular formation of collagen fibrils was blocked, indicating that the cells on the nanofibrous scaffold may be interacting directly with the synthetic scaffold[86, 95].

Cells cultured on nanofibrous material also have a cellular morphology more similar to in vivo compared to cells cultured on control materials[86, 87, 96]. Mouse pre-osteoblasts cultured on nanofibrous matrices exhibited processes interacting with nanofibers while cells on the flat (solid) films were flat and spread over large areas

(Figure 2.3)[95]. Mouse pre-osteoblasts cultured on nanofibrous matrices also exhibited fewer stress fibers than cells on the flat (solid) films[95]. In several cell types these morphological characteristics have been linked to increased Rac expression[97], a regulator of actin cytoskeleton assembly known to affect attachment and other cellular functions.

After cells attach, they must then proliferate in order to fully populate the scaffold and form tissue. Nanofibrous materials have enhanced the proliferation of several cell types compared to various control materials that do not have nanofibrous features[65, 87-89, 93, 94, 96, 98]. In one study, after 7 days of growth nearly 3 times more osteoblasts were present on the nanofibrous scaffold compared to the solid-walled scaffold[65].

2.5.2 Differentiation and Tissue Formation

Various cells types, including osteoblasts[65, 86], chondrocytes[94, 99],neural progenitors[90, 100], and hepatocytes[101, 102] have shown enhanced differentiation on a few types of nanofibrous materials compared to their corresponding control materials. For this review, we will focus on osteoblast differentiation as an example.

In addition to their role in cellular attachment, integrins also activate signalling pathways which stimulate cellular differentiation. After 24hrs of culture increased paxillin and focal adhesion kinase phosphorylation, components of integrin activated differentiation pathways[103], were observed in osteoblasts grown on nanofibrous scaffolds compared to solid-walled scaffolds similar to those described above in the protein adsorption studies[86]. This indicates that the increased integrin signalling during the cellular attachment translates into increased cellular differentiation and underscores

how the selective adsorption of serum proteins onto nanofibrous materials creates a different micro-environment from the solid-walled materials, which then alters the pathways which contribute to differentiation.

As the extracellular matrix matures, the osteoblasts and their progenitor cells express osteogenic markers. Increased expression of alkaline phosphatase, an early marker of osteogenic differentiation, has been seen in cells grown on nanofibrous matrices compared to solid-walled scaffolds after 3 or more days of culture[86, 104], while increased expression of bone sialoprotein and osteocalcin, later markers of osteogenic differentiation, have been seen in cells grown on nanofibrous matrices compared to solid-walled scaffolds after 1 week of culture[65, 86, 95]. The expression of these later bone markers is typically accompanied by mineralization of the extracellular matrix. Upon quantification, the nanofibrous scaffolds have been found to contain up to 13 times more calcium content compared to solid-walled scaffolds[65, 86]. The mineral on the nanofibrous matrix spread more evenly throughout the scaffolds, while the mineral on the solid-walled scaffold is principally in its exterior (Figure 2.4). Overall, thes data suggest that nanofibrous scaffolds better promote cellular differentiation and tissue formation over more traditional scaffolds.

2.6 Conclusions

Tissue engineering is a rapidly evolving field in which scaffolding plays a pivotal role. As our understanding of tissue development expands, the complexity of the scaffolding has increased to mimic the native ECM. Currently, there are three techniques capable of producing nanofibrous scaffolds. Of these, phase separation has shown high

potential to meet the needs of three dimensional tissue regeneration due to its ability to incorporate any pore shape and size or any overall 3-D geometry. Through mimicking the natural extracellular matrix, the interactions of the cells and matrix have been enhanced over previous scaffolding strategies. Increased cellular attachment, proliferation, and differentiation have all been observed on nanofibrous scaffolding compared to more traditional scaffolds. However, completely duplicating the ECM may not be the best strategy since mature ECM often does not contain highly interconnected pores to allow for the quick even cell dispersion that tissue engineering strives. Additionally, tissue engineering seeks to accelerate the natural development and wound healing processes which may render mimicking some aspects of the ECM unnecessary. As the field continues to mature, the scaffolds will most likely become more complex and bring us closer to the goal of functional tissue regeneration.

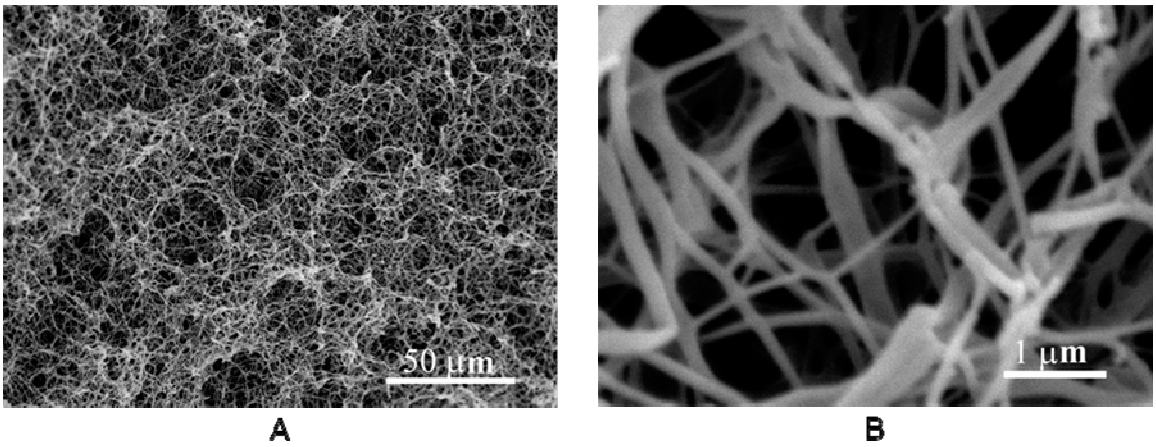

Figure 2.1: SEM micrographs of a PLLA nanofibrous matrix prepared from 2.5% (wt/v) PLLA/THF solution at a phase separation temperature of 8°C. (A) 500x; (B) 20,000x.From Ma and Zhang[63], Copyright ©John Wiley & Sons. Reprinted by permission of John Wiley & Sons.

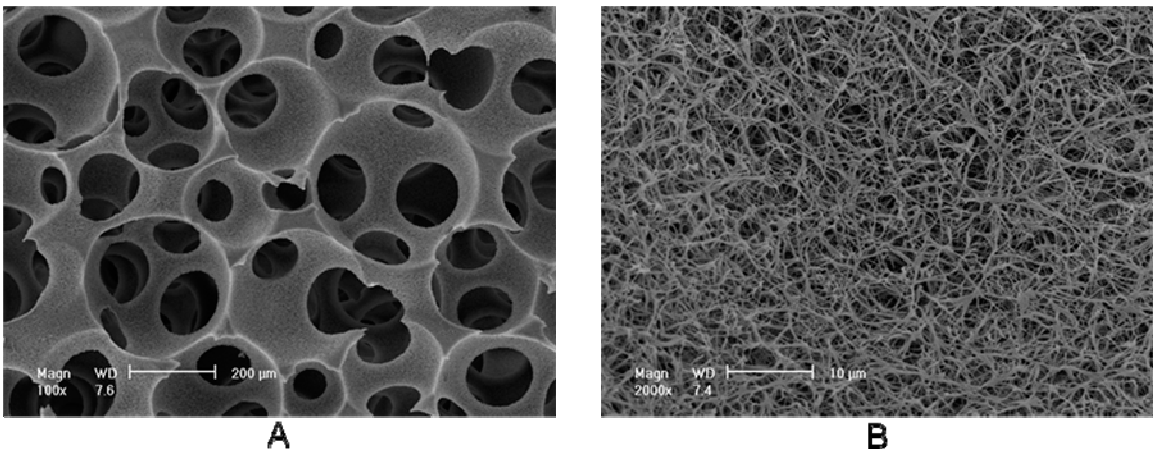

Figure 2.2: SEM micrographs of PLLA nanofibrous scaffolds prepared from 10% (wt/v) PLLA/THF solutions at a phase separation temperature of -20°C. (A) 100x; (B) 2000x.From Liu et al.[66], Copyright © American Scientific Publishers. Reprinted by permission of American Scientific Publishers.

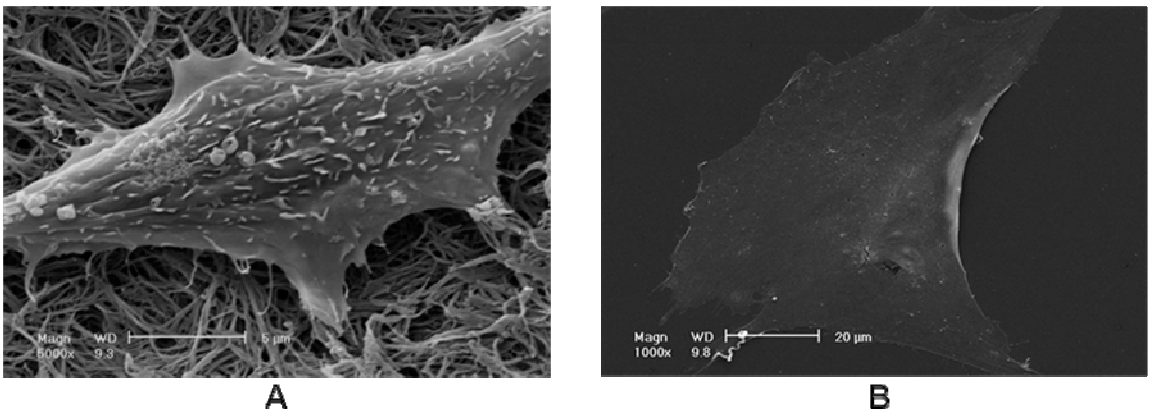

Figure 2.3: SEM of MC-4 cells after 24 hours of culture on (A) nanofibrous matrices and (B) flat (solid) films. From Hu et al.[95], Copyright © 2008 by Elsevier.

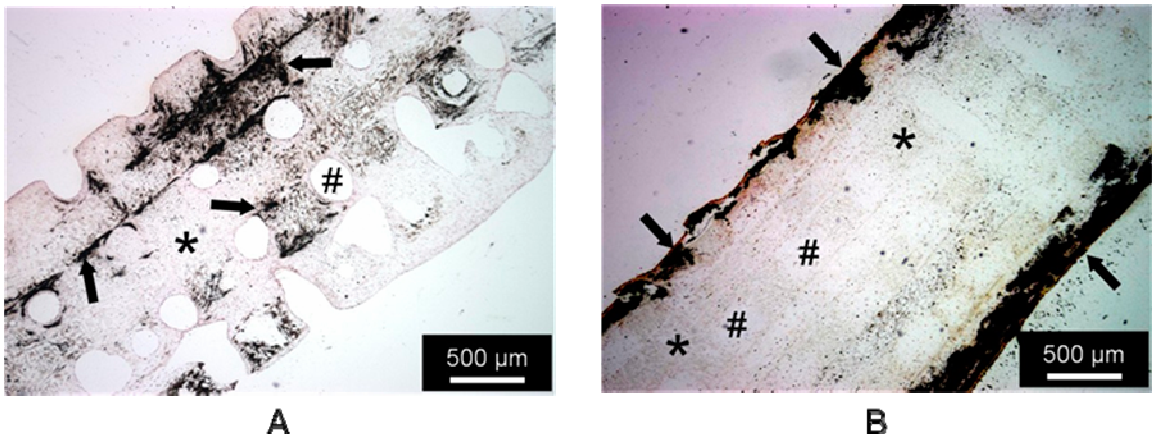

Figure 2.4: Von Kossa's silver nitrate staining of histological sections after 6 weeks of MC3T3-E1 osteoblast cultured on (A) nanofibrous scaffolds and (B) solid-walled scaffold Scale bars are 500 µm. * denotes the PLLA scaffold, # a scaffold pore. Arrows denote mineralization.From Chen et al.[65], Copyright © 2006 by Elsevier.

2.7 References

1. Karp, J.M. and R. Langer. Development and therapeutic applications of advanced biomaterials Current Opinion in Biotechnology, 2007. **18**: p. 454-459.

2. *2006 Annual Report of the U.S. Organ Procurement and Transplantation Network and the Scientific Registry of Transplant Recipients: Transplant Data 1996-2005.* 2006, Health Resources and Services Administration, Healthcare Systems Bureau, Division of Transplantation: Rockville, MD. p. I1-I14.

3. *Statistical Abstract of the United States: 2004-2005 Section 3 Health and Nutrition, No 161 Organ Transplants and Grafts: 1990 to 2001.* . 2004, U.S. Census Bureau: Washington DC. p. 114.

4. Wang, S., C. Zinderman, R. Wise, and M. Braun. Infections and human tissue transplants: review of FDA MedWath reports 2001-2004. Cell and tissue Banking, 2007. **8**: p. 211-219.

5. Langer, R. and J. Vacanti. Tissue Engineering. Science, 1993. **260**: p. 920-926.

6. Ma, P.X. Scaffolds for tissue fabrication. Materials Today, 2004. **7**: p. 30-40.

7. Ma, P.X. Biomimetic materials for tissue engineering. Adv Drug Deliv Rev, 2008. **60**: p. 184-189.

8. Abbott, A. Cell culture:biology's new dimension. Nature, 2003. **424**: p. 870-872.

9. Cukierman, E., R. Pankov, D. Stevens, and K. Yamada. Taking Cell-matrix adhesions to the third dimensions. Science, 2001. **294**: p. 1708-1712.

10. Schmeichel, K.L. and M.J. Bissell. Modeling tissue-specific signaling and organ function in three dimensions. J Cell Sci, 2003. **116**(Pt 12): p. 2377-2388.

11. Elsdale, T. and J. Bard. Collagen substrata for studies on cell behavior. J cell biology, 1972. **54**: p. 626-637.

12. Kadler, K. Matrix loading: assembly of extracellular matrix collagen fibrils during embryogenesis. Birth Defects Res C Embryo Today, 2004. **72**: p. 1-11.

13. Marks, S. and P. Odgren. Structure and Development of the Skeleton, in *Principles of Bone Biology*, J. Bilezikian, L. Raisz, and G. Rodan. Editors. 2002, Academic Press: San Diego, CA. p. 3-16.

14. Smith, A. A glossary for stem-cell biology. Nature, 2006. **441**: p. 1060.

15. Alison, M. Liver stem cells: a two compartment system. Curr Opin Cell Biol, 1998. **10**: p. 710-715.

16. Clarke, D.L., C.B. Johansson, J. Wilbertz, B. Veress, E. Nilsson, H. Karlstrom, U. Lendahl, and J. Frisen. Generalized Potential of Adult Neural Stem Cells. Science, 2000. **288**: p. 1660-1663.

17. Lee, M.W., J. Choi, M.S. Yang, Y.J. Moon, J.S. Park, H.C. Kim, and Y.J. Kim. Mesenchymal stem cells from cryopreserved human umbilical cord blood Biochem Biophys Res Commun, 2004. **320**: p. 273-278.

18. Pittenger, M.F., A.M. Mackay, S.C. Deck, R.K. Jaiswal, R. Douglas, J.D. Mosca, M.A. Moorman, D.W. Simonetti, S. Craig, and D.R. Marshak. Multi-lineage potential of adult human mesenchymal stem cells. Science, 1999. **284**: p. 143-147.

19. Yang, L., S. LI, H. Hatch, K. Ahrens, J.G. Cornelius, B.E. Petersen, and A.B. Peck. In vitro trans-differentiation of adult hepatic stem cells into pancreatic endocrine hormone-producing cells Proc Natl Acad Sci U S A, 2002. **99**: p. 8078-8083.

20. Zuk, P.A., M. Zhu, H. Mizuno, J. Huang, J.W. Futrell, A.J. Katz, P. Benhaim, H.P. Lorenz, and M.H. Hedrick. Multilineage cells from human adipose tissue: implications for cell-based therapies. Tissue Eng, 2001. **7**: p. 211-228.

21. De Coppi, P., G. Bartsh Jr, M.M. Siddiqui, T. Xu, C.C. Santos, L. Perin, G. Mostoslavsky, A.C. Serre, E.Y. Snyder, J.J. Yoo, M.E. Furth, S. Soker, and A. Atala. Isolation of amniotic stem cell lines with potential for therapy. Nat Biotechnol, 2007. **25**: p. 100-106.

22. Thomson, J.A., J. Itskovitiz-Eldor, S.S. Shapiro, M.S. Waknitz, J.J. Swiergiel, V.S. Marshall, and J.M. Jones. Embryonic stem cell lines derived from human blastocysts. Science, 1998. **282**: p. 1145-1147.

23. Mathe, G., J. Amiel, L. Schwarzenberg, A. Cattan, and M. Schneider. Haematopoietic Chimera in Man After Allogenic (Homologous) Bone-marrow Transplantation. Br Med J, 1963. **2**: p. 1633-1635.

24. Bang, O.Y., J.S. Lee, P.H. Lee, and G. Lee. Autologous mesenchymal stem cell transplantation in stroke patients. Ann Neurol, 2005. **57**: p. 874-882.

25. Chen, S.L., W.W. Fang, F. Ye, Y.H. Lui, J. Qian, S.J. Shan, J.J. Zhang, R.Z. Chunhua, L.M. Liao, S. Lin, and J.P. Sun. Effect on left ventricular function of intracoronary transplantation of autologous bone marrow mesenchymal stem cell in patients with acute myocardial infarction. Am J Cardiol, 2004. **94**: p. 92-95.

26. Horwitz, E.M., P.L. Gordon, W.K. Koo, J.C. Marx, M.D. Neel, R.Y. McNall, L. Muul, and T. Hofmann. Isolated allogeneic bone marrow-derived mesenchymal cells engraft and stimulate growth in children with osteogenesis imperfecta: implications for cell therapy of bone. Proc Natl Acad Sci U S A, 2002. **99**: p. 8932-8937.

27. Karitisis, D.G., P.A. Sotiropoulou, E. Karvouni, I. Karabinos, S. Korovesis, S.A. Perez, E.M. Voridis, and M. Papamichail. Transcoronary transplantation of autologous mesenchymal stem cells and endothelial progenitors into infarcted human myocardium. Catheter Cardiovas Interv, 2005. **65**: p. 321-329.

28. Koc, O.N., J. Day, M. Nieder, S.L. Gerson, H.M. Lazarus, and W. Krivit. Allogeneic mesenchymalstem cell infusion for treatment of metachromatic leukodystrophy (MLD) and Hurler syndrome (MPS-IH). Bone Marrow Transplant, 2002. **30**: p. 215-222.

29. Jiang, Y., B.N. Jahagirdar, R.L. Reinhardt, R.E. Schwartz, C.D. Keene, X.R. Ortiz-Gonzalez, M. Reyes, T. Lenvik, T. Lund, M. Blackstad, J. Du, S. Alsrich, A. Lisberg, W.C. Low, D.A. Largaespada, and C.M. Verfaillie. Pluripotency of mesenchymal stem cells derived from adult marrow. Nature, 2002. **418**: p. 41-49.

30. Aggarwal, S. and M.F. Pittenger. Human mesenchymal stem cells modulate allogeneic immune cell responses Blood, 2005. **105**: p. 1815-1822.

31. Beyth, S., Z. Borovsky, D. Mevorach, M. Liebergall, Z. Gazit, H. Aslan, E. Galun, and J. Rachmilewitz. Human mesenchymal stem cells alter antigen-presenting cell maturation and induce T-cell unresponsiveness. Blood, 2005. **105**(2214-2219).

32. Corcione, A., F. Benvenuto, E. Ferretti, D. Giunti, V. Cappiello, F. Cazzanti, M. Risso, F. Gualandi, G. Mancardi, V. Pistoia, and A. Uccelli. Human mesenchymal stem cells modulate B-cell functions. Blood, 2006. **107**: p. 367-372.

33. Di Nicola, M., C. Carlo-Stella, M. Magni, M. Milanesi, P. Longoni, P. Matteucci, S. Grisanti, and A. Gianni. Human bone marrow stromal cells suppress T-lymphocyte proliferation induced by cellular or nonspecific mitogenic stimuli. Blood, 2002. **99**: p. 3838-3843.

34. Fehrer, C. and G. Lepperdinger. Mesenchymal stem cell aging. Exp Gerontol, 2005. **40**: p. 926-930.

35. Muraglia, A., R. Cancedda, and R. Quarto. Clonal mesenchymal progenitors from human bone marrow differentiate in vitro according to a hierarchical model. J Cell Sci, 2000. **113**: p. 1161-1166.

36. Drukker, M., H. Katchman, G. Katz, S.E. Friedman, E. Shezen, E. Hornstein, O. Mandelboim, Y. Reisner, and N. Benvenisty. Human Embryonic Stem Cells and Their Differentiated Derivatives Are Less Susceptible to Immune Rejection Than Adult Cells Stem Cells, 2006. **24**: p. 221-229.

37. Martin, M.J., A. Muotri, R. Gage, and A. Varki. Human embryonic stem cells express an immunogenic nonhuman sialic acid. Nat Med, 2005. **11**: p. 228-232.

38. Formhals, A., *Process and apparatus for pareparing artificial threads*, U.S.P. Office, Editor. 1934: US. p. 1-7.

39. Li, W.J., C.T. Laurencin, E.J. Caterson, R.S. Tuan, and F.K. Ko. Electrospun nanofibrous structure: A novel scaffold for tissue engineering. Journal of Biomedical Materials Research, 2002. **60**(4): p. 613-621.

40. Reneker, D.H. and I. Chun. Nanometre diameter fibres of polymer, produced by electrospinning. Nanotechnology, 1996. **7**(3): p. 216-223.

41. Bhattarai, N., D. Edmondson, O. Veiseh, F.A. Matsen, and M.Q. Zhang. Electrospun chitosan-based nanofibers and their cellular compatibility. Biomaterials, 2005. **26**(31): p. 6176-6184.

42. Deitzel, J.M., J.D. Kleinmeyer, J.K. Hirvonen, and N.C.B. Tan. Controlled deposition of electrospun poly(ethylene oxide) fibers. Polymer, 2001. **42**(19): p. 8163-8170.

43. Jin, H.J., J.S. Chen, V. Karageorgiou, G.H. Altman, and D.L. Kaplan. Human bone marrow stromal cell responses on electrospun silk fibroin mats. Biomaterials, 2004. **25**(6): p. 1039-1047.

44. Kenawy, E.R., J.M. Layman, J.R. Watkins, G.L. Bowlin, J.A. Matthews, D.G. Simpson, and G.E. Wnek. Electrospinning of poly(ethylene-co-vinyl alcohol) fibers. Biomaterials, 2003. **24**(6): p. 907-913.

45. Li, M.Y., M.J. Mondrinos, M.R. Gandhi, F.K. Ko, A.S. Weiss, and P.I. Lelkes. Electrospun protein fibers as matrices for tissue engineering. Biomaterials, 2005. **26**(30): p. 5999-6008.

46. Luu, Y.K., K. Kim, B.S. Hsiao, B. Chu, and M. Hadjiargyrou. Development of a nanostructured DNA delivery scaffold via electrospinning of PLGA and PLA-PEG block copolymers. Journal of Controlled Release, 2003. **89**(2): p. 341-353.

47. Ma, Z.W., M. Kotaki, T. Yong, W. He, and S. Ramakrishna. Surface engineering of electrospun polyethylene terephthalate (PET) nanofibers towards development of a new material for blood vessel engineering. Biomaterials, 2005. **26**(15): p. 2527-2536.

48. Matthews, J.A., G.E. Wnek, D.G. Simpson, and G.L. Bowlin. Electrospinning of collagen nanofibers. Biomacromolecules, 2002. **3**(2): p. 232-238.

49. Min, B.M., G. Lee, S.H. Kim, Y.S. Nam, T.S. Lee, and W.H. Park. Electrospinning of silk fibroin nanofibers and its effect on the adhesion and spreading of normal human keratinocytes and fibroblasts in vitro. Biomaterials, 2004. **25**(7-8): p. 1289-1297.

50. Smith, L.A. and P.X. Ma. Nano-fibrous scaffolds for tissue engineering. Colloids and Surfaces B-Biointerfaces, 2004. **39**(3): p. 125-131.

51. Wnek, G.E., M.E. Carr, D.G. Simpson, and G.L. Bowlin. Electrospinning of nanofiber fibrinogen structures. Nano Letters, 2003. **3**(2): p. 213-216.

52. Yoshimoto, H., Y.M. Shin, H. Terai, and J.P. Vacanti. A biodegradable nanofiber scaffold by electrospinning and its potential for bone tissue engineering. Biomaterials, 2003. **24**(12): p. 2077-2082.

53. Whitesides, G.M., J.P. Mathias, and C.T. Seto. Molecular Self-Assembly and Nanochemistry - a Chemical Strategy for the Synthesis of Nanostructures. Science, 1991. **254**(5036): p. 1312-1319.

54. Decher, G. Fuzzy nanoassemblies: Toward layered polymeric multicomposites. Science, 1997. **277**(5330): p. 1232-1237.

55. Philp, D. and J.F. Stoddart. Self-assembly in natural and unnatural systems. Angewandte Chemie-International Edition in English, 1996. **35**(11): p. 1155-1196.

56. Kadler, K.E., D.F. Holmes, J.A. Trotter, and J.A. Chapman. Collagen fibril formation. Biochemical Journal, 1996. **316**: p. 1-11.

57. Hartgerink, J.D., E. Beniash, and S.I. Stupp. Self-assembly and mineralization of peptide-amphiphile nanofibers. Science, 2001. **294**(5547): p. 1684-1688.

58. Yu, Y.C., M. Tirrell, and G.B. Fields. Minimal lipidation stabilizes protein-like molecular architecture. Journal of the American Chemical Society, 1998. **120**(39): p. 9979-9987.

59. Zhang, S.G. Fabrication of novel biomaterials through molecular self-assembly. Nature Biotechnology, 2003. **21**(10): p. 1171-1178.

60. Lee, S.H., B.S. Kim, S.H. Kim, S.W. Kang, and Y.H. Kim. Thermally produced biodegradable scaffolds for cartilage tissue engineering. Macromolecular Bioscience, 2004. **4**(8): p. 802-810.

61. Nam, Y.S. and T.G. Park. Porous biodegradable polymeric scaffolds prepared by thermally induced phase separation. Journal of Biomedical Materials Research, 1999. **47**(1): p. 8-17.

62. Zhang, R.Y. and P.X. Ma. Poly(alpha-hydroxyl acids) hydroxyapatite porous composites for bone-tissue engineering. I. Preparation and morphology. Journal of Biomedical Materials Research, 1999. **44**(4): p. 446-455.

63. Ma, P.X. and R.Y. Zhang. Synthetic nano-scale fibrous extracellular matrix. Journal of Biomedical Materials Research, 1999. **46**(1): p. 60-72.

64. Zhang, R.Y. and P.X. Ma. Synthetic nano-fibrillar extracellular matrices with predesigned macroporous architectures. Journal of Biomedical Materials Research, 2000. **52**(2): p. 430-438.

65. Chen, V.J., L.A. Smith, and P.X. Ma. Bone regeneration on computer-designed nano-fibrous scaffolds. Biomaterials, 2006. **27**: p. 3973-3979.

66. Liu, X.H., L.A. Smith, G. Wei, Y.J. Won, and P.X. Ma. Surface engineering of nano-fibrous poly(L-lactic acid) scaffolds via self-assembly technique for bone tissue engineering. Journal of Biomedical Nanotechnology, 2005. **1**(1): p. 54-60.

67. Chen, V.J. and P.X. Ma. Nano-fibrous poly(L-lactic acid) scaffolds with interconnected spherical macropores. Biomaterials, 2004. **25**(11): p. 2065-2073.

68. Wei, G.B. and P.X. Ma. Macroporous and nanofibrous polymer scaffolds and polymer/bone-like apatite composite scaffolds generated by sugar spheres. Journal of Biomedical Materials Research Part A, 2006. **78A**(2): p. 306-315.

69. Liu, X.H. and P.X. Ma. Polymeric scaffolds for bone tissue engineering. Annals of Biomedical Engineering, 2004. **32**(3): p. 477-486.

70. Cai, K.Y., K.D. Yao, Y.L. Cui, S.B. Lin, Z.M. Yang, X.Q. Li, H.Q. Xie, T.W. Qing, and J. Luo. Surface modification of poly (D,L-lactic acid) with chitosan and its effects on the culture of osteoblasts in vitro. J. Biomed. Mater. Res., 2002. **60**(3): p. 398-404.

71. Gao, J.M., L. Niklason, and R. Langer. Surface hydrolysis of poly(glycolic acid) meshes increases the seeding density of vascular smooth muscle cells. Journal of Biomedical Materials Research, 1998. **42**(3): p. 417-424.

72. Hu, Y.H., S.R. Winn, I. Krajbich, and J.O. Hollinger. Porous polymer scaffolds surface-modified with arginine-glycine-aspartic acid enhance bone cell attachment and differentiation in vitro. J. Biomed. Mater. Res. A., 2003. **64A**(3): p. 583-590.

73. Nitschke, M., G. Schmack, A. Janke, F. Simon, D. Pleul, and C. Werner. Low pressure plasma treatment of poly(3-hydroxybutyrate): Toward tailored polymer surfaces for tissue engineering scaffolds. Journal of Biomedical Materials Research, 2002. **59**(4): p. 632-638.

74. Liu, X.H., Y.J. Won, and P.X. Ma. Surface modification of interconnected porous scaffolds. Journal of Biomedical Materials Research Part A, 2005. **74A**(1): p. 84-91.

75. Liu, X.H., Y.J. Won, and P.X. Ma. Porogen-induced surface modification of nano-fibrous poly(L-lactic acid) scaffolds for tissue engineering. Biomaterials, 2006. **27**(21): p. 3980-3987.

76. Smith, L.A., J. Beck, and P.X. Ma. Fabrication and Tissue formation with Nano-Fibrous Scaffolds, in *Nanotechnologies for Tissue, Cell and Organ Engineering*, C. Kumar. Editor. 2007, Wiley-VCH: Weinheim, Germany.

77. Tysseling-Mattiace, V., V. Sahni, K.L. Niece, D. Birch, C. Czeisler, M. Fehling, S. Stupp, and J. Kessler. Self-assembling nanofibers inhibit glial scar formation and promote axon elongation after spinal cord injury. J Neurosci, 2008. **28**: p. 3814-3814.

78. Olsen, B., A. Reginato, and W. Wang. Bone Development. Ann Rev Cell Dev Biol, 2000. **16**(191-220).

79. Hall, B. and T. Miyake. Divide, accumulate, differentiate: cell condensation in skeletal development revisited. Int J Dev Biol, 1995. **39**: p. 881-893.

80. Bielby, R., E. Jones, and D. McGonagle. The role of mesenchymal stem cells in maintenance and repair of bone. Injury, 2007. **38S1**: p. S26-S32.

81. Duplomb, L., M. Dagouassat, P. Jourdon, and D. Heymann. Concise review: embryonic stem cells: a new tool to study osteoblast and osteoclast differentiation. Stem Cells, 2006. **25**: p. 544-552.

82. Satija, N., G. Gurudutta, S. Sharma, F. Afrin, P. Gupta, Y. Verma, V. Singh, and R. Tripathi. Mesenchymal stem cells: molecular targets for tissue engineering. stem Cells Dev, 2007. **16**: p. 7-23.

83. Olivier, E., A. Rybicki, and E. Bouhassira. Differentiation of human embryonic stem cells into bipotent mesenchymal stem cells. Stem Cells, 2006. **24**: p. 1914-1922.

84. Barberi, T., L. Williz, N. Socci, and L. Studer. Derivation of multipotent mesenchymal precursors from human embryonic stem cells. PLoS Med, 2005. **2**: p. e161.

85. Woo, K.M., V.J. Chen, and P.X. Ma. Nano-fibrous scaffolding architecture selectively enhances protein adsorption contributing to cell attachment. J Biomed Mater Res A, 2003. **67**(2): p. 531-537.

86. Woo, K.M., J.H. Jun, V.J. Chen, J. Seo, J.H. Baek, H.M. Ryoo, G.S. Kim, M.J. Somerman, and P.X. Ma. Nano-fibrous scaffolding promotes osteoblast differentiation and biomeneralization. Biomaterials, 2007. **28**: p. 335-343.

87. Schindler, M., I. Ahmed, J. Kamal, A. Nur-E-Kamal, T.H. Grafe, H.Y. Chung, and S. Meiners. A synthetic nanofibrillar matrix promotes in vivo-like organization and morphogenesis for cells in culture. Biomaterials, 2005. **26**: p. 5624-5631.

88. Chen, M., K. Prabir, S.B. Warner, and S. Bhowmick. Role of Fiber Diameter in Adhesion and Proliferation of NIH 3T3 Fibroblast on Electrospun Polycaprolactone Scaffolds. Tissue Eng, 2007. **13**: p. 579-587.

89. Xu, C.Y., R. Inai, M. Kotaki, and S. Ramakrishna. Aligned biodegradable nanofibrous structure: a potential scaffold for blood vessel engineering. Biomaterials, 2004. **25**: p. 877-886.

90. Yang, F., C.Y. Xu, M. Kotaki, S. Wang, and S. Ramakrishna. Characterization of Neural stem cells on electrospun poly(L-lactic acid) nanofibrous scaffolds. J Biomater Scit Polymer Edn, 2004. **15**(12): p. 1483-1497.

91. Nur-E-Kamal, A., I. Ahmed, J. Kamal, M. Schindler, and S. Meiners. Three-demensional nanofibrillar surfaces promote self-renewal in mouse embryonic stem cells. Stem Cells, 2006. **24**: p. 426-433.

92. Storrie, H., M.O. Guler, S.N. Abu-Amara, T. Volberg, M. Rao, B. Geiger, and S.I. Stupp. Supramolecular crafting of cell adhesion Biomaterials, 2007. **28**: p. 4608-4618.

93. Bondar, B., S. Fuchs, A. Motta, C. Migliaresi, and C.J. Kirkpatrick. Functionality of endothelial cells on silk fibroin nets: Comparative study of micro- and nanometric fibre size Biomaterials, 2008. **29**: p. 561-572.

94. Li, W.J., K.G. Danielson, P.G. Alexander, and R.S. Tuan. Biological response of chondrocytes cultured in three-dimensional nanofibrous poly(E-caprolactone) scaffolds. J Biomed Mater Res, 2003. **67A**: p. 1105-1114.

95. Hu, J., X. Liu, and P.X. Ma. Induction of osteoblast differentiation phenotype on poly(L-lactic acid) nanofibrous matrix. Biomaterials, 2008. **29**: p. 3815-3821.

96. Shih, Y.V., C.N. Chen, S.W. Tsai, Y.J. Wang, and O.K. Lee. Growth of Mesenchymal Stem ells on Electrospun Type I collagen Nanofibers. Stem Cells, 2006. **24**: p. 2391-2397.

97. Nur-E-Kamal, A., I. Ahmed, J. Kamal, M. Schindler, and S. Meiners. Three dimensional nanofibrillar surfaces induces the activation of Rac. Biochem Biophys Res Commun, 2005. **331**: p. 428-434.

98. Lee, C.H., H.O. Shin, I.H. Cho, Y.M. Kang, I.A. Kim, K.D. Park, and J.W. Shin. Nanofiber alignment and direction of mechanical strain affect the ECM productions of human ACL fibroblast. Biomaterials, 2005. **26**: p. 1261-1270.

99. Li, W.J., Y.J. Jiang, and R.S. Tuan. Chondrocyte phenotype in engineered fibrous matrix is regulated by fiber size. Tissue Eng, 2006. **12**: p. 1775-1785.

100. Silva, G.A., C. Czeisler, K.L. Niece, E. Beniash, D.A. Harrington, J.A. Kessler, and S.I. Stupp. Selective Differentiation of Neural Progenitor Cells by High-Epitope Density Nanofibers. Science, 2004. **303**: p. 1352-1355.

101. Chua, K.N., W.S. Lim, P. Zhang, H. LU, J. Wen, S. Ramakrishna, K.W. Leong, and H.Q. Mao. Stable immobilization of rat hepatocyte spheroids on galactosylated nanofibers. Biomaterials, 2005. **26**: p. 2537-2547.

102. Semino, C.E., J.R. Merok, G.G. Crane, G. Panagiotakos, and S. Zhang. Functional differentiation of hepatocyte-like spheroid structures from putative liver progenitor cells in three-deminional peptide scaffolds. Differentiation, 2003. **71**: p. 262-270.

103. Parson, J.T. Focal adhesion kinase: the first ten years. J Cell Sci, 2003. **116**: p. 1409-1416.

104. Li, W., R. Tuli, X. Huang, P. Laquerriere, and R. Tuan. Multilineage differentiation of human mesnchymal stem cells in a three-dimensional nanofibrous scaffold. Biomaterials, 2005. **26**: p. 5158-5166.

Chapter 3

Osteogenic Differentiation of Mouse Embryonic Stem Cells on Nanofibers

3.1 Introduction

Embryonic stem cells (ESC) typically isolated from the inner cell mass of blastocyts are pluripotent and possess the ability to differentiate into all tissues derived from the three germ layers[1, 2]. Due to this, ESC hold great promise as a cell source for tissue engineering[3]. Additionally, ESC have been found to proliferate longer than other types of stem cells making them a potentially adventageous cell source. ESC derived cells have just begun to be explored as the cell source for tissue engineering applications [4-7].

Much of the effort to control the differentiation of ESC into specific lineages has focused on the use of biological factors [8-10]. However, it is known that extracellular matrix (ECM) contributes to the osteogenic lineage selection during embryonic development through cytoskeletal and surface receptor interactions[11-13]. Therefore to successfully use ESC in tissue engineering we need to understand and mimic the contributions of the ECM. The scaffold should act as a directive template for the ESC, stimulating the desired differentiation pathway much as the ECM does during embryonic

development. As such, the scaffold should mimic the natural ECM of the desired tissue[14]. Type I collagen, consisting of three collagen polypeptide chains wound together to form a ropelike superhelix that assembles into the fibers ranging in size from 50 to 500nm[15, 16], is a major component of the ECM in many tissues.

We hypothesize that such nanofibers advantageously support ESC differentiation since they provide a microenvironment for cells more similar to type 1 collagen ECM than traditional smooth surfaces. Synthetic three dimensional nanofibers of the same size scale as natural type I collagen have been developed in our lab using a novel phase separation technique[17-21]. To test our hypothesis, thin poly (L-lactic acid) (PLLA) matrices with nanofibrous (NF) architecture and flat (solid) films were used as a model to study the effects of scaffold wall architecture on the differentiation of mouse ESC to osteoblastic lineage as a precursor to their use as a cell source for bone tissue engineering.

3.2 Materials and Methods

3.2.1 Materials

PLLA with an inherent viscosity of 1.6 dl/g was purchased from Alkermes (Medisorb, Cambridge, Massachusetts) and used without further purification. Dubecco's Modified Eagle Media (DMEM), 0.5M EDTA, trypsin, Hank's buffered salt solution and PCR primers were obtained from Invitrogen (Carlsbad, CA). Fetal bovine serum was obtained from Harlan Biological (Indianapolis, IN). Human recombinant leukemia inhibitory factor (LIF), and Neuronal Class III β-Tubulin (TUJ1) antibody were obtained

from Chemicon (Temecula, CA). Brachyury antibody was obtained from Santa Cruz Biotechnology (Santa Cruz, CA). LEAF anti-mouse/rat CD49e, LEAF anti-mouse/rat CD49b and LEAF Purified Armenian Hamster IgG Isotype Control were obtained from Biolegend (San Diego, CA). All secondary antibodies and normal donkey serum were obtained from Jackson ImmunoResearch (West Grove, PA). RNeasy Mini Kit and Rnase-Free DNase set were obtained from Qiagen (Valencia, California). TaqMan reverse transcription reagents, real-time PCR primers, and TaqMan Universal PCR Master mix were obtained from Applied Biosystems (Foster City, California). Chemicals were obtained from Sigma Chemical Co. (St. Louis, MO) unless otherwise noted above.

3.2.2 Thin Matrix Preparation for Cell Culture

PLLA was dissolved in tetrahydrofuran at 60^{o}C to make a 10% (w/v) PLLA solution. The NF PLLA matrix (thickness~40μm) was fabricated by first casting 0.4 mL of the PLLA solution on a glass support plate that had been pre-heated at 45^{o}C for 10 min and then sealing the polymer solution on the glass support plate by covering it with another pre-heated glass plate. The polymer solution was phase separated at -20°C for 2 hrs and then immersed into a mixture of ice and water to exchange tetrahydrofuran for 24 hrs. The matrix was washed with distilled water at room temperature for 24 hrs with water changed every 8 hrs. The matrix was then freeze-dried. The porosity and fiber diameter were determined as previously described[17]. Briefly, the volume and the weight of the matrix was determined and then the density was calculated. The porosity was then calculated from the measured overall densities. The average fiber diameter was

calculated from SEM micrographs. Fifty fibers per sample were measured their averages and standard deviations are reported.

The matrices were cut to fit into a 35 mm Petri dish and secured in place with a disk of silicone elastomer from Dow Corning (Midland, MI) containing a 1.5 mm by 1.5 mm opening which had been cast from a 1:10 mix of curing agent to base. The matrices were then sterilized with ethylene oxide, wet with Hank's buffered salt solution 2 times for 0.5 hrs each and rinsed with differentiation media (DMEM supplemented with 20% FBS, 10^{-4}M β-mercaptoethanol, and 1.33 μg/ml HEPES) for 1hr.

Solid films were fabricated in a similar manner excluding the phase separation step. Instead, the solvent was evaporated at room temperature in a fume hood. The flat (solid) films and 0.1% gelatin coated Petri dishes were then treated similarly to the NF matrices.

3.2.3 Mouse Embryonic Stem Cell Culture and Seeding

D3 mouse ESC[22] were cultured on 0.1% gelatin-coated tissue culture flasks in ESC media (DMEM supplemented with 10% FBS, 10^{-4}M β-mercaptoethanol, 0.224 μg/ml L-glutamine, 1.33 μg/ml HEPES, and 1,000 units/ml human recombinant LIF).

15,000 (for SEM in order to see the interactions of individual cells with the matrices) or 60,000 cells were seeded on each of the prepared matrices or 0.1% gelatin-coated tissue culture dish controls. Upon seeding, cells were cultured in differentiation media (DMEM supplemented with 20% FBS, 10^{-4}M β-mercaptoethanol, and 0.224 μg/ml L-glutamine, and 1.33 μg/ml HEPES) or osteogenic media (differentiation media supplemented with 1 μM dexamethasone, 50 μg/mL ascorbic acid and 10 mM β-glycerol

phosphate). The media was changed 12 hrs after seeding and then every other day for the remainder of the culture period.

For the α2 integrin blocking studies, 6μg/ml LEAF anti-mouse/rat CD49b antibody[23] was added to the media from day 7 onward. While for the α5 integrin blocking studies 6μg/ml LEAF anti-mouse/rat CD49e antibody was added to the media after a 24hr attachment period.

3.2.4 Scanning Electron Microscopy

Twelve hours after seeding, the matrices and control were washed with PBS and 0.1M cacodylate buffer, then fixed with 2.5% glutaraldehyde in 0.1M cacodylate buffer over night. The matrices were washed again with 0.1M cacodylate buffer and post-fixed in 1% osmium tetroxide for 1 hr. The fixed samples were then dehydrated through an ethanol gradient (50%, 70%, 90%, 95%, and 100%) over 3 hrs and dried with hexamethyldisilazane. Samples were then gold coated and observed using scanning electron microscopy (S-3200, Hitachi, Japan). Cell spreading area was calculated from at least 20 cells per sample in the SEM images using the automated measure function of J Image (downloaded from the National Institute of Health, Bethesda, MD, USA, free download available at http://rsb.info.nih.gov/ij/).

3.2.5 Immunofluorescence and Alizarin Red S Staining

For quantitative analysis, the ESC were removed from the matrices and 0.01% gelatin coated tissue culture plastic control with 0.25% trypsin/ 1mM EDTA then fixed with 4% paraformaldhyde, 0.2% Triton-X100 washed twice in 0.1% goat serum, and

stained in 1 μg of Runx2 and TUJ1 antibodies in 100 μl of 0.2% triton-X100 and 2% goat serum in PBS. The ESC were then washed twice with PBS and stained with the appropriate secondary antibodies and dapi. The cells from each 12-day sample were then placed on a cover slip and the number of ESC expressing Runx2 and TUJ1 were then counted in 4 random fields of view in each of 3 replicates. At least 900 cells as determined by dapi staining in images taken with an RT Slider Spot camera (Diagnostic Instraments Inc, Sterling Heights, MI) on a Eclispe TE 300 fluorescence microscope (Nikon Instruments Inc, Melville, NY) were counted per sample using Image-Pro Plus (Media Cybernetics Inc, Bethesda, MD). Images of Runx2 and TUJ1 staining were overlaid with matching images of dapi staining in Photoshop CS (Abode, San Jose, CA). Areas of Runx2 and TUJ1 staining not associated with a nucleus were then manually excluded in Image-Pro Plus. All counts were checked with a counter by hand and found to be similar.

After 26 days of culture, the matrices and controls were fixed with 2% paraformaldehyde/PBS, washed, and stored at 4°C in PBS. Nonspecific antibody binding was blocked by incubating in 10% donkey or goat serum, then the matrices and controls were exposed to TUJ1 (1:250) or osteocalcin (1:50) antibodies, followed by appropriate secondary antibodies conjugated to FITC (TUJ1), or TRITC (ostoecalcin). Dapi was used to stain cell nuclei.

For Alizarin Red S staining, the matrices and controls were fixed using the same method as described above and then stained with 40mM Alizarin Red S solution, pH 4.2 at room temperature for 10 minutes. Matrices and controls were then rinsed 5 times in

distilled water and washed 3 times in PBS on an orbital shaker at 40 rpm for 5 minutes each to reduce nonspecific binding.

3.2.6 Western Blotting Analysis

Films were pre-wetted with PBS according to protocol described above, then cell culture medium or 100ug/ml bovine fibronectin were added and incubated for 1hr. For cell culture medium treatment, three films were pooled for sample collection, while 1 film was used to form fibronectin collection sample. Films were then washed with PBS for 2 times (1 min each), cut into pieces and transferred to 1.5ml tubes. 1ml of PBS was added, and the films were washed three times. PBS was then removed, and the films were centrifuged for 1min at 12,000rpm 2 times to remove any remaining liquid. 100ul of 1% SDS was added and incubated for 1hr. This was repeated two more times and the samples pooled to form a 300ul sample. 30 ul of the collection sample was used for each gel. Western blot analysis was conducted as previously described[19]. Briefly, the recovered serum protein samples were subject to fractionation through 4-12% SDS-polyacrylamide gel electrophoresis (PAGE). The fractionated proteins were transferred to a PVDF membrane (Sigma). The blots were washed with TBST (10 m*M* Tris-HCl, 150 m*M* NaCl, 0.05% Tween-20, pH 8.0), and blocked with Blotto (5% nonfat milk in TBST) at room temperature for 1 h. The blots were incubated in anti-bovine fibronectin polyclonal antibody (Santa Cruz Biotechnology, Santa Cruz, CA) at room temperature for 1 h. After washing with TBST, the blots were incubated in anti-goat immunoglobulin G-horseradish peroxidase-conjugated antibody (Sigma), and then in chemiluminescence reagent

(SuperSignal West Dura; Pierce). The relative densities of the protein bands were analyzed with QualityOne (Biorad).

3.2.7 PCR and Real Time PCR

Total RNA was isolated from at least 3 replicates using an RNeasy Mini Kit according to the manufacturer's protocol after films were mechanically homogenized with a Tissue-Tearor (BioSpec Products, Bartlesville, OK) while cells cultured on gelatin-coated tissue culture plate controls were harvested with a cell scraper. Based on absorbance reading at 260nm, 1μg of RNA from samples an optical density ratio greater than 1.6 was used to make cDNA using a Geneamp PCR (Applied Biosystems) with TaqMan reverse transcription reagents and 10 min incubation at 25 °C, 30 min reverse transcription at 48 °C, and 5 min inactivation at 95 °C. 5 μL of each reaction was subject to PCR using AmpliTaq Gold DNA polymerase (Applied Biosystems) for each of the following: Brachyury (5'- gctgtgactgcctaccagcagaatg-3' and 5'-gagagagagcgagcctccaaac-3'); Nestin (5'- gtgcctctggatgatg-3' and 5'- ttgaccttcctccccctc-3'); α5 integrin (5'-cgttgagtcattcgcctct-3' and 5'-ctaccgcgtctaggttgaagc-3'); α2 integrin (5'- acccgccccttctgtatcttt-3' and 5'-ggcagtcatagccaacagcaa-3'); β1 integrin (5'-ggtgtcgtgtttgtgaatgc-3' and 5'-cacagttgtcacggcactct-3'); Collagen type I (5'-gaagtcagctgcatacac-3' and 5'-aggaagtccaggctgtcc-3'); Runx2 (5'-ccgcacgacaaccgcaccat-3' and 5'-cgctccggcccacaaatctc-3'); Bone sialoprotein (5'- gtcaacggcaccagcaccaa-3' and 5'-gtagctgtattcgtcctcat-3'); Osteocalcin (5'-cggccctgagtctgacaaa-3' and 5'-accttattgccctcctgcctt-3') and β actin (5'- caggattccatacccaagaag-3' and 5'-

aaccctaaggccaaccgtg-3'). The cycling conditions were: 94°C for 5 min followed by 94°C for 30s, 55°C for 60s, 72°C for 60s 35 cycles for brachyury and β actin, 94°C for 120s, 55°C for 30s, 72°C for 45s 35 cycles for nestin, 94°C for 60s, 60°C for 120s, 72°C for 180s 40 times for α5 integrin and 94°C for 30s, 55°C for 60s, 72°C for 60s 30 cycles for α2 integrin, β1 integrin, Runx2, bone sialoprotein, and osteocalcin. These amplifications were followed by a 10 min extension at 72°C. The relative densities of the bands were analyzed with QualityOne (Biorad) to obtain a semi-quantitative assessment.

Real-time PCR was set up using TaqMan Universal PCR Master mix and specific primer sequence for brachyury, nestin, bone sialoprotein, osteocalcin and β actin with 2 min incubation at 50 °C, a 10 min Taq Activation at 95 °C, and 50 cycles of denaturation for 15 s at 95 °C followed by an extension for 1 min at 72 °C on an ABI Prism 7500 Real-Time PCR System (Applied Biosystems). Target genes were normalized against β actin using a relative standard curve.

3.2.8 Statistical Analysis

All experiments were conducted at least three times. All quantifiable data are reported with the means and standard deviations. Student t-tests were performed where applicable. Significance was set at a p-value of less than 0.05.

3.3 Results

The surface characterization of the NF matrix (Figure 3.1A) and the solid film (Figure 3.1B) via SEM shows the differences in matrix architecture prior to cell culture.

The NF matrix was found to contain fibers ranging in diameter from 50 to 500nm with an average fiber diameter of 148nm±21nm (standard deviation) and calculated to have a porosity of 92.9%. The NF matrix contains very small pores preventing cellular penetration so that the effects of scaffold wall architecture can be studied without complications from cell distribution and mass transport conditions associated with pore size and inter-pore connectivity. Figure 3.1C illustrates the difference in cell morphology after 12 hrs on NF PLLA matrix, solid PLLA film and control surface (gelatin coated tissue culture plastic). The differentiating ESC extended more processes on the NF matrix and spread to a greater degree (278±56 μm^2 reported as area ± standard deviation) compared with ESC grown on either the solid film (110±12μm^{2*}, *indicates p value<0.05 compared to NF matrix) or control surface (203±26 μm^2). Measurements of DNA content indicate that a similar number of cells have attached to each of the materials (data not shown), indicating that the cell morphology difference is not an effect of additional available surface area on the NF matrices.

Based on these initial morphological differences on the films, we examined cellular differentiation over longer culture periods. Brachyury mRNA expression (a mesodermal marker) and nestin mRNA expression (a neural marker) was examined in samples cultured in osteogenic media for 12 days (Figure 3.2A). ESC cultured on the NF matrices were found to have increased brachyury expression and reduced nestin expression compared to those on either the solid films and gelatin control surface. Quantitative PCR results for brachyury espression (Figure 2B) and nestin expression(Figure 2C) show these relationships to be significant.

Early osteogenic markers (Type I Collagen and Runx2) were also examined via mRNA expression at day 12(Figure 3.2A). Type I Collagen was found to be expressed more strongly in the ESC on the NF matrix and control then those on the solid films, while Runx2 was found to be expressed more strongly in the ESC on the NF matrix than either of those on the solid films or control. Later markers of bone differentiation, bone sialoprotein and osteocalcin, were not detectable at this time point.

Next the percentage of cells on the matrices committed to the osteogenic lineage was examined after 12 days of osteogenic culture. Approximately, (60±6)% (expression ±std) of ESC on the NF matrices expressed Runx2 at this time point, while only (33±11)% of ESC on the solid films and (38±2)% of ESC on the control. Expression a TUJ1, a neuronal marker, was also examined at this time. Approximately, (37±11)% (expression ±std) of ESC on the NF matrices expressed TUJ1, while (61±13)% of ESC on the solid films and (35±10)% of ESC on the control.

The expression of transcripts for several integrins (α2, α5, and β1), cell membrane proteins which mediate cellular adhesion to substrates, were also examined after 12 days of culture in osteogenic media (Figure 3.2A). Several integrin subunits associated with cellular adhesion to type I collagen (α2β1) and fibronectin (α5β1) were found to be up regulated on the NF matrices compared to the solid films. The increase in β1 integrin transcription in ESC on NF matrices compared to solid films and control surface supports the lineage differenitation data, as increased β1 integrin is associated with increased mesodermal differentiation while inhibiting neuronal differentiation[24]. Since integrin expression varies during osteogenesis as the ECM develops[25], the ESC on the NF matrices may be changing their adhesion patterns and therefore gene

expression as a response to more developed ECM being presented on the NF matrices than on either the solid films or the control surface.

To examine the effects of α2 and α5 integrins on the differentiation of ESC on the matrices, blocking studies were conducted (Figure 3.3). Since α2 integrin expression is developmentally regulated[26] and not expressed at the mRNA level in our undifferentiated cell population, a time course was conducted to determine when α2 integrin mRNA begins being transcribed during the differentiation process (Figure 3.3A). Since this does not occur until after day 7 of differentiation, the blocking antibody was only administered to the cells from day 7 onward in the study. Figure 3.3B shows that blocking α2 integrin interactions substantially decreases mesodermal differentiation on both architectures. Runx2 was also examined after blocking α2 integrin, but after 70 amplification cycles no Runx2 expression was found in the samples treated with the α2 integrin blocking antibody while the samples treated with the IGG isotype control antibody expressed Runx2 mRNA at a level similar to samples not exposed to antibodies (Figure 3.3C). Measurements of DNA content indicate that a similar number of cells have attached to each of the NF matrices and solid film samples regardless of antibody treatment (data not shown), indicating that changes in cellular differentiation are not the result of variations in cell number present on the samples. Since α2 integrin interactions have been found to be necessary for the osteogenic differentiation of pre-osteoblasts, the lack of Runx2 mRNA expression, a characteristic of a more committed cell type[23, 27], in the samples where α2 integrin interactions were blocked was not surprising. Since α5 integrin is strongly expressed in our undifferentiated ESC[28], blocking antibody was added to culture after a short attachment period to block its additional stimulation of

differentiation signal transduction pathways such as focal adhesion kinase. Blocking α5 integrin interactions has a significant effect on both the mesodermal (Figure 3.3-D) and the osteogenic (Figure 3.3E) differentiation of ESC cultured on the NF matrices but little effect on the mesodermal (Figure 3.3D) and the osteogenic (Figure 3.3E) differentiation of ESC cultured on the solid films. Since α5 integrin was down regulated at the mRNA level (Figure 3.2A) on the solid films compared to the NF matrices and the effects of its stimulation on osteogenic differentiation have been shown to be dependent on culture conditions[23, 29], these indicate that the NF matrcies and the solid films expose the ESC grown on them to different microenvironments. One of the differences between the NF matix and the solid film appears to be associated with the α5 integrin interactions.

To examine the initial microenvironment created on each architecture, the protein adsorption from the differentiation media was examined (Figure 4A). The NF matrices were found to adsorb more protein than the solid films. Western blots for fibronectin on NF matrices exposed to with media (Figure 4B) or pure bovine fibronectin (Figure 4C) were shown to adsorb more fibronectin than similarly treated solid films, supporting the α5 integrin blocking data.

The expression of bone markers was examined after 26 days of differentiation (Figure 3.5A). Type I collagen, unlike 12 days of differentiation, was expressed at a similar level on all materials and controls. While after the additional culture time, Runx2 was more strongly expressed on all materials and controls, it was still expressed more strongly on NF matrices than on solid films. Later markers of osteogenic differentiation (bone sialoprotein and osteocalcin) were now detected unlike the earlier time point. ESC grown on the NF matrices expressed higher levels of osteocalcin (Figure 3.5B) and bone

sialoprotein (Figure 3.5C) compared to both flat (solid) films (3 times for both markers) and control surfaces (1.8 and 5.5 times respectively).

The expression of these late stage bone markers coincides with the mineralization of the matrix during bone formation. After 26 days of osteogenic culture, the samples were stained for calcium to examine mineral deposition on each of the surfaces (Figure 3.6A). Although all the samples showed some degree of calcium deposition, there was substantially more calcium on the NF matrices than on the solid films or the controls. NF matrix without cells cultured in media for the same time period did not show significant staining (Figure 3.6B), signifying that the mineralization on the NF matrices is due to cellular deposition and not biomimetic absorption from the media. Immunohistochemical localization of osteocalcin and TUJ1 was used to determine the distribution of the mature osteoblasts across the matrices (Figure 3.7). NF matrices had an even distribution of osteocalcin across the surface with very little neuronal differentiation, while solid films and controls had less osteocalcin protein and increased neuronal differentiation. NF matrix controls run either without cells or without antibodies indicate that the staining is specific for osteocalcin and TUJ1 and not nonspecific binding of the antibody to the NF matrix. In combination with the mRNA and mineralization data, this indicates a more mature osteogenic cell population has differenitated on the NF matrix than on either the flat (solid) films or the control surface, suggesting that the NF matrix promotes greater differentiation of ESC toward the osteogenic lineage than the solid films or control surface.

3.4 Discussion

The controlled differentiation of embryonic stem cells is a necessary first step in using them as a cell source for tissue engineering applications[30]. Current attempts focus on the addition of biochemical factors to direct the differentiation of the cells to a particular lineage. However, biochemical cues are only part of the complex environment, which controls lineage fate in vivo. To elicit more control over lineage fate, one must move beyond chemical cues and examine how other components contribute. In this study, we have examined the effects of NF architecture on ESC differentiation using thin PLLA NF matrices as a model for tissue engineering applications.

With osteoblasts and their precursors, it has been shown that substrate architecture independent of material chemistry can significantly affect cellular behavior [31-33]. Osteoblasts in short term culture on material with NF architecture have been shown to extend more processes then osteoblasts cultured on material with solid architecture[34]. This is consistent with the enhanced ESC spreading and process outgrowth observed after 12 hrs on NF matrices compared to flat (solid) films. This is significant because the flat (solid) films were made of the same polymer indicating that the NF architecture was contributing to the difference in cellular response and not the polymer itself. The increased cell spreading and process outgrowth with the NF matrices compared to the solid films may lead to increased activation of intercellular signaling pathways affecting lineage fate and the type of tissue formed.

As culture time increased, ESC on NF matrices with osteogenic supplementation continued to exhibit increased differentiation toward bone than ESC on the flat (solid) films. Increased differentiation on NF architecture compared to solid architecture has also been observed with osteoblasts[20, 34]. In addition to the size scale of the material

architecture, increased matrix rigidity have been shown to increased osteogenic differentiation of pre-osteoblastic cells[35-37].

Several factors likely contribute to the differences in differentiation observed between the NF matrices and the flat (solid) films. Similar to the thin matrices and film (figure 3.4), previous work with macro-porous NF PLLA scaffolds formed by a similar phase separation process, showed that NF scaffolds absorbed more serum proteins than solid -walled scaffolds and the profile of the adsorbed proteins was different from those absorbed by the solid-walled scaffolds[19]. Differences in the amount or type of absorbed serum proteins provide a better niche for directing the differentiation of ESC. Previously, we reported that similar NF scaffolds adsorb nearly 4 times more fibronectin than their solid counterparts[19]. Increased fibronectin adsorbed to the NF matrices may accelerate ESC differentiation to the mesodermal and osteogenic lineages on the NF matrices compared to the solid films, which is further supported by our α5 blocking results. Increased integrin signaling and differentiation has been observed in ESC cultured on fibronectin[28]. Fibronectin is the earliest of the matrix proteins synthesized by osteoblasts[38, 39]. During embryonic development, integrin-fibronectin interactions have been shown to be important to early mesodermal development[40].

A previous study found increased β1 integrin expression and osteogenic differentiation in neonatal mouse osteoblasts on NF scaffolds compared to their solid counterparts[34]. β1 integrin expression is up regulated in a similar manner on the thin NF matrices compared to the solid films, which is consistent with the increased osteogenic differentiation and consistent with the observation that β1 integrin plays a role in mesodermal lineage commitment of ESC[24]. As such, increased stimulation of β1

integrin, which has been shown to regulate ESC differentiation through the MAP kinase signaling pathway[41, 42], could also be contributing to this increased ESC differentiation on the NF matrices compared to the solid films.

The NF matrices themselves mimic the fiber diameter of type I collagen, a major component of the bone ECM[27]. α2β1 integrin is the major type I collagen binding integrin[43, 44]. Although α2 integrin expression is developmentally regulated[26], its up regulation has been linked to a increase in ESC differentiation[28] and is necessary for osteogenic differentiation[23, 27] as seen in our α2 integrin blocking data (Figure 3). A study of neonatal mouse osteoblasts on NF scaffolds indicates that α2β1 integrin could directly interact with the nanofibers based on their unaltered expression when collagen fiber formation was blocked[34]. Additionally, pre-osteoblasts were found to have unaltered cytoskeleton structure (in terms of stress fiber and focal adhesion formation) on gelatin modified and unmodified NF matrices[45]. As both eliminating the cell produced collagen fibers and providing a biomimic surface chemistry on the NF matrices do not eliminate or induce the NF effect, the NF architecture itself could be influencing cell behavior directly in a manner similar to type I collagen.

3.5 Conclusions

These results indicate that NF architecture contributes to promoting the osteogenic lineage fate of ESC cells. We observed morphological differences in ESC cultured on NF matrices compared to solid films in short time frames and increased differentiation to the mesodermal and osteogenic lineage (osteogenic media) over longer time frames. Based on these results, we believe that NF architecture plays an important

role in differentiation and should be used in combination with soluble factors to achieve the directed differentiation necessary for tissue engineering applications.

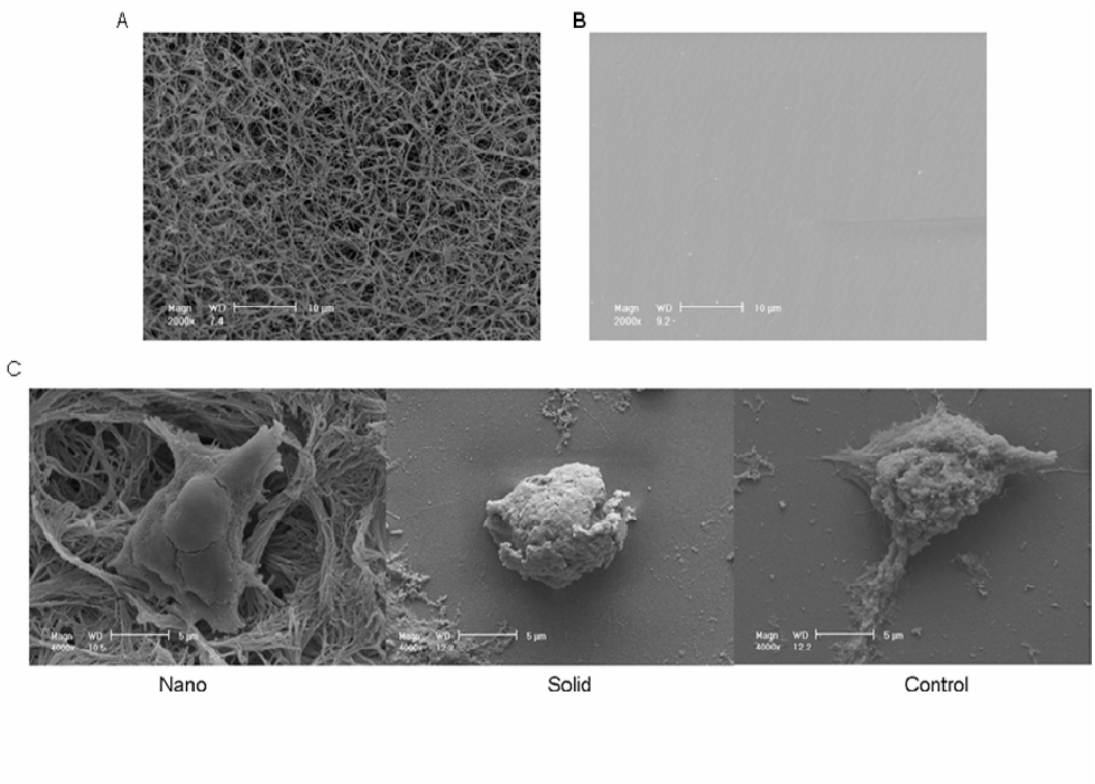

Figure 3.1: SEM micrographs of (A) nanofibrous matrix, Scale bar =10µm; (B) solid films, Scale bar=10µm; (C) D3 cells after 12 hrs under differentiation conditions on nanofibrous matrix (Nano), flat (solid) films (Solid), gelatin coated tissue culture plastic (Control), Scale bar =5µm.

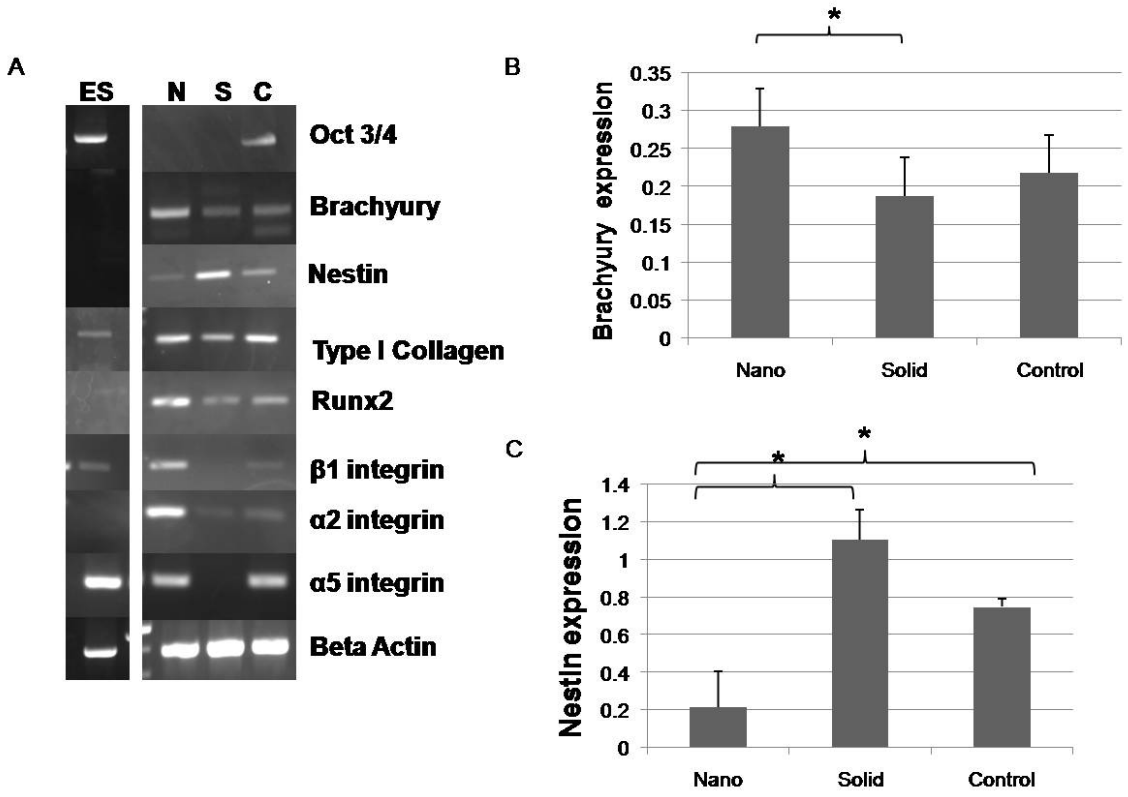

Figure 3.2: Expression of neuronal, mesodermal, and early osteogenic markers and integrins after 12 days of culture under osteogenic conditions: (A) PCR of RNAs isolated from cells grown on nanofibrous matrix (N), solid films (S) and gelatin coated tissue culture plastic (C); (B) Quantitative PCR of brachyury of RNAs isolated from cells grown expression on nanofibrous matrix (Nano), solid films (Solid) and gelatin coated tissue culture plastic (Control) * denotes p-value <0.05; (C) Quantitative PCR of nestin of RNAs isolated from cells grown expression on nanofibrous matrix (Nano), solid films (Solid) and gelatin coated tissue culture plastic (Control) * denotes p-value <0.05.

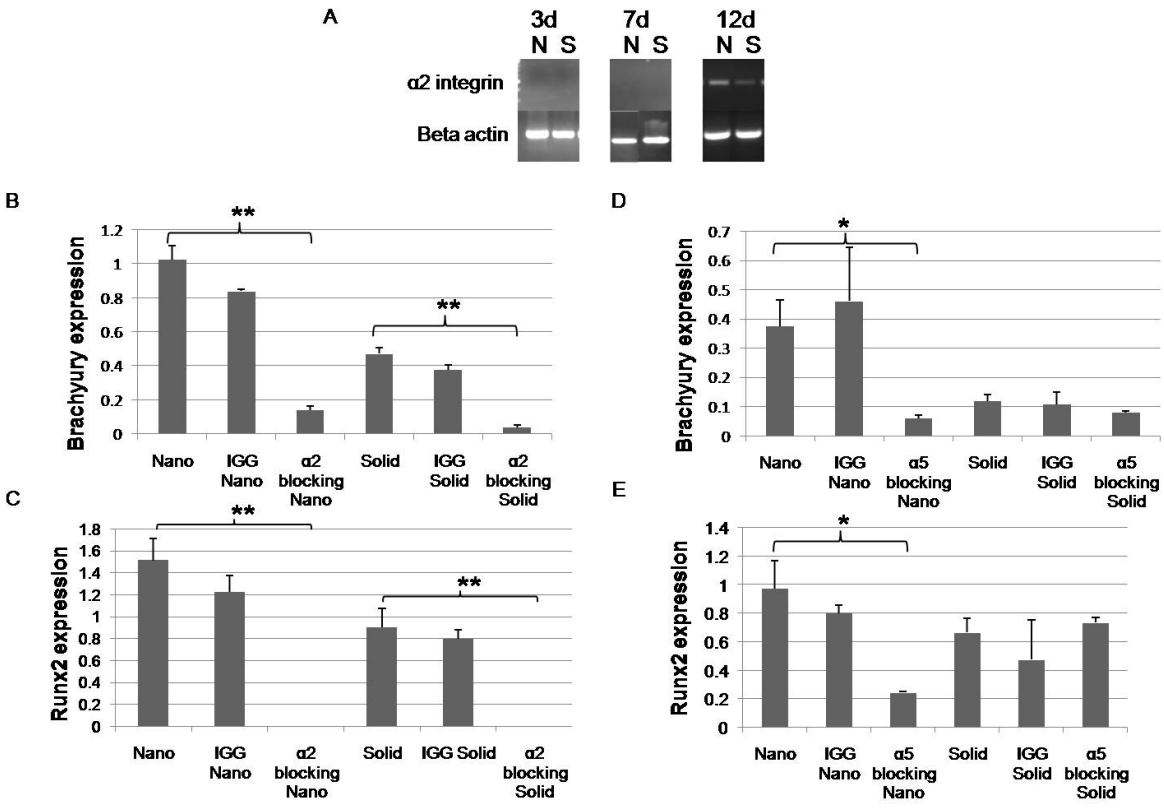

Figure 3.3: Effects of integrin blocking on mesodermal and osteogenic differentiation after 12 days of differentiation culture. (A) PCR of α2 integrin RNAs expression over time on nanofibrous matrix (N) and flat (solid) films (S); (B) quantitative PCR of brachyury RNAs isolated from cells grown on nanofibrous matrix (Nano), on nanofibrous matrix with control IGG isotype (IGG nano), on nanofibrous matrix with CD49b antibody (α2 blocking nano), on flat (solid) films (Solid), on flat (solid) films with control IGG isotype (IGG solid), and on flat (solid) films with CD49b antibody (α2 blocking solid) ** denotes p-value <0.01; (C) quantitative PCR of Runx2 RNAs isolated from cells grown on nanofibrous matrix (Nano), on nanofibrous matrix with control IGG isotype (IGG nano), on nanofibrous matrix with CD49b antibody (α2 blocking nano), on solid-walled matrix (Solid), on flat (solid) films with control IGG isotype (IGG solid), and on flat (solid) films with CD49b antibody (α2 blocking Solid) ** denotes p-value <0.01; (D) quantitative PCR of brachyury RNAs isolated from cells grown on nanofibrous matrix (Nano), on nanofibrous matrix with control IGG isotype (IGG nano), on nanofibrous matrix with CD49e antibody (α5 blocking nano), on flat (solid) films (Solid), on flat (solid) films with control IGG isotype (IGG solid), and on solid-walled matrix with CD49e antibody (α5 blocking solid) * denotes p-value <0.05; (E) quantitative PCR of Runx2 RNAs isolated from cells grown on nanofibrous matrix (Nano), on nanofibrous matrix with control IGG isotype (IGG nano), on nanofibrous matrix with CD49e antibody (α5 blocking nano), on flat (solid) matrix (Solid), on flat (solid) films with control IGG isotype (IGG solid), and on flat (solid) films with CD49e antibody (α5 blocking solid) * denotes p-value <0.05.

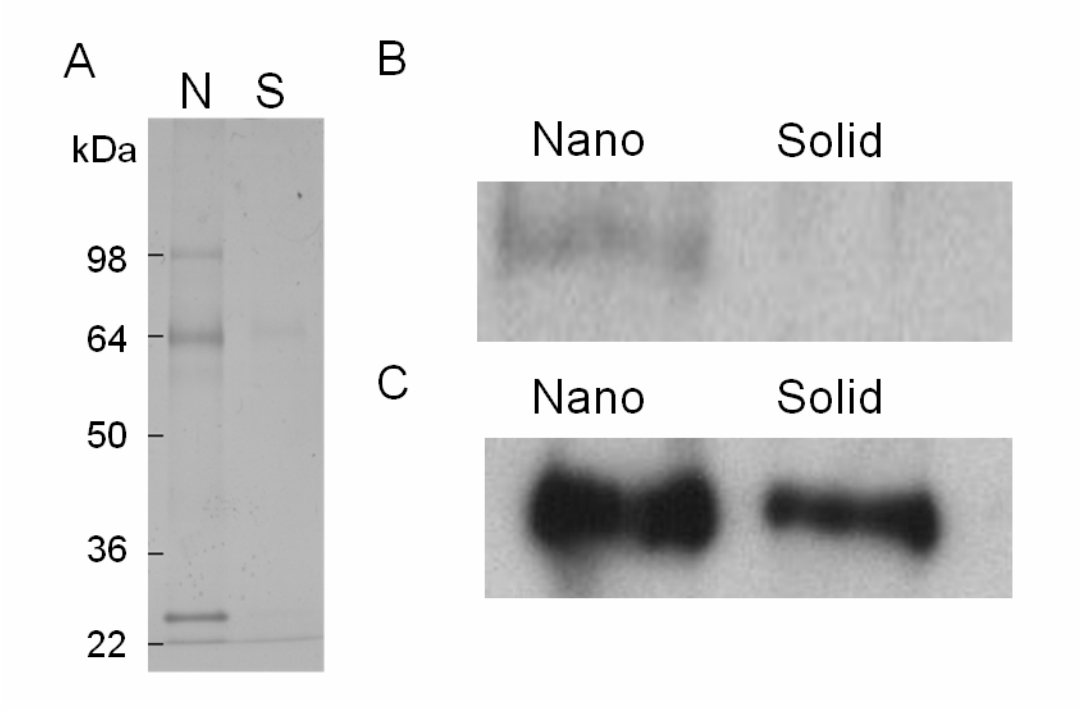

Figure 3.4: Protein adsorption to materials after exposure to differentiation media containing 20% bovine serum protein or purified bovine fibronectin(100μg/ml) for 1 hr: (A) 4-12% polyacrylamide gels stained with Coomassie blue from protein extracts from nanofibrous matrix (N) and flat (solid) films (S) treated with media; (B) western blot of fibronectin extracted from nanofibrous matrix (Nano) and flat (solid) films (Solid) treated with media; (C) western blot of fibronectin extracted from nanofibrous matrix (Nano) and flat (solid) films (Solid) treated with purified bovine fibronectin.

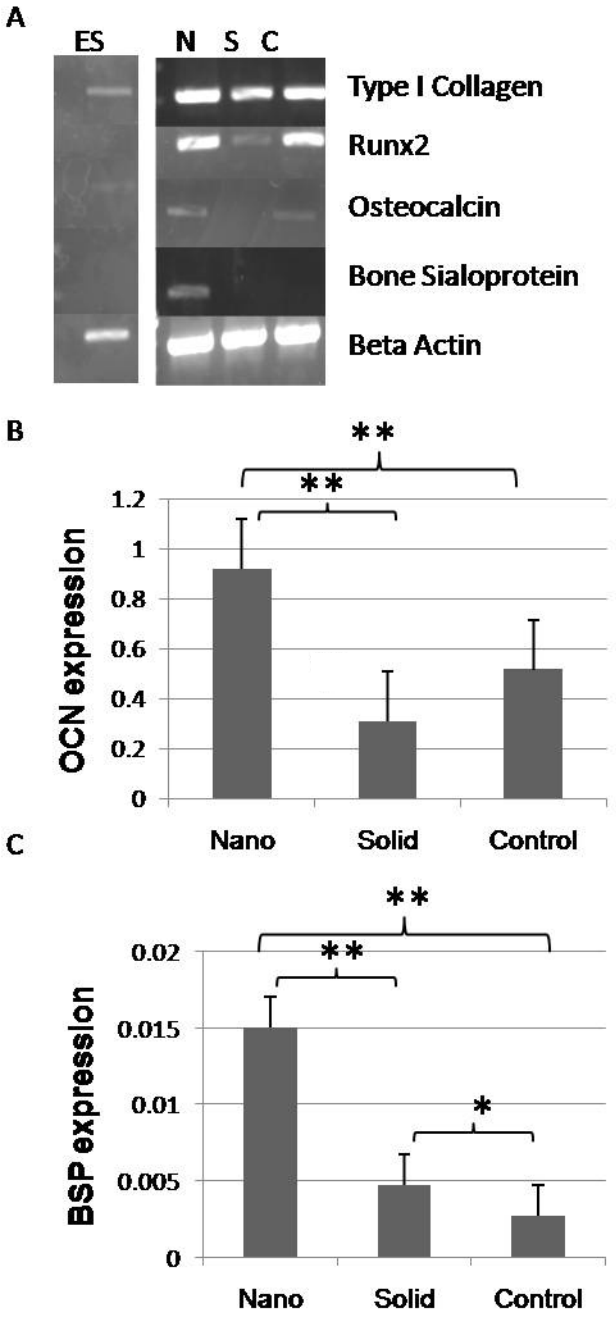

Figure 3.5: Expression of osteogenic markers after 26 days of culture under osteogenic differentiation conditions: (A) PCR of RNAs isolated from cells grown on nanofibrous matrix (N), flat (solid) films (S) and gelatin coated tissue culture plastic (C); (B) quantitative PCR of bone sialoprotein RNAs isolated from cells grown on nanofibrous matrix (Nano), flat (solid) films (Solid) and gelatin coated tissue culture plastic (Control) * denotes p-value <0.05; (C) quantitative PCR of osteocalcin RNAs isolated from cells grown on nanofibrous matrix (Nano), flat (solid) films (Solid) and gelatin coated tissue culture plastic (Control) * denotes p-value <0.05; ** denotes p-value <0.01.

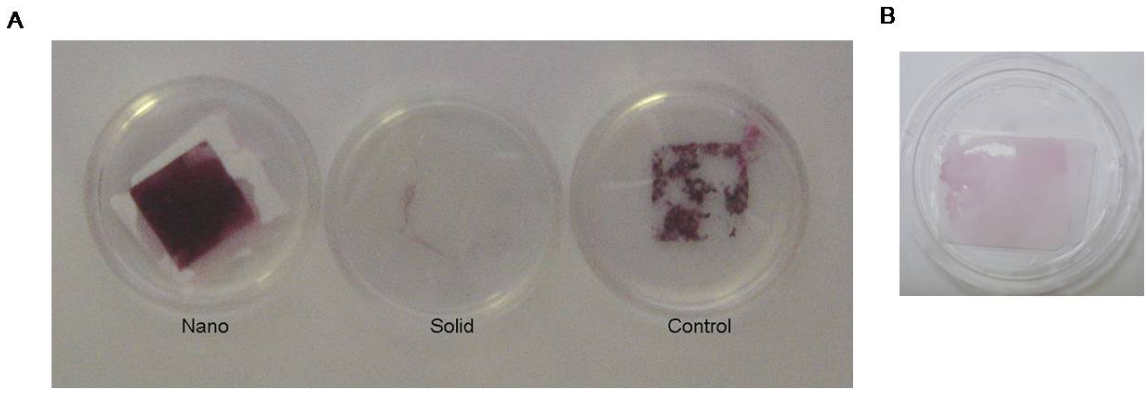

Figure 3.6: Mineralization characterization after 26 days of culture under osteogenic differentiaion conditions (A) Calcium staining after 26 days under osteogenic differentiation conditions on nanofibrous matrix (Nano), flat (solid) films (Solid) and gelatin coated tissue culture plastic (Control); (B) Calcium staining after 26 days under osteogenic differentiation conditions on nanofibrous matrix without ESC.

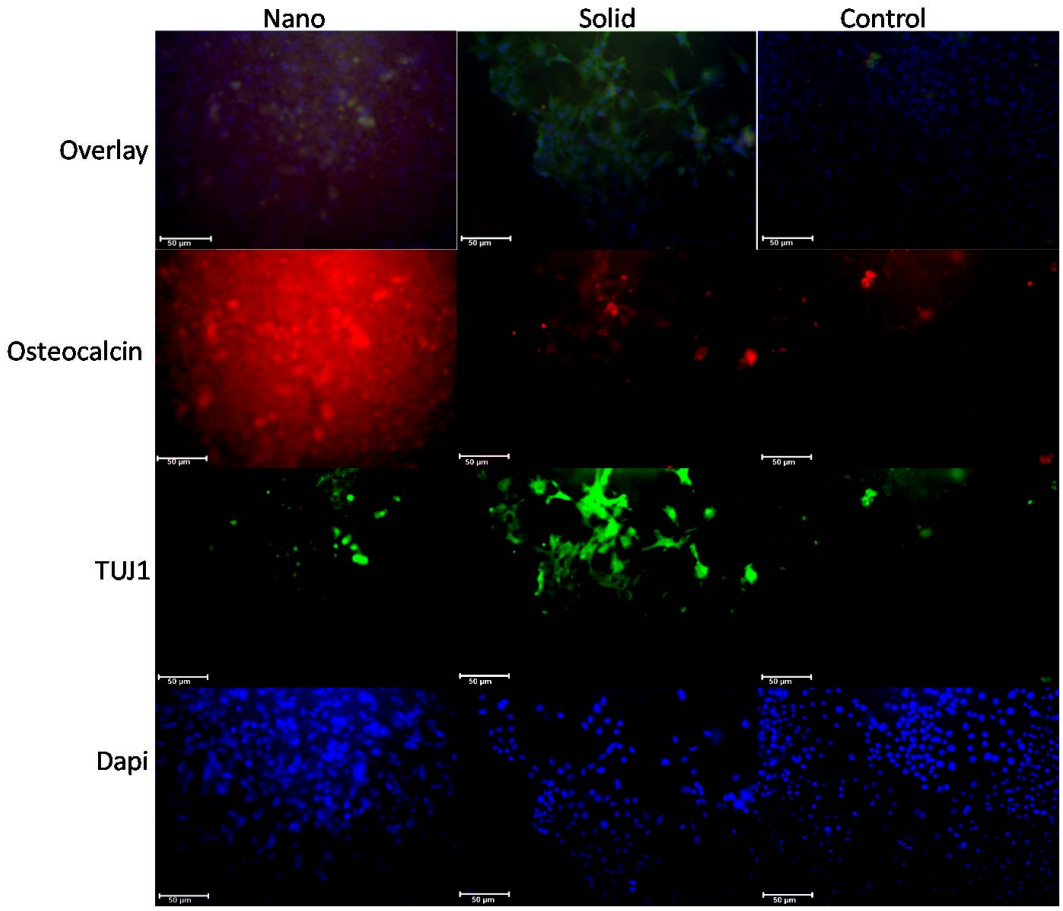

Figure 3.7: Immunofluorescence localization of neuronal (TUJ1) and late bone differentiation (Osteocalcin) Marker expression after 26 days under osteogenic differentiation conditions on nanofibrous matrix (Nano), flat (solid) films (Solid) and gelatin coated tissue culture plastic (Control). Scale bar =50μm.

3.6 References

1. Martin, G.R. Isolation of a pluripotent cell line from early mouse embryos cultured in medium conditioned by teratocarcinoma stem cells. Proc Natl Acad Sci USA, 1981. **78**: p. 7634-7638.

2. Evans, M.J. and M.H. Kaufman. Establishment in culture of pluripotential cells from mouse embryos. Nature, 1981(292): p. 154-156.

3. Guillot, P.V., W. Cui, N.M. Fisk, and D.J. Polak. Stem cell differentiation and expansion for clinical applications of tissue engineering. J Cell Mol Med, 2007. **11**: p. 935-944.

4. McCloskey, K., M. Gilroy, and R. Nerem. Use of Embryonic Stem Cell-Derived Endothelial Cells as a Cell Source to Generate Vessel Structures in vitro. Tissue engineering, 2005. **11**: p. 497-505.

5. Ke, Q., Y. Yang, J. Rana, C. Yu, J. Morgan, and X. Yong-Fu. Embryonic stem cells cultured in biodegradable scaffold repair infarcted myocardium in mice. Acta Physiologica Sinica, 2005. **57**: p. 673-681.

6. Chaudhry, G., D. Yao, A. Smith, and A. Hussain. Osteogenic Cells Derived from Embryonic Stem Cells Produced Bone Nodules in Three-Dimensional Scaffolds. Journal of Biomedicine and Biotechnology, 2004. **4**: p. 203-310.

7. Randle, W.L., J.M. Cha, Y.S. Hwang, K.L. Chan, S.G. Kazarian, J. Polak, and A. Mantalaris. Integrated 3-dimensional expansion and osteogenic differentiation of murine embryonic stem cells. Tissue engineering, 2007. **13**: p. 2957-2970.

8. Buttery, L., S. Bourne, J. Xynos, H. Wood, F. Hughes, S. Hughes, V. Episkopou, and J. Polak. Differentiation of Osteoblasts and in vitro bone formation of murine embryonic stem cells. Tissue engineering, 2001. **7**: p. 89-99.

9. Kramer, J., F. Bohrnsen, P. Schlenke, and J. Rohwedel. Stem Cell-Derived Chondrocytes for Regenerative Medicine Transplantation Proceedings, 2006. **38**: p. 762-765

10. Lavon, N. and N. Benvenisty. Study of hepatocyte differentiation using embryonic stem cells. J Cell Biochem, 2005. **96**: p. 1193-1202.

11. Hall, B. and T. Miyake. Divide, accumulate, differentiate: cell condensation in skeletal development revisited. Int. J. Dev. Biol., 1995. **39**: p. 881-893.

12. Aszodi, A., J.F. Bateman, E. Gustafsson, R. Boot-Handford, and R. Fassler. Mammalian Skeletogenesis and Extracellular Matrix: What can We Learn from Knockout Mice? Cell Struct Funct, 2000. **25**: p. 73-84.

13. MacDonald, M. and B. Hall. Altered Timing of the Extracellular-Matrix-Mediated Epithelial-Mesenchymal Interaction That Initiates Mandibular Skeletogenesis in Three Inbread Strains of Mice: Development, Heterchrony and Evolutionary Change in Morphology. J Exp Zool, 2001. **291**: p. 258-273.

14. Ma, P.X. Biomimetic materials for tissue engineering. Adv Drug Deliv Rev, 2008. **60**: p. 184-189.

15. Elsdale, T. and J. Bard. Collagen substrata for studies on cell behavior. J cell biology, 1972. **54**: p. 626-637.

16. Birk, D.E., F.H. Silver, and R.L. Trelstad. Matrix Assembly, in *Cell Biology of the Extracellular Matrix*, H.E. D. Editor. 1991, Plenum Press: New York.

17. Ma, P.X. and R. Zhang. Synthetic nano-scale fibrous extracellular matrix. Biomed Mater Res, 1999. **46**: p. 60-72.

18. Chen, V. and P.X. Ma. Nano-fibrous poly(L-lactic acid) scaffolds with interconnected spherical macropores. Biomaterials, 2004. **25**: p. 2065-2073.

19. Woo, K.M., V.J. Chen, and P.X. Ma. Nano-fibrous scaffolding architecture selectively enhances protein adsorption contributing to cell attachment. J Biomed Mater Res, 2003. **67A**: p. 531-537.

20. Chen, V., L. Smith, and P.X. Ma. Bone regeneration on computer-designed nano-fibrous scaffolds. Biomaterials, 2006. **27**: p. 3973-3979.

21. Zhang, R. and P.X. Ma. Synthetic nano-fibrillar extracellar matrices with predesigned macroporous architectures. J Biomedi Mater Res, 2000. **52**: p. 430-438.

22. Doetschman, T., H. Eistetter, M. Katz, W. Schmidt, and R. Kemler. The in vitro development of blastocyst-derived embryonic stem cell lines: formation of visceral yolk sac, blood island and myocardium. J Embryol Exp Mophol, 1985. **87**: p. 27-45.

23. Xiao, G., D. Wang, D. Benson, G. Karsenty, and R.T. Franceschi. Role of the a2-Integrin Osteoblast-specific Gene Expression and Activation of the OSF2 Transcription Factor. J Biol Chem, 1998. **273**: p. 32988-32994.

24. Rohwedel, J., K. Guan, and W. Zuschratter. Loss of Beta 1 integrin function results in a retardation of myogenic, but an acceleration of neuronal, differentiation of embryonic stem cells in vitro. Del Biol, 1998. **201**(167-184).

25. Siebers, M., P. ter Brugge, X. Walboomers, and J. Jansen. Integrins as a linker protein between osteoblasts and bone replacing materials. A critical review. Biomaterials, 2005. **26**(2): p. 137-146.

26. Sutherland, A.E., C.P. G, and C.H. Damsky. Developmental regulation of integrin expression at the time of implantation in the mouse embryo. Development, 1993. **119**: p. 1175-1185.

27. Mizuno, M., R. Fujisawa, and Y. Kuboki. Type I collagen-induced osteoblastic differentiation of bone-marrow cells mediated by collagen-alpha2beta1 integrin interaction. J Cell Physiol, 2000. **184**: p. 207-213.

28. Hayashi, Y., M.K. Furue, T. Okamoto, Y. Myoishi, Y. Fukuhara, T. Abe, J.D. Sato, R.I. Hata, and M. Asashima. Integrins Regulate Mouse Embryonic Stem Cell Self-Renewal. Stem Cells, 2007. **25**: p. 3005-3015.

29. Jikko, A., S.E. Harris, D. Chen, D.L. Mendrick, and C.H. Damsky. Collagen Integrin Receptors Regulate Early Osteoblast Differentiation Induced by BMP-2. J Bone Miner Res, 1999. **14**: p. 1075-1083.

30. Vats, A., N. Tolley, A. Bishop, and J. Polak. Embryonic stem cells and tissue engineering: delivering stem cells to the clinic. J R Soc Med 2005. **98**(8): p. 346-350.

31. Fleming, R., C. Murphy, G. Abrams, S. Goodman, and P. Nealey. Effects of synthetic micro-and nano-structured surfaces on cell behavior. Biomaterials, 1999. **20**: p. 573-588.

32. Keselowsky, B.G., L. Wang, Z. Schwartz, A.J. Garcia, and B.D. Boyan. Integrin alpha(5) controls osteoblastic proliferation and differentiation responses to titanium substrates presenting different roughness characteristics in a roughness independent manner. J Biomed Mater Res A, 2007. **80**: p. 700-710.

33. Lim, J.Y., J.C. Hansen, C.A. Siedlecki, J. Runt, and H.J. Donahue. Human foetal osteoblastic cell response to polymer-demixed nanotopographic interfaces. J R Soc Interface, 2005. **22**: p. 97-108.

34. Woo, K., J.-H. Jun, V. Chen, J. Seo, J.-H. Baek, H.-M. Ryoo, G.-S. Kim, M. Somerman, and P. Ma. Nano-fibrous scaffolding promotes osteoblast differentiation and biomineralization. Biomaterials, 2007. **28**(2): p. 335-343.

35. Khatiwala, C.B., S.R. Peyton, and A.J. Putnam. Intrinsic mechanical properties of the extracellular matrix affect the behavior of pre-osteoblastic MC3T3-E1 cells. Am J Physiol Cell Physiol, 2006. **290**: p. C1640-C1650.

36. Khatiwala, C.B., S.R. Peyton, M. Metzke, and A.J. Putnam. The Regulation of Osteogenesis by ECM Rigidity in MC3t3-E1 Cells Requires MAPK Activation. J Cell Physiol, 2007. **211**: p. 661-672.

37. Engler, A.J., S. Sen, H.L. Sweeney, and D.E. Dishcer. Matrix Elasticity Directs Stem Cell Lineage Specification. Cell, 2006. **126**: p. 677-689.

38. Weiss, R. and A. Reddi. Role of Fibronectin in collagenous matrix-induced mesenchymal cell proliferation and differentiation in vivo. Exp Cell Res, 1981. **133**: p. 247-254.

39. Cowles, E., M. DeRome, G. Pastizzo, L. Brailey, and G. Gronowicz. Mineralization and the Expression of the Matrix Proteins During In Vivo Bone Development. Calcif Tissue Int, 1998. **62**: p. 74-82.

40. Yang, J.T., B.L. Bader, J.A. Kredberg, M. Ullman-Cullere, J. Trevithick, and R.O. Hynes. Overlapping and Independent Functions of Fibronectin Receptor Integrins in Early Mesodermal Development. Developmental Biology, 1999. **215**: p. 264-277.

41. Watt, F. and B. Hogan. Out of Eden: Stem Cells and their Niches. Science, 2000. **287**: p. 1427-1430.

42. Czyz, J. and A. Wobus. Embryonic stem cell differentiation: The role of extracellular factors. Differentiation, 2001. **68**: p. 167-174.

43. Tulla, M., O.T. Pentikainen, T. Viitasalo, J. Kapyla, U. Impola, P. Nykvist, L. Nissinen, M.S. Johnson, and J. Heino. Selective binding of collagen subtypes by integrin alpha 1I, alpha 2I, and alpha 10I domains. J Biol Chem, 2001. **276**: p. 48206-48212.

44. Kapyla, J., J. Ivaska, R. Riikonen, P. Nykvist, O. Pentikainen, M.S. Johnson, and J. Heino. Integrin alpha(2)I domain recognizes type I and type IV collagens by different mechanisms. J Biol Chem, 2000. **275**: p. 3348-3354.

45. Hu, J., X. Liu, and P.X. Ma. Induction of osteoblast differentiaion phenotype on poly(L-lactic acid) nanofibrous matrix. Biomaterials, 2008. **29**: p. 3815-3821.

Chapter 4

Osteogenic Differentiation of Mouse Embryonic Stem Cells on Nanofibrous Scaffolds

4.1 Introduction

Over the past 10 years, the number of surgical procedures to correct bone defects has been increasing[1]. Currently, these procedures utilize autografts, allografts or metallic and ceramic implants to correct the bone defect. Each of these options has its own drawbacks such as donor site morbidity, pathogen transmission, and mismatching material properties with those of the native bone respectively[2, 3]. As an alternative to these procedures, tissue engineering has emerged to create de novo tissue by growing cells on three-dimensional(3-D) scaffolding [4, 5]. Ideally, this scaffolding should recapitulate the key structural and biochemical signals of the tissue's natural extracellular matrix (ECM)[6], which is primarily composed of type I collagen in bone. Several fabrication methods are capable of mimicking the size scale of type I collagen[7], however most are incapable of incorporating a designed 3-D macro pore structure. We

have developed a synthetic nanofibrous (NF) scaffold capable of generating well-defined anatomical shapes and pore structures[8].

Once a bone defect reaches a certain size, cells in addition to the scaffolds are required to generate functional tissue. Currently, most cells used for this type of tissue engineering are isolated from an autologous source[9]. This yields a limited number of cells that may lose the ability to generate the desired tissue during expansion culture prior to seeding on the scaffolding. Embryonic stem cells (ESC) represent a potential advance in cell sourcing for tissue engineering because they proliferate longer than other types of stem cells and possess the ability to differentiate to any tissue type within the body.

Although nano-scale architecture affects cellular proliferation, migration, and orientation[10], few studies have examined the effects of these architectures on ESC[11, 12]. Most studies using ESC for tissue engineering have focused simply on the addition of biochemical cues to control ESC differentiation[13-16]. However, during embryonic development both the ECM and the biochemical cues play a vital role in tissue development[17]. In this study, we will examine the effects of both the NF architecture and biochemical cues on both two dimensional (2-D) thin matrices or films, and 3-D scaffolds in vitro to assess their combined effect on the osteogenic differentiation of ESC compared to flat (solid) films and more traditional solid-walled (SW) scaffolds.

4.2 Materials and Methods

Poly(L-lactic acid) (PLLA) with an inherent viscosity of 1.6 dl/g was purchased from Alkermes (Medisorb, Cambridge, Massachusetts) and used without further purification. Wax and polysulphonamide for 3-D printing were purchased from

Solidscape Inc. (Merrimack, New Hampshire). Cyclohexane, dioxane, ethanol, hexane, and methanol were purchased from Fisher Scientific (Pittsburgh, Pennsylvania). Dubecco's Modified Eagle Media (DMEM), 0.5M EDTA, trypsin, Hank's buffered salt solution (HBSS) and PCR primers were obtained from Invitrogen (Carlsbad, CA). Fetal Bovine Serum was obtained from Harlan Biological (Indianapolis, IN). Human recombinant leukemia inhibitory factor (LIF), and Neuronal Class III β-Tubulin (TUJ1) antibody and goat serum were obtained from Sigma (St. Louis, MO). Human transforming growth factor-beta1 (TGF-β1), insulin-like growth factor I (IGF) and bone morphogenic protein-2 (BMP-2) were obtained from Peprotech (Rocky Hill, New Jersey). Osteocalcin antibody and all secondary antibodies were obtained from Santa Cruz Biotechnology (Santa Cruz, CA). RNeasy Mini Kit and Rnase-Free DNase set were obtained from Qiagen (Valencia, California). TaqMan reverse transcription reagents, real-time PCR primers, and TaqMan Universal PCR Master mix were obtained from Applied Biosystems (Foster City, California). Chemicals were obtained from Sigma Chemical Co. (St. Louis, MO) unless otherwise noted.

4.2.1 2-D Thin Matrix and Film Preparation for Cell Culture

PLLA was dissolved in tetrahydrofuran at 60^{o}C to make a 10% (wt/v) PLLA solution. The NF PLLA matrix (thickness~40μm) was fabricated by first casting 0.4 mL of the PLLA solution on a glass support plate which had been pre-heated at 45^{o}C for 10 min and then sealing the polymer solution on the glass support plate by covering it with another pre-heated glass plate. The polymer solution was phase separated at -20°C for 2 hrs and then immersed into ice-water mixture to exchange tetrahydrofuran for 24 hrs. The

matrix was washed with distilled water at room temperature for 24 hrs with water changed every 8 hrs. The matrix was then freeze-dried.

The matrices were cut to fit into a 35 mm Petri dish and secured in place with a disk of silicone elastomer from Dow Corning (Midland, MI) containing a 1.5 mm by 1.5 mm opening. The matrices were then sterilized with ethylene oxide, wet with HBSS 2 times for 0.5hrs each and rinsed with differentiation media (DMEM supplemented with 20% FBS, 10^{-4}M β-mercaptoethanol, and 1.33μg/ml HEPES) for 1hr.

PLLA thin flat (solid) films were fabricated in a similar manner excluding the phase separation step. Instead, the solvent was evaporated at room temperature in a fume hood. The thin flat (solid) films were then treated similarly to the NF matrices.

4.2.2 3-D Scaffold Preparation for Cell Culture

Scaffolds were fabricated as previously described[8]. Briefly, negative molds were designed and converted into stereolithography data using Rhinoceros software (Robert McNeel & Associates, Seattle, Washington), and then imported into Modelworks software (Solidscape) to convert the files for 3-D printing. Molds were fabricated in a layer-by-layer fashion with the molten wax and polysulphonamide printed separately using a Modelmaker II (Solidscape). The polysulphonamide was dissolved in ethanol.

External dimensions of the scaffolds were (LxWxH) 6.6×6.6×2.45 mm. Internally, the scaffold contains partially overlapping orthogonally stacked layers (thickness) of parallel rectangular open channels with dimensions of (WxH) 400×300 μm and closed struts of (WxH) 350×300 μm.

For NF scaffolds, a 9% (wt/v) solution of PLLA in 4:1 (v/v) dioxane:methanol was stirred at 60 °C until homogeneous. Dioxane was dripped into the mold to wet the wax surface, the polymer solution was cast into the mold, and the polymer/mold composite was phase separated overnight at −20 °C. The solvent was extracted with cold ethanol (−20 °C) for 1 d and ice-cold water for 1 d. Excess polymer was trimmed with a razor blade, and the polymer/mold composite was washed in 37 °C cyclohexane to dissolve the wax mold, followed by washings in 37 °C ethanol and water, and subsequent freeze-drying.

For SW scaffolds, a 9% (wt/v) PLLA/dioxane solution was similarly cast and phase separated. The polymer/mold composites were lyophilized at −5 to −10 °C to sublimate dioxane crystals. Excess polymer was trimmed with a razor blade and wax molds were dissolved similarly to those in NF samples.

4.2.3 D3 Culture and Seeding

D3 mouse ESC[18] were cultured on 0.1% gelatin-coated tissue culture flasks in ESC media (DMEM supplemented with 10% FBS, 10^{-4}M β-mercaptoethanol, 0.224 µg/ml L-glutamine, 1.33 µg/ml HEPES, and 1,000 units/ ml human recombinant LIF). Media formulations used are contained in Table 1.

Embryoid bodies (EBs) were formed by seeding $3x10^6$ cells into a 60 mm polystyrene dish containing EB media (ESC media without LIF supplement and with the addition of 1 µM dexamethasone, 50 mg/mL ascorbic acid and 10 mM β-glycerol phosphate in osteogenic cultures). The media was changed every 2 to 3 days. After 5 days, EBs were dissociated with 0.25% trypsin/ 1mM EDTA. $1.5x10^5$ EB-derived cells

were seeded on each of the prepared 2-D matrices, films or 0.1% gelatin-coated tissue culture dish controls, while 2 x10^6 EB-derived cells where seeded onto each 3-D scaffold. Upon seeding, cells were cultured in differentiation media, osteogenic media, BMP media or TBI media (Table 1 contains media formulations). TBI media was used unless otherwise stated. On the thin matrices and controls the media was changed 12 hrs after seeding and then every other day for the remainder of the culture period. For scaffolds, the media was changed every 12 hrs for 72 hrs. The scaffolds were then transferred from the Telfon seeding trays to 6-well plates and the media was changed every other day.

4.2.4 PCR and Real Time PCR

Total RNA was isolated using an RNeasy Mini Kit with Rnase-Free DNase set according to the manufacturer's protocol after thin matrices and scaffolds were mechanically homogenized with a Tissue-Tearor (BioSpec Products, Bartlesville, OK) while cells cultured on gelatin-coated tissue culture plate controls were harvested with a cell scraper. The cDNA was made using a Geneamp PCR (Applied Biosystems) with TaqMan reverse transcription reagents and 10 min incubation at 25 °C, 30 min reverse transcription at 48 °C, and 5 min inactivation at 95 °C. 5μL of each reaction was subject to PCR using AmpliTaq Gold DNA polymerase (Applied Biosystems) for each of the following: collagen type I (5'-gaagtcagctgcatacac-3' and 5'-aggaagtccaggctgtcc-3'); runx2 (5'-ccgcacgacaaccgcaccat-3' and 5'-cgctccggcccacaaatctc-3'); bone sialoprotein (5'- gtcaacggcaccagcaccaa-3' and 5'-gtagctgtattcgtcctcat-3'); osteocalcin (5'-cggccctgagtctgacaaa-3' and 5'-accttattgccctcctgcctt-3') and β actin (5'-caggattccatacccaagaag-3' and 5'- aaccctaaggccaaccgtg-3'). The conditions were: 94°C

for 5mins followed by 94°C for 30s, 55°C for 60s, 72°C for 60s 35 cycles for β actin, and 94°C for 30s, 55°C for 60s, 72°C for 60s 30 cycles for runx2, bone sialoprotein, and osteocalcin. These amplifications were followed by a 10min extension at 72°C.

Real-time PCR was set up using TaqMan Universal PCR Master mix and specific primer sequence for collagen type I, runx2, bone sialoprotein, osteocalcin and β actin with 2 min incubation at 50 °C, a 10 min Taq Activation at 95 °C, and 50 cycles of denaturation for 15 s at 95 °C followed by an extension for 1 min at 72 °C on an ABI Prism 7500 Real-Time PCR System (Applied Biosystems). Expression of target genes was normalized against β actin.

4.2.5 Immunofluorescence and Histological Staining

Cells growing on NF matrices, flat (solid) films and gelatin coated tissue culture plastic controls were fixed in 2% paraformaldehyde/PBS, washed, and stored at 4°C in PBS. For histological analysis, cells grown on scaffolds were fixed in 10% neutral buffered formalin solution (Sigma, St. Louis, Missouri), dehydrated through an ethanol gradient, and embedded in paraffin. Samples were cut at 5 μm. The paraffin was dissolved with xylene and the sections were rehydrated through an ethanol gradient. The sections were then incubated in 0.5% pepsin for 10min at 30°C for antigen retrieval. Nonspecific antibody binding was blocked by incubating in 10% goat serum, then the matrices and control were exposed to TUJ1 (1:250) or osteocalcin (1:50) antibodies, followed by appropriate secondary antibodies conjugated to FITC (TUJ1) or TRITC (ostoecalcin). DAPI was used to stain cell nuclei.

For Alizarin Red S staining, the matrices, controls, and scaffold sections were fixed by the same method and then stained with 40mM Alizarin Red S solution, pH 4.2 at room temperature for 10min. Thin matrices and controls were then rinsed 5 times in distilled water and washed 3 times in PBS on an orbital shaker at 40rpm for 5 minutes each to reduce nonspecific binding. Scaffold sections were dehydrated in acetone and rinsed in xylene before mounting with permamount. Scaffold sections were also stained with hematoxylin and eosin-phloxine.

4.2.6 Western Blotting Analysis

Scaffolds were treated with ethanol and PBS as described above for cell culture. Scaffolds were then incubated with cell culture medium or FBS. Scaffolds were quickly washed with PBS for 2 times (1 min each), cut into pieces and transferred to 1.5ml tubes. 600ul PBS was added, and the scaffolds were washed for three times. PBS was removed, and the scaffolds were centrifuged for 1min at 12,000rpm for 2 times to remove any liquid remained. 100µl 1% SDS was added and incubated for 1hr, then it was repeated twice. The 3 samples were pooled to form a total collection sample of 300µl. For microBCA (Pierce, Rockford, IL), 50µl of the collection sample was used (n=3), while 30 µl of the collection sample was used for each gel. Western blot analysis was conducted as previously described[19]. Briefly, the recovered serum protein samples were subject to fractionation through 4-12% SDS-polyacrylamide gel electrophoresis (PAGE). The fractionated proteins were transferred to a PVDF membrane (Sigma). The blots were washed with TBST (10 m*M* Tris-HCl, 150 m*M* NaCl, 0.05% Tween-20, pH 8.0), and blocked with Blotto (5% nonfat milk in TBST) at room temperature for 1 h. The

blots were incubated in anti-bovine fibronectin polyclonal antibody (Santa Cruz Biotechnology, Santa Cruz, CA) at room temperature for 1 h. After being washed with TBST, the blots were incubated in anti-goat immunoglobulin G-horseradish peroxidase-conjugated antibody (Sigma), and then in chemiluminescence reagent (SuperSignal West Dura; Pierce). The relative densities of the protein bands were analyzed with QualityOne (Biorad).

4.2.7 Mineral Quantification

After 4 weeks of culture, scaffolds for mineralization quantification were washed three times for 5 min each in double-distilled water and then homogenized with a Tissue-Tearor in 1 mL of double-distilled water. Samples were then incubated in 0.5 M acetic acid overnight. The total calcium content of each scaffold was determined by the *o*-cresolphthalein-complexone method following the manufacturer's instructions (Calcium LiquiColor, Stanbio Laboratory, Boerne, Texas).

4.2.8 Collagen Quantification

The collagen content of the scaffolds was determined using a colormetric hydroxyproline quantification method[20]. Briefly, scaffolds for collagen quantification were washed three times for 5 min each in double-distilled water and then homogenized with a Tissue-Tearor in 500 μL of double-distilled water. 600 μL of 12N hydrochloric acid was added and the samples were incubated at 100-110°C for 18-24 hrs. 10 μL of methyl red was added and the samples were neutralized to a PH between 6-7 with sodium hydroxide and hydrochloric acid. 320 μL of Chloramine T assay solution was added to

640 μL of the sample, which was placed on an orbital shaker for 20min at 100rpm. 320 μL of dimethylaminobenzaldehyde assay solution was added and the samples were placed at 50°C for 30min. After which, the samples were read at 550nm. Collagen content was estimated assuming a ratio of 1 μg hydroxyproline: 7.46 μg collagen[21].

4.2.9 Statistical Analysis

All experiments were conducted at least 3 times. All quantifiable data is reported with the mean and standard deviation. Student t-tests were performed where applicable. Significance was set at a p-value of less than 0.05.

4.3 Results

After 3 weeks of culture, ESC cultured on NF matrices in basic differentiation media without the addition of any osteogenic growth factors expressed osteocalcin and bone sialoprotein (Figure 4.1). While the addition of pro-osteogenic growth factors (ascorbic acid, β-glycerolphosphate, and dexamethasone) to the media increased the expression of the bone markers in the ESC on the NF matrices, only the addition of BMP-2 to the osteogenic media lead to the expression of both osteocalcin and bone sialoprotein in the ESC cultured on the flat (solid) films and controls. However, bone sialoprotein was expressed by ESC on the flat (solid) films without osteogenic supplementation. Runx2, an early bone marker, exhibited increased expression in ESC on the NF matrices compared to the ESC on the flat (solid) films in all media. ESC on the NF matrices expressed Runx2 at a similar level to ESC on the control in diffentiation media, while ESC on the NF matrices exhibited increased Runx2 expression compared to

ESC on the control in osteogenic and BMP media. Collagen type I was expressed at a similar level on all materials in all tested media at this time. These results indicate that the NF matrices promote osteogenic differentiation which can then be enhanced by the addition of biochemical cues. However, the flat (solid) films and controls rely more on biochemical cues to drive the ESC differentiation toward the desired lineage.

ESC were then cultured on the 2-D NF thin matrices or films and 3-D scaffolds in BMP-media, which leads to the eventual osteogenic differentiation of the ESC on all thin matrices and films to examine the effects of the different culture conditions on differentiation (Figure 4.2). After 1 week of culture, Runx2, an early osteogenic marker, was expressed by ESC on the 3-D scaffolds, but not on any of the 2-D NF thin matrices and flat (solid) films until week 2 of culture. Similarly, bone sialoprotein and osteocalcin were expressed by the ESC on the 3-D NF scaffold after 1 week of culture, but not by ESC on the 2-D NF thin matrices, 2-D flat (solid) films or the 3-D solid-walled scaffold until 2 weeks. This indicates that 3-D culture promotes osteogenic differentiation compared to 2-D culture. NF materials also expedite differentiation compared to both 2-D flat (solid) films and 3-D SW scaffold cultures.

Although BMP media leads to acceptable differentiation of ESC, it does not produce the development of tissue like cellular growth within scaffolds. To increase the production of a more tissue-like ECM, IGF-1 and TGF-β1 were added to the media to create TBI media. After 1 week of culture ESC cultured in TBI media expressed more collagen type I and osteocalcin than cells cultured in BMP media (Figure 4.3). Increased expression of collagen type I (7 times) and osteocalcin (2.6 times) in ESC cultured in TBI

media compared to BMP media continued after two weeks of culture. TBI media was therefore used in the remainder of the experiments.

After 4 weeks of culture in TBI media, the expression of bone differentiation markers was examined on scaffolds (Figure 4.4). ESC growing on NF scaffolds expressed higher levels of type I collagen (5.5 times), runx2 (5 times), bone sialoprotein (8.5 times), and osteocalcin (2.9 times) compared to those on the SW scaffolds.

The appearance of these late stage bone markers coincides with the mineralization of the matrix during bone formation. The NF thin matrices and films (Figure 4.5) were stained for calcium to examine mineral deposition on each of the surfaces. After one week of culture, there was significantly more mineralization on the NF matrices compared to the flat (solid) films. It is only after 3 weeks of culture that the flat (solid) films appear to have a similar amount of mineral to the NF matrices after one week of culture. This indicates that the NF matrices better promotes mineralization. NF matrix controls cultured in media for the same time periods without cells did not show significant calcium suggesting that the mineralization on the NF matrix is due to active cellular deposition and not biomimic absorption from the media. This indicates a more mature osteogenic cell population developed on the NF matrix than on either the flat (solid) films or the control surface and suggests that the NF matrix better promotes the differentiation of ESC toward the osteogenic lineage than the flat (solid) films or control surface.

A similar phenomenon was observed in the 3-D scaffolds (Figure 4.6A), where the NF scaffolds mineralized to a greater degree and more quickly than the SW scaffolds. Upon quantification, NF scaffolds were found to contain 3 times more calcium than the

SW scaffolds after 4 weeks of culture (Figure 4.6B). NF scaffolds were also found to contain over 3 times more collagen than the SW scaffolds after 4 weeks of culture (Figure 4.6C).

Additionally, after 2 weeks of culture, ESC were found to be distributed throughout the NF scaffold while the ESC on the SW scaffold were still primarily in embryoid bodies and not directly interacting with the scaffolds (Figure 4.7). After 4 weeks of culture the ESC on the SW scaffolds did associate with the scaffolds like the ESC on the NF scaffolds at both 2 and 4 weeks (Figure 4.7). However, the ESC on the SW scaffold did not express osteocalcin in the center regions of the scaffold as strongly as the ESC on the NF scaffolds at either time point.

A previous study found that differences in the amount of protein adsorbed from the media on the NF matrices compared to that on the flat (solid) films[22], which could contribute to the differences in osteogenic differentiation on substrates with different the architectures. The initial microenvironment created by protein adsorption from the medium was examined on the scaffolds to see if a similar trend occurs. The NF scaffolds were found to adsorb significantly more protein from the media than the SW scaffolds (Figure 4.8A). Western blots for fibronectin on NF scaffolds exposed to serum-containing media (differentiation media) or pure fetal bovine serum were shown to adsorb more fibronectin than similarly treated solid scaffolds (Figure 4.8B).

4.4 Discussion

ESC hold great promise as a tissue engineering cell source. However, their ability to form multiple lineages must be contained and the ESC must be directed toward only

the lineages needed for the desired tissue[23-25]. In bone, the development process involves ECM proteins, growth factors, signaling molecules, hormones and transcription factors in a temporary and spatially organized process[17, 26]. In this study we examine the effects of NF materials and biochemical cues in 2-D and 3-D on the osteogenic differentiation of ESC compared to SW materials.

Through mimicking the ECM, 2-D NF matrices without osteogenic supplements are able to induce osteogenic differentiation, while flat (solid) films require both osteogenic supplements and growth factors to achieve the same results. The NF matrices may provide a better niche for ESC osteogenesis due to improved protein adsorption from the serum[22]. Fibronectin, the earliest of the bone matrix proteins synthesized by osteoblasts, is thought to play an important role particularly in early osteogenesis[27, 28]. A previous study found that NF scaffolds adsorb nearly 4 times more fibronectin than their SW counterparts[29], which may contribute to increased differentiation on NF scaffolds without the addition of osteogenic factors.

The addition of osteogenic supplements and growth factors enhanced the osteogenic differentiation on all materials tested illustrating that signaling molecules play an important role in the lineage selection process. This differentiation was further enhanced on NF scaffolds (Figure 4.3) by crudely mimicking the temporal expression of growth factors (TGF- β1, BMP-2 and IGF-1) during development. During skeletogenesis, TGF-β1 induces cells to migrate along ECM molecules such as fibronectin to bone formation sites[30]. After the migration, TGF-β1 then promotes cellular proliferation and ECM production during development[31]. BMP-2 is essential in limb patterning and is thought to induce commitment to osteoprogenitors[32].

Following this, IGF-1 plays a pivotal role in longitudinal bone growth during development[33] and has been shown to increase collagen type I in the ECM[34]. Although these additional growth factors have been shown to enhance the osteogenic differentiation, additional study is needed to identify the optimal combinations of growth factors for the directed osteogenic differentiation of ESC.

During embryogenesis, cell-cell interactions are thought to contribute to cell lineage differentiation[35]. The stimulation of these cellular communication pathways through 3-D culture on the scaffolds may explain the enhanced differentiation in 3-D culture compared to 2-D culture. However, for functional bone formation further work is needed to determine the optimal 3-D culture conditions.

Previous studies with pre-osteoblasts showed enhanced differentiation and tissue formation on NF scaffolds compared to SW scaffolds[8, 36]. As the NF architecture was designed to mimic collagen type I, which modulates osteoblast behavior through integrin interactions[37, 38] and adsorbs more protein from the media (Figure 4.8); additional stimulation of integrin signalling could be occurring on the NF scaffolds compared to the SW scaffolds. A previous study with NF materials found expression of α2 and β1 integrin expression to be up-regulated compared to their SW counterparts even when collagen fibril formation was inhibited, implying a direct interaction between the NF material and the cells[36]. This increased α2β1expression particularly could enhance the osteoblast differenitiation of the ESC since increased α2 integrin expression is associated with increased differentiation of ESC[39] and is considered necessary for osteogenic differentiation[40, 41], while increased β1 integrin expression has been linked to enhanced ESC mesodermal lineage commitment of ESC[42]. Additional integrins

associated with collagen and fibronectin binding are also up-regulated on NF materials compared to SW materials[36], which could further lead to enhancement of the osteogenic phenotype due to their importance in osteogenesis.

4.5 Conclusion

ESC grown on NF architecture exhibited enhanced osteogenic differentiation and mineralization compared to SW architecture. 3-D culture and supplementation of media with osteogenic growth factors further enhanced the effects of NF architecture over SW architecture on ESC differentiation. NF scaffolds with osteogenic growth factors provided the best environment for ESC osteogenic differentiation and mineralization. These findings suggest the NF scaffolds provide a suitable environment for bone tissue engineering with ESC and merit further testing.

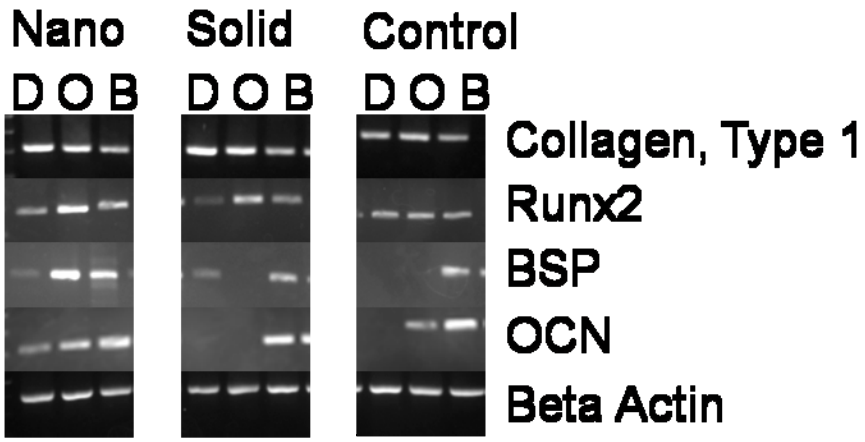

Figure 4.1: Expression of bone differentiation markers on nanofibrous thin matrices (Nano), flat films (Solid) and gelatin-coated tissue culture plastic (Control) with various media supplementations ((D) basic differentiation media, (O) osteogenic media, and (B) BMP media) after 3 weeks of culture

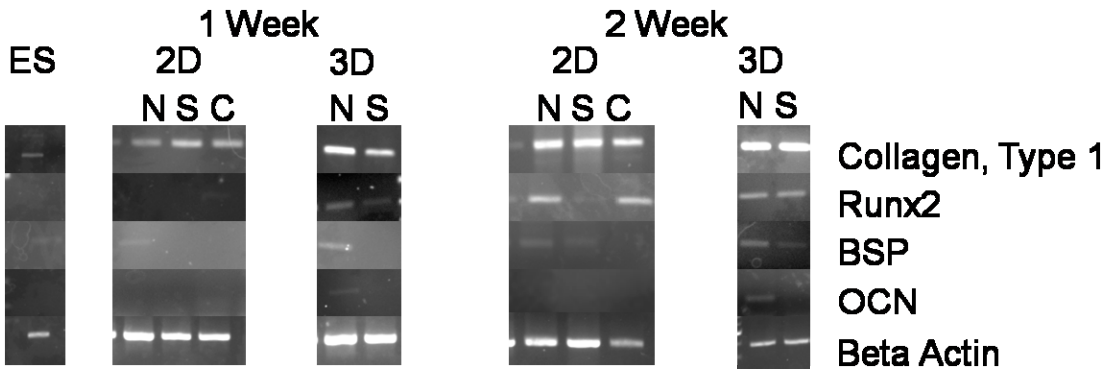

Figure 4.2: Expression of bone differentiation markers on 2D nanofibrous thin matrices (N), flat films (S) and control (C) and 3D nanofibrous (N) and solid-walled (S) scaffolds (3-D) in BMP media over 2 weeks of culture.

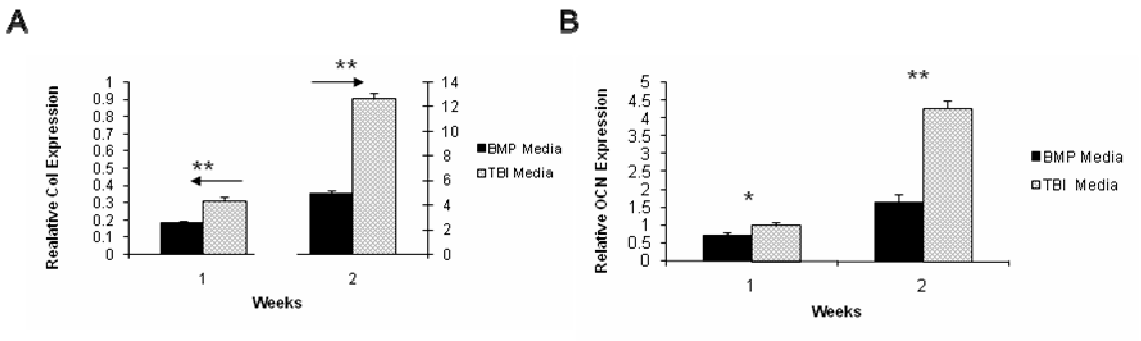

Figure 4.3: Expression of bone differentiation markers on nanofibrous scaffolds comparing cellular (A) type I collagen and (B) osteocalcin expression in BMP media and TBI media over 2 weeks. * denotes a $p<0.05$. ** denotes a $p<0.01$.

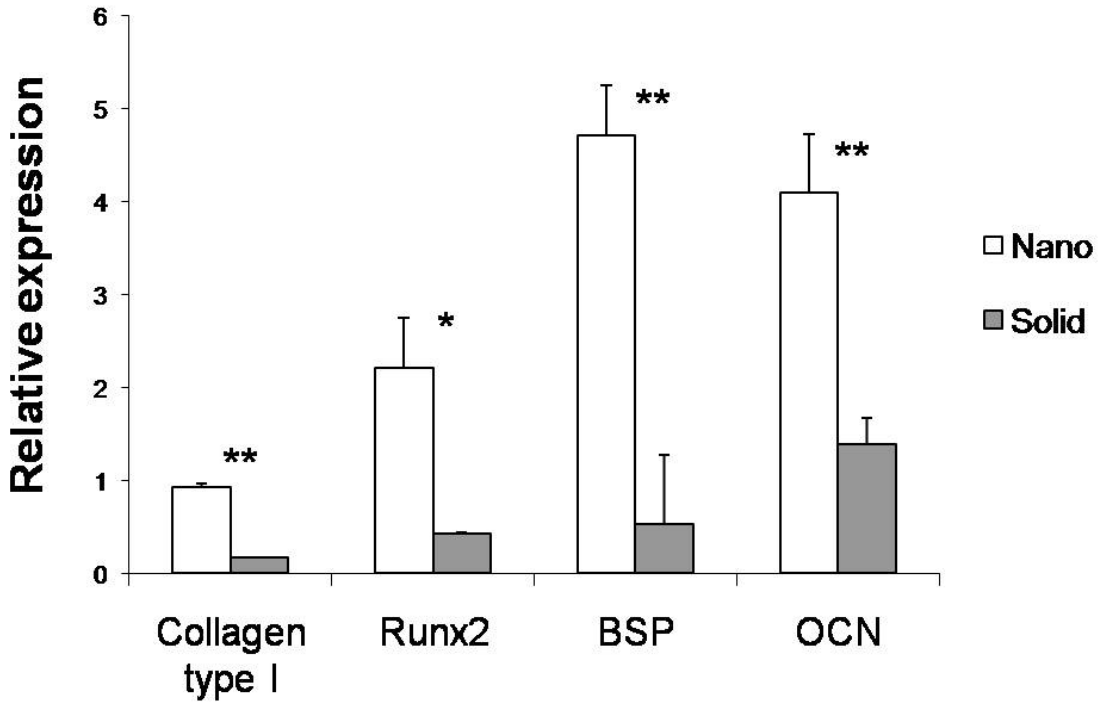

Figure 4.4: Expression of bone differentiation markers on nanofibrous (Nano) and solid-walled (Solid) scaffolds after 4 weeks of culture in TBI media. * denotes a $p<0.05$. ** denotes a $p<0.01$.

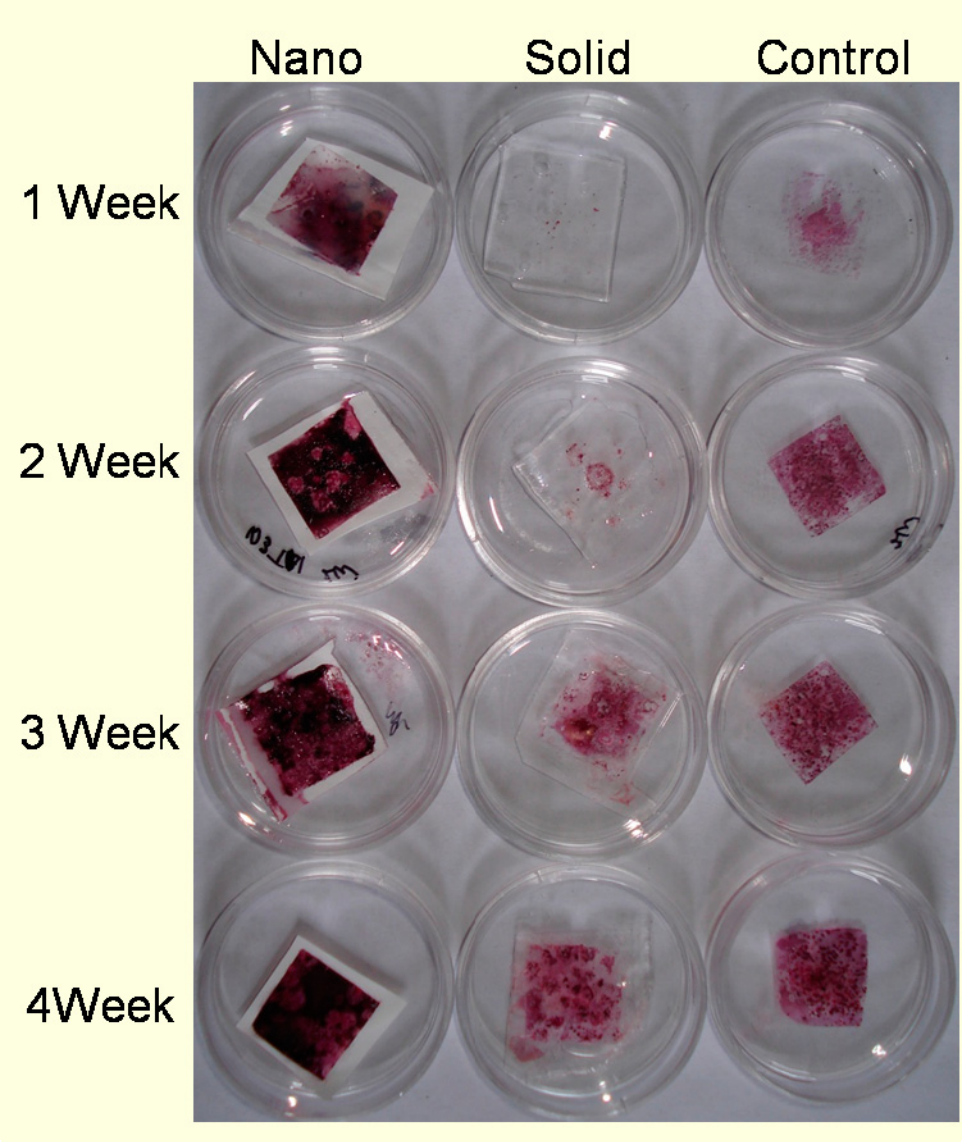

Figure 4.5: Calcium staining over 4 weeks of culture on nanofibrous matrices (Nano), flat films (Solid) and Control in TBI media.

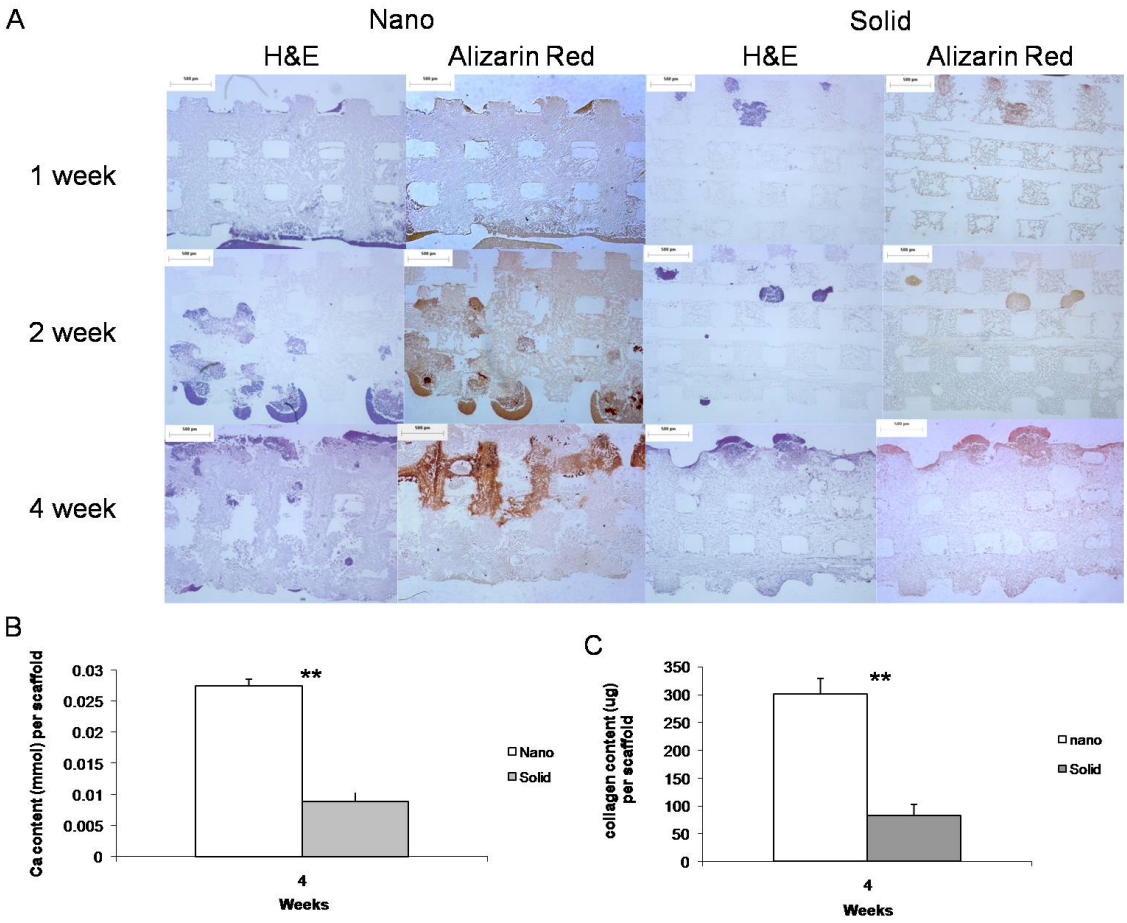

Figure 4.6: (A) Histology of cellular (H&E) and calcium (Alizarin Red) staining over 4 weeks of culture on nanofibrous (Nano) and solid-walled (Solid) scaffolds in TBI media. Scale bar =500μm. (B) Quantification of scaffold calcium content after 4 weeks of culture in TBI media. (C) Quantification of scaffold collagen content after 4 weeks of culture in TBI media. ** denotes a $p<0.01$.

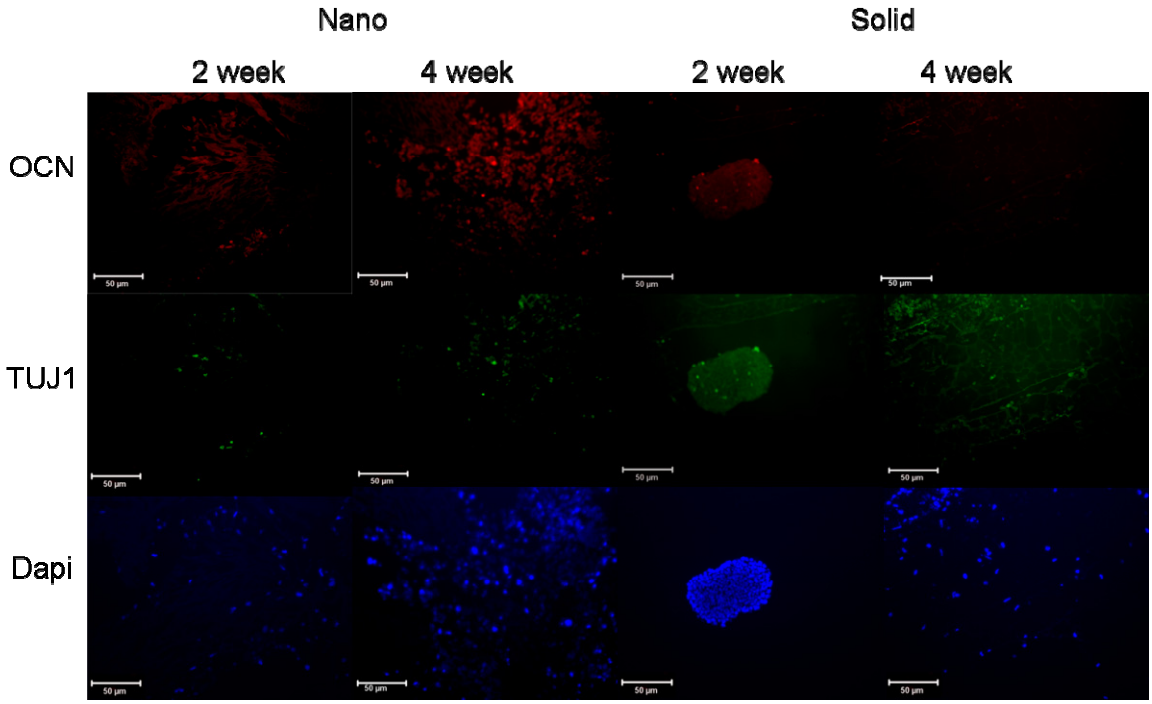

Figure 4.7: Immunofluorescence of late bone differentiation (Osteocalcin-red) and neuronal (TUJ1-green) marker expression over 4 weeks of culture in TBI media on nanofibrous (Nano), solid-walled (Solid) scaffolds. Scale bar =50µm.

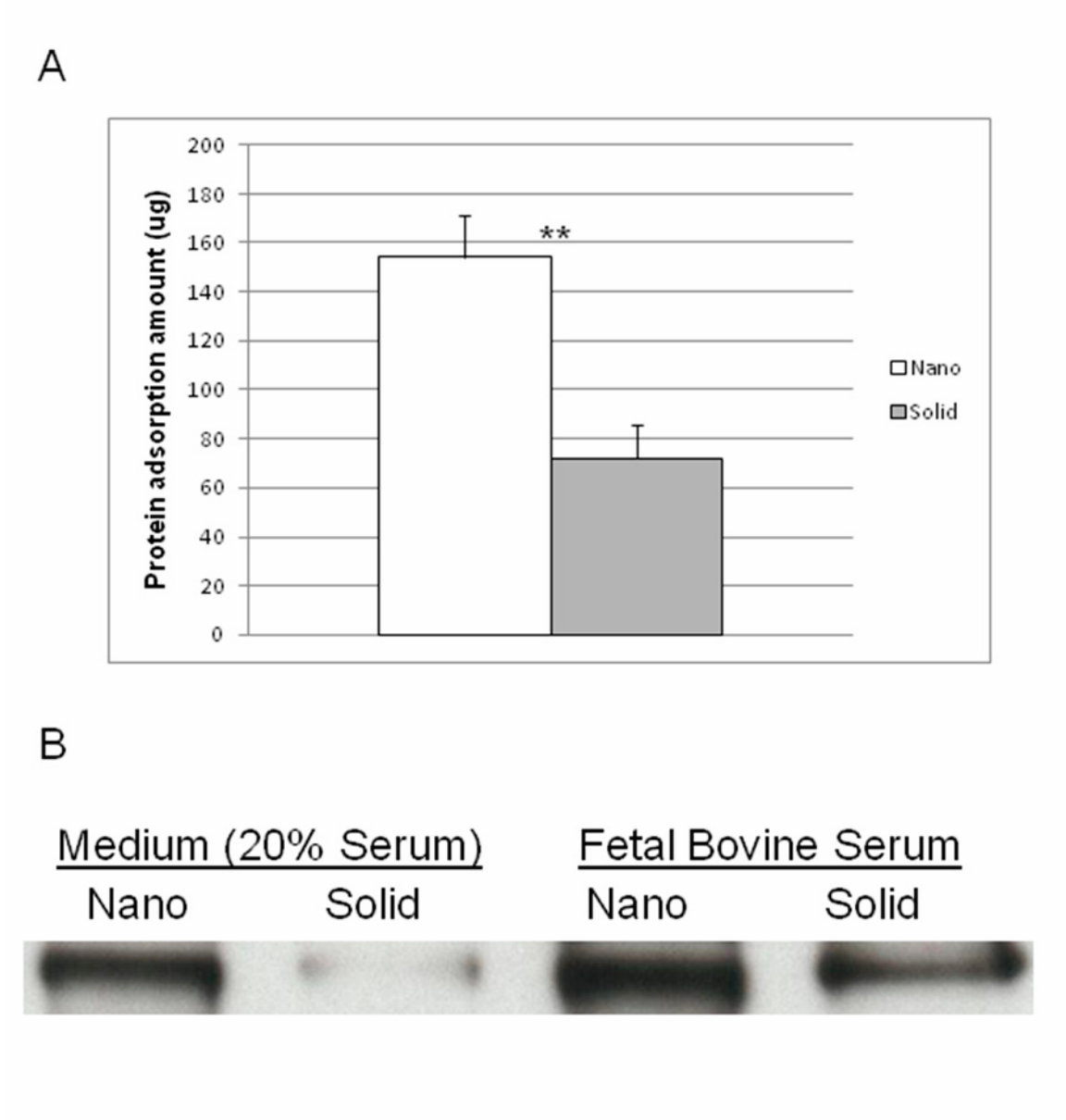

Figure 4.8: Protein adsorption to materials after exposure to medium containing bovine serum protein or fetal bovine serum for 4 hr: (A) MicroBCA of protein extracts from nanofibrous scaffolds (Nano) and solid-walled scaffolds (Solid) treated with media; ** denotes a p-value < 0.01. (B) western blot of fibronectin extracted from nanofibrous scaffolds (Nano) and solid-walled scaffolds (Solid) treated with differentiation media or fetal bovine serum.

Media Title	Media Formulations
ESC Media	DMEM supplemented with 10% FBS, 10^{-4}M β-mercaptoethanol, 0.224 μg/ml L-glutamine, 1.33 μg/ml HEPES and 1,000 units/ ml human recombinant LIF
EB Media	DMEM supplemented with 10% FBS, 10^{-4}M β-mercaptoethanol, 0.224 μg/ml L-glutamine, and 1.33 μg/ml HEPES. For osteogenic cultures 1 μM dexamethasone, 50 mg/mL ascorbic acid and 10 mM β-glycerol phosphate were added
Differentiation Media	DMEM supplemented with 20% FBS, 10^{-4}M β-mercaptoethanol, 0.224 μg/ml L-glutamine, and 1.33 μg/ml HEPES
Osteogenic Media	DMEM supplemented with 20% FBS, 10^{-4}M β-mercaptoethanol, 0.224 μg/ml L-glutamine, 1.33 μg/ml HEPES 1 μM dexamethasone, 50 mg/mL ascorbic acid and 10 mM β-glycerol phosphate
BMP Media	DMEM supplemented with 20% FBS, 10^{-4}M β-mercaptoethanol, 0.224 μg/ml L-glutamine, 1.33 μg/ml HEPES 1 μM dexamethasone, 50 mg/mL ascorbic acid, 10 mM β-glycerol phosphate and 25ng/mL of BMP-2 for days 6-9 of differentiation.
TBI Media	DMEM supplemented with 20% FBS, 10^{-4}M β-mercaptoethanol, 0.224 μg/ml L-glutamine, 1.33 μg/ml HEPES 1 μM dexamethasone, 50 mg/mL ascorbic acid, 10 mM β-glycerol phosphate 2.5ng/mL of TGF-β1 for 2-5days of differentiation, 25ng/mL of BMP-2 for days 6-9 of differentiation and 100ng/mL of IGF-1 for days 10-13 of differentiation

Table 4. 1: Media Formulations used for ESC culture and differentiation

4.6 References

1. Kurtz, S., F. Mowat, K. Ong, N. Chan, E. Lau, and M. Halpern. Prevalence of Primary and Revision Total Hip and Knee Arthroplasty in the United States From 1990 Through 2002 J Bone Joint Surg, 2005. **87**: p. 1487-1497.

2. Liu, X. and P.X. Ma. Polymeric Scaffolds for Bone Tissue Engineering. Annals of Biomedical Engineering, 2004. **32**(3): p. 477-486.

3. Christenson, E.M., K.S. Anseth, J.J.J.P. vanden Beucken, C.K. Chan, B. Ercan, J.A. Janson, C.T. Laurencin, W.J. Li, R. Murugan, L.S. Nair, S. Ramakrishna, R.S. Tuan, T.H. Webster, and A.G. Mikos. Nanobiomaterial Applications in Orthopedics. J Orthop Res, 2007. **25**: p. 11-22.

4. Ma, P.X. Scaffolds for tissue fabrication. Materials Today, 2004. **7**: p. 30-40.

5. Langer, R. and J. Vacanti. Tissue Engineering. Science, 1993. **260**: p. 920-926.

6. Ma, P.X. Biomimetic materials for tissue engineering. Adv Drug Deliv Rev, 2008. **60**: p. 184-189.

7. Smith, L.A., J.A. Beck, and P.X. Ma. Fabrication and Tissue formation with Nano-Fibrous Scaffolds, in *Nanotechnologies for Tissue, Cell and Organ Engineering*, C. Kumar. Editor. 2007, Wiley-VCH: Weinheim. p. 188-215.

8. Chen, V.J., L.A. Smith, and P.X. Ma. Bone regeneration on computer-designed nano-fibrous scaffolds. Biomaterials, 2006. **27**: p. 3973-3979.

9. Atala, A. Recent developments in tissue engineering and regenerative medicine. Current Opinion in Pediatrics, 2006. **18**: p. 167-171.

10. Fleming, R.G., C.J. Murphy, G.A. Abrams, S.L. Goodman, and P.F. Nealey. Effects of synthetic micro-and nano-structured surfaces on cell behavior. Biomaterials, 1999. **20**: p. 573-588.

11. Gerecht, S., C.J. Bettinger, Z. Zhang, J.T. Borenstein, G. Vunjak-Novakovic, and R. Langer. The effect of actin disrupting agents on contact guidance of humand embryonic stem cells. Biomaterials, 2007. **28**: p. 4068-4077.

12. Nur-E-Kamal, A., I. Ahmed, J. Kamal, M. Schindler, and S. Meiners. Three-dimensional nanofibrillar surfaces promote self-renewal in mouse embryonic stem cells. Stem Cells, 2006. **24**: p. 426-433.

13. Hwang, Y.S., W.L. Randle, R.C. Bielby, J.M. Polak, and A. Mantalaris. Enhanced derivation of osteogenic cells from murine embryonic stem cells after treatment with HepG2-conditioned medium and modulation of the embryoid body

formation period: application to skeletal tissue engineering. Tissue Eng, 2006. **12**: p. 835-843.

14. Chaudhry, G.R., D. Yao, A. Smith, and A. Hussain. Osteogenic Cells Derived from Embryonic Stem Cells Produced Bone Nodules in Three-Dimensional Scaffolds. Journal of Biomedicine and Biotechnology, 2004. **4**: p. 203-310.

15. Hwang, Y., S. Varghese, P. Theprunsirikul, A. Canver, and J. Elisseeff. Enhanced chondrogenic differentiation of murine embryonic stem cells in hydrogels with glucosamine. Biomaterials, 2006. **27**: p. 6015-6023.

16. McCloskey, K.E., M.E. Gilroy, and R.M. Nerem. Use of Embryonic Stem Cell-Derived Endothelial Cells as a Cell Source to Generate Vessel Structures in Vitro. Tissue engineering, 2005. **11**: p. 497-505.

17. Aszodi, A., J.F. Bateman, E. Gustafsson, R. Boot-Handford, and R. Fassler. Mammalian Skeletogenesis and Extracellular Matrix: What can We Learn from Knockout Mice? Cell Struct Funct, 2000. **25**: p. 73-84.

18. Doetschman, T., H. Eistetter, M. Katz, W. Schmidt, and R. Kemler. The in vitro development of blastocyst-derived embryonic stem cell lines: formation of visceral yolk sac, blood island and myocardium. J Embryol Exp Mophol, 1985. **87**: p. 27-45.

19. Woo, K.M., V.J. Chen, and P.X. Ma. Nano-fibrous scaffolding architecture selectively enhances protein adsorption contributing to cell attachment. J Biomed Mater Res, 2003. **67A**: p. 531-537.

20. Woessner, J.F. The Determination of Hydroxyproline in Tissue and Protein Samples Containing Small proportions of this Imino Acid. Achivers of Biochemistry and Biophysics, 1961. **93**: p. 440-447.

21. Neuman, R. and M. Logan. The determination of collagen and elastin in tissues. J Biol Chem, 1950. **186**: p. 549-556.

22. Smith, L.A., X. Liu, P. Wang, J. Hu, and P.X. Ma. Enhancing Osteogenic Differentiation of Mouse Embryonic Stem Cells by Nanofibers. In preparation.

23. Vats, A., N. Tolley, A. Bishop, and J. Polak. Embryonic stem cells and tissue engineering: delivering stem cells to the clinic. J R Soc Med 2005. **98**(8): p. 346-350.

24. Vats, A., N.S. Tolley, A.E. Bishop, and J.M. Polak. Embryonic stem cells and tissue engineering: delivering stem cells to the clinic. J R Soc Med 2005. **98**(8): p. 346-350.

25. Kaplan, D.L., R.T. Moon, and G. Vunjak-Novakovic. It takes a village to grow a tissue. Nat Biotechnol, 2005. **23**: p. 1237-1239.

26. Karaplis, A. Embryonic Development of Bone and the Molecular Regulation of Intramembranous and Endochondral Bone Formations, in *Principles of Bone Biology*, J. Bilezikian, L. Raisz, and G. Rodan. Editors. 2002, Academic Press: San Diego. p. 33-58.

27. Cowles, E.A., M.E. DeRome, G. Pastizzo, L.L. Brailey, and G.A. Gronowicz. Mineralization and the Expression of the Matrix Proteins During In Vivo Bone Development. Calcif Tissue Int, 1998. **62**: p. 74-82.

28. Weiss, R.E. and A.H. Reddi. Role of Fibronectin in collagenous matrix-induced mesenchymal cell proleration and differentiation in vivo. Exp Cell Res, 1981. **133**: p. 247-254.

29. Woo, K.M., V.J. Chen, and P.X. Ma. Nano-fibrous scaffolding architecture selectively enhances protein adsoption contributing to cell attachement. J Biomed Mater Res, 2003. **67A**: p. 531-537.

30. Atchley, W.R. and B.K. Hall. A model for development and evolution of complex morphological structures. Biol Rev Camb Philos So, 1991. **66**: p. 101-157.

31. Kanaan, R.A. and L.A. Kanaan. Transforming growth factor B1, bone connection. Med Sci Monit, 2006. **12**: p. RA164-169.

32. Rosen, V. and J.M. Wozney. Bone Morphogenetic Proteins, in *Principles of Bone Biology*, J. Bilezikian, L. Raisz, and G. Rodan. Editors. 2002, Academic Press: San Diego. p. 919-928.

33. Karaplis, A.C. Embryonic Development of Bone and the Molecular Regulation of Intramembranous and Endochondral Bone Formation, in *Principles of Bone Biology*, J. Bilezikian, L. Raisz, and G. Rodan. Editors. 2002, Academic Press: San Diego. p. 33-58.

34. Rossert, J. and B. de Crombugghe. Type I Collagen, in *Principles of Bone Biology*, J. Bilezikian, L. Raisz, and G. Rodan. Editors. 2002, Academic Press: San Diego. p. 189-210.

35. Stains, J.P. and R. Civitelli. Cell-Cell Interactions in Regulatin Osteogenesis and Osteoblast Function. Birth Defects Research (Part C), 2005. **75**: p. 72-80.

36. Woo, K.M., J.-H. Jun, V.J. Chen, J. Seo, J.-H. Baek, H.-M. Ryoo, G.-S. Kim, M.J. Somerman, and P.X. Ma. Nano-fibrous scaffolding promotes osteoblast differentiation and biomineralization. Biomaterials, 2007. **28**(2): p. 335-343.

37. Lynch, M.P., J.L. Stein, G.S. Stein, and J.B. Lian. The influence of type I collagen on the development and maintenance of the osteoblast phenotype in primary and passaged rat calvarial osteoblasts: modifcation of expression of genes supporting cell growth, adhesion, and extracellular matrix mineralization. Exp Cell Res, 1995. **216**: p. 35-45.

38. Mizuno, M., R. Fujisawa, and Y. Kuboki. Type I collagen-induced osteoblastic differentiation of bone-marrow cells mediated by collagen-alpha2beta1 integrin interaction. J Cell Physiolo, 2000. **184**: p. 207-213.

39. Hayashi, Y., M.K. Furue, T. Okamoto, Y. Myoishi, Y. Fukuhara, T. Abe, J.D. Sato, R.I. Hata, and M. Asashima. Integrins Regulate Mouse Embryonic Stem Cell Self-Renewal. Stem Cells, 2007. **25**: p. 3005-3015.

40. Mizuno, M., R. Fujisawa, and Y. Kuboki. Type I collagen-induced osteoblastic differentiation of bone-marrow cells mediated by collagen-alpha2beta1 integrin interaction. J Cell Physiol, 2000. **184**: p. 207-213.

41. Xiao, G., D. Wang, D. Benson, G. Karsenty, and R.T. Franceschi. Role of the a2-Integrin Osteoblast-specific Gene Expression and Activation of the OSF2 Transcription Factor. J Biol Chem, 1998. **273**: p. 32988-32994.

42. Rohwedel, J., K. Guan, and W. Zuschratter. Loss of Beta 1 integrin function results in a retardation of myogenic, but an acceleration of neuronal, differentiation of embryonic stem cells in vitro. Del Biol, 1998. **201**(167-184).

Chapter 5

Osteogenic Differentiation of Human Embryonic Stem Cells on Nanofibrous Scaffolds

5.1 Introduction

Pluripotent human embryonic stem cells (hESC) isolated from the inner cell mass of blastocysts represent a potentially unlimited source of cells for bone tissue engineering[1]. While the proliferative ability of adult stem cells is limited by donor age and time in expansion culture[2, 3], hESC proliferate much longer and can differentiate into any cell type within the body. However, there are several obstacles to using hESC (tumorgencity of the undifferentiated cells and the heterogeneous cell population generated using the current differentiation protocols) which must be overcome prior to their clinical use as a cell source for tissue engineering.

Most attempts to direct hESC differentiation to the osteogenic lineage have focused on the addition of biologically active molecules to hESC in a culture dish[4-7]. However in previous studies with mouse embryonic stem cells, we have found that biologically active molecules in combination with a nanofibrous (NF) architecture of the substrate enhance the osteogenic differentiation of the embryonic stem cells[8, 9]. Type I collagen is a major component of the extracellular matrix (ECM) in bone and consists of

three collagen polypeptide chains wound together to form a ropelike superhelix that assembles into the fibers ranging in size from 50 to 500nm[10]. Using phase separation, we have developed synthetic three dimensional nanofibers of the same size scale as natural type I collagen[11-15].

When polymeric scaffolds have been used to facilitate differentiation or tissue formation, hESC have been encapsulated within an ECM hydrogel in order to maintain the cells within the scaffold[16-18]. We hypothesize that the collagen mimicking synthetic nanofibers generated by phase separation advantageously enhance hESC differentiation and tissue formation, eliminating potential problems associated with pathogen transmission and immune response to ECM. To test this hypothesis, we will examine the effects of the NF architecture of both two dimensional (2-D) poly(L-lactic acid) (PLLA) thin matrices and 3-D PLLA scaffolds in vitro on the osteogenic differentiation of hESC compared with more traditional flat (solid) films and solid-walled (SW) scaffolds.

5.2 Methods and Materials

Poly(L-lactic acid) (PLLA) with an inherent viscosity of 1.6 dl/g was purchased from Alkermes (Medisorb, Cambridge, Massachusetts) and used without further purification. Cyclohexane, dioxane, ethanol, hexane, and methanol were purchased from Fisher Scientific (Pittsburgh, Pennsylvania). Dubecco's Modified Eagle Media (DMEM), Dulbecco's Modified Eagle Medium: Nutrient Mix F-12 (D-MEM/F-12), alpha Minimum Essential Medium (αMEM), Dulbecco's Phosphate Buffered Saline (D-PBS), fibroblast growth factor 2 (FGF2), knockout Serum replacer, non-essential amino acids,

glutaMAX-I support supplement, TrypLE Express stable trypsin replacement enzyme and PCR primers were obtained from Invitrogen (Carlsbad, CA). Fetal Bovine Serum was obtained from Harlan Biological (Indianapolis, IN). Neuronal Class III β-Tubulin (TUJ1) antibody and goat serum were obtained from Sigma (St. Louis, MO). Human transforming growth factor-beta1 (TGF-β1) and bone morphogenic protein-2 (BMP-2) were obtained from Peprotech (Rocky Hill, New Jersey). Osteocalcin antibody and all secondary antibodies were obtained from Santa Cruz Biotechnology (Santa Cruz, CA). Mouse anti-human integrin alpha 2 monoclonal antibody and purified mouse IgG1 antibody were obtained from Millipore (Danvers, MA). RNeasy Mini Kit and Rnase-Free DNase set were obtained from Qiagen (Valencia, California). TaqMan reverse transcription reagents, real-time PCR primers, and TaqMan Universal PCR Master mix were obtained from Applied Biosystems (Foster City, California). Chemicals were obtained from Sigma Chemical Co. (St. Louis, MO) unless otherwise noted.

5.2.1 2-D Thin Matrix and Film Preparation for Cell Culture

PLLA was dissolved in tetrahydrofuran at 60^{o}C to make a 10% (wt/v) PLLA solution. The NF PLLA matrix (thickness~40μm) was fabricated by first casting 0.4 mL of the PLLA solution on a glass support plate which had been pre-heated at 45^{o}C for 10 min and then sealing the polymer solution on the glass support plate by covering it with another pre-heated glass plate. The polymer solution was phase separated at -20°C for 2 hrs and then immersed into ice-water mixture to exchange tetrahydrofuran for 24 hrs. The matrix was washed with distilled water at room temperature for 24 hrs with water changed every 8 hrs. The matrix was then freeze-dried.

The matrices were cut to fit into a 35mm Petri dish and secured in place with a disk of silicone elastomer from Dow Corning (Midland, MI) containing a 1.5mm by 1.5mm opening. The matrices were then sterilized with ethylene oxide and wet with αMEM containing 20% Fetal Bovine Serum, 1% non-essential amino acid, 0.1mM β mercaptoethanol and 1mM glutaMAX-I support supplement for 1hr.

PLLA thin flat (solid) films were fabricated in a similar manner excluding the phase separation step. Instead, the solvent was evaporated at room temperature in a fume hood. The thin flat (solid) films and controls were then treated similarly to the NF matrices. The NF matrices (average fiber diameter of 148nm±21nm(standard deviation)) and films (smooth surface) were previously characterized[8, 19].

5.2.2 Fabrication of NF-PLLA and SW-PLLA Scaffolds

NF-PLLA scaffolds were fabricated as described previously[12, 15]. Briefly, paraffin spheres (diameter = 250-420 μm) were added to Teflon molds, and the top surface was leveled. The molds were preheated at 37^{o}C for 40 min to ensure that paraffin spheres were interconnected. PLLA was dissolved in 4/1 (v/v) dioxane/methanol solvent mixture and was cast onto paraffin sphere assemblies. The polymer/paraffin composite was cooled to –76 ^{o}C overnight to phase separate the polymer solution. Hexane was used for solvent extraction and leaching the paraffin spheres for a total of 4 days. Hexane in the scaffolds was then exchanged with cyclohexane. The polymer scaffolds were lyophilized and cut to samples with 3.8 mm diameter and 1.0 mm thickness.

For comparison, SW PLLA scaffolds were also prepared using PLLA solution in dioxane. The paraffin sphere mold preparation and the polymer casting procedure were

performed in the same way as for NF PLLA scaffolds. After PLLA solution casting, the polymer/paraffin composites were dried under low vacuum overnight (about 300 mmHg) and under high vacuum (about 30 mmHg) for 3 days. Paraffin leaching and lyophilizing procedure were performed in the same manner as for NF PLLA scaffolds.

5.2.3 Human Embryonic Stem Cell Culture

The human embryonic stem cell line, BG01, was purchased from Bresagen (Athens, Georgia) and cultured as previously described[1]. The cells were expanded manually on mouse embryonic fibroblasts obtained from the University of Michigan Center for Human Embryonic Stem Cell Research, plated at 4 $x10^5$ per 60mm dish in DMEM/ F-12 media containing 20% knockout serum replacer, 1% non-essential amino acids, 1mM glutaMAX-I support supplement, 0.1 mM β mercaptoethanol and 4ng/ml FGF2. Media was changed daily.

To induce the formation of embryoid bodies for osteogenic differentiation, cells were manually passaged in small clumps and transferred to non-adhesive petri plates in DMEM/ F-12 media containing 20% knockout serum replacer, 10% Fetal Bovine Serum, 1% non-essential amino acids, 1mM glutaMAX-I support supplement, 0.1 mM β mercaptoethanol, 1 μM dexamethasone, 50 mg/mL ascorbic acid and 10 mM *β*-glycerol phosphate. After 2 days of embryoid body formation, 2.5ng/mL of TGF-β1 was added to the media for 3 days. After 5 days of suspension culture, the embryoid bodies were plated onto 0.1% gelatin coated dishes in αMEM containing 20% Fetal Bovine Serum, 1% non-essential amino acids, 1mM glutaMAX-I support supplement, 0.1 mM β mercaptoethanol, 1 μM dexamethasone, 50 μg/mL ascorbic acid, 10 mM *β*-glycerol

phosphate and 25ng/ml BMP-2. On day 8 of the differentiation protocol, hESC growing on the 0.1% gelatin coated dishes were washed with D-PBS and passaged to tissue culture plastic using TrypLE Express stable trypsin replacement enzyme in αMEM containing 20% Fetal Bovine Serum, 1% non-essential amino acids, 1mM glutaMAX-I support supplement, and 2ng/ml FGF2. After 7 days of culture on tissue culture plastic, hESC were passaged with tryLE express stable trypsin replacement enzyme and seeded on materials in αMEM containing 20% Fetal Bovine Serum, 1% non-essential amino acid, 1mM glutaMAX-I support supplement, 0.1 mM β mercaptoethanol, 1 μM dexamethasone, 50 mg/mL ascorbic acid and 10 mM β-glycerol phosphate. 7.5×10^4 hESC were seeded on thin matrices and films, while 2.5×10^6 hESC were seeded on scaffolds. Media was changed every other day throughout the differentiation process.

For blocking studies, 6μg/ml of mouse anti-human integrin alpha 2 monoclonal antibody or purified mouse IgG1 antibody were added to the media after a 48hr attachment period, since alpha 2 integrin was expressed in our seeding population. The media was changed every other day.

5.2.4 Human Mesenchymal Stem Cell and Mesenchymal-like Embryonic Stem Cell Derived Culture

In order to assess the ability of this protocol to promote osteogenic differentiation, human mesenchymal stem cells and mesenchymal-like embryonic stem cell derived cells were used. All cell types were seeded to tissue culture plastic at a density of 3.3×10^4 cells per cm^2. Human mesenchymal stem cells were obtained from Cambrex (East Rutherford, NJ) and expanded in mesenchymal stem cell growth media.

Mesenchymal-like embryonic stem cell derived cells were obtained as previously described[20]. Briefly, BG01 cells were allowed to form embryoid bodies for 10 days in DMEM/ F-12 media containing 20% knockout serum replacer, 1% non-essential amino acids, 1mM glutaMAX-I support supplement, and 0.1 mM β mercaptoethanol. The embryoid bodies were then plated to 0.1% gelatin coated dishes and cultured in DMEM with 10% fetal bovine serum, 100 U/mL penicillin and100 mg/mL streptomycin.

5.2.5 Scanning Electron Microscopy

Twelve hours after seeding, the matrices and control were washed with PBS followed by 0.1M cacodylate buffer and then fixed with 2.5% glutaraldehyde in 0.1M cacodylate buffer over night. The cells were washed again with 0.1M cacodylate buffer and post-fixed in 1% osmium tetroxide for 1 hr. The fixed samples were then dehydrated through an ethanol gradient (50%, 70%, 90%, 95%, and 100%) over 3hrs and dried with hexamethyldisilazane (HMDS). Samples were then gold coated and observed using scanning electron microscopy (S-3200, Hitachi, Japan). Cell spreading area was calculated from at least 20 cells per sample in the SEM images using the automated measure function of J Image (downloaded from the National Institute of Health, Bethesda, MD, USA, free download available at http://rsb.info.nih.gov/ij/) .

5.2.6 Real Time PCR

Total RNA was isolated using an RNeasy Mini Kit with Rnase-Free DNase set according to the manufacturer's protocol after thin matrices and scaffolds were mechanically homogenized with a Tissue-Tearor (BioSpec Products, Bartlesville, OK)

while cells cultured on gelatin-coated tissue culture plate controls were harvested with a cell scraper. The cDNA was made using a Geneamp PCR (Applied Biosystems) with TaqMan reverse transcription reagents and 10 min incubation at 25 °C, 30 min reverse transcription at 48 °C, and 5 min inactivation at 95 °C. Real-time PCR was set up using TaqMan Universal PCR Master mix and specific primer sequences for collagen type I, Runx2, osteocalcin, TUJ1 and β actin with 2 min incubation at 50 °C, a 10 min Taq Activation at 95 °C, and 50 cycles of denaturation for 15 s at 95 °C followed by an extension for 1 min at 72 °C on an ABI Prism 7500 Real-Time PCR System (Applied Biosystems). Target genes were normalized against β actin.

5μL of each reaction was subject to PCR using AmpliTaq Gold DNA polymerase (Applied Biosystems) for each of the following: ITGAV (αV) integrin (5'-TCGCCGTGGATTTCTTCGT-3' and 5'- TCGCTCCTGTTTCATCTCAGTTC-3'); ITGA2 (α2) integrin (5'- TCCAAGCCTTCAGTGAGAGC-3' and 5'-ATGTGTATCGATCTCTGCCG-3'); ITGA5 (α5) integrin (5'-AGATGAGTTCAGCCGATTCG-3' and 5'- TGGAAGTCAGGAACAGTGCC-3'); ITGB1 (β1) integrin (5'- ACATGGACGCTTACTGCAGG-3' and 5'-GAACAATTCCAGCAACCACG-3'); ITGB3 (β3) integrin (5'-ATTGGCTGGAGGAATGACG-3' and 5'- AAGACTGCTCCTTCTCCTGG-3'); and β actin (5'- ATCTGGCACCACCTTCTACAATGAGCTGCG-3' and 5'-CGTCATACTCCTGCTTGCTGATCCACATCTGC-3'). The cycling conditions used were 94°C for 5mins followed by 94°C for 30s, 56°C for 60s, 72°C for 60s 40 times for integrin primers, and 94°C for 30s, 55°C for 30s, 72°C for 120s 40 times for β actin. These amplifications were followed by a 10min extension at 72°C.

5.2.7 Immunofluorescence and Histological Staining

The NF matrices, flat (solid) films and controls were fixed with 2% paraformaldehyde/PBS, washed, and stored at 4°C in PBS. For histological analysis, scaffolds were fixed in 10% neutral buffered formalin solution (Sigma, St. Louis, Missouri), dehydrated through an ethanol gradient, and embedded in paraffin. Embedded samples were cut at 5 μm. The paraffin was dissolved with xylene and the sections were rehydrated through an ethanol gradient. The sections were then incubated in 0.5% pepsin for 10min at 30°C for antigen retrieval. Nonspecific antibody binding was blocked by 10% goat serum, then the matrices and control were exposed to TUJ1 (1:250) or osteocalcin (1:50) antibodies, followed by appropriate secondary antibodies conjugated to FITC (TUJ1) or TRITC (ostoecalcin). DAPI was used to stain cell nuclei.

For Alizarin Red S staining, the matrices, controls, and scaffold sections were fixed by the same method and then stained with 40mM Alizarin Red S solution, pH 4.2 at room temperature for 10min. Thin matrices and controls were then rinsed 5 times in distilled water and washed 3 times in PBS on an orbital shaker at 40rpm for 5 min each to reduce nonspecific binding. Scaffold sections were dehydrated in acetone and rinsed in xylene before mounting with Permamount. Scaffold sections were also stained with hematoxylin and eosin-phloxine and von Kossa.

5.2.8 Mineral Quantification

After 6 weeks of culture, scaffolds for mineralization quantification were washed three times for 5 min each in double-distilled water and then homogenized with a Tissue-

Tearor in 1 mL of double-distilled water. Samples were then incubated in 0.5 M acetic acid overnight. Total calcium content of each scaffold was determined by *o*-cresolphthalein-complexone method following the manufacturer's instructions (Calcium LiquiColor, Stanbio Laboratory, Boerne, Texas).

5.2.9 Collagen Quantification

The collagen content of the cell/scaffold constructs was determined using a colormetric hydroxyproline quantification method [21]. Briefly, scaffolds for collagen quantification were washed three times for 5 min each in double-distilled water and then homogenized with a Tissue-Tearor in 500 μL of double-distilled water. 600 μL of 12N hydrochloric acid was added and the samples were incubated at 100-110°C for 18-24hrs. 10μL methyl red was added and the samples were neutralized to a PH 6-7 with sodium hydroxide and hydrochloric acid. 320 μL of chloramine T assay solution (211.5mg chloramine T, 12mL Citrate buffer, ph6, 1.5ml isopropanol) was added to 640 μL of the sample, which was placed on an orbital shaker for 20min at 100rpm. 320 μL of dimethylaminobenzaldehyde assay solution (2.250g dimethylaminobenzaldehyde, 9mL isopropanol, 3.9mL 60% perchloric acid) was added and the samples placed at 50°C for 30min. The samples were read at 550nm. Collagen content was estimated assuming a ratio of 1 μg hydroxyproline: 7.46 μg collagen[22].

5.2.10 Western Blot Analysis

Scaffolds were treate with ethanol and PBS in the same way discribed above for cell culture. Scaffolds were incubated with cell culture medium or FBS for 4 hours.

Scaffolds were quickly washed with PBS for 2 times, cut into pieces and transferred to 1.5ml tubes. 600µl of PBS was added and the scaffolds were washed three times. PBS was removed, and the scaffolds were centrifuged for 1min at 12,000rpm for 2 times to remove any liquid remained. 25µl 1% SDS was added and incubated for 1hr. This was repeated twice. A total of 75µl was pooled to form the collection sample. For microBCA (Pierce, Rockford, IL), 50ul of the collection sample was used (n=3), while 30 µl of the collection sample was used for each gel. Western blot analysis was conducted as previously described[15]. Briefly, the recovered serum protein samples were subject to fractionation through 4-12% SDS-polyacrylamide gel electrophoresis (PAGE). The fractionated proteins were transferred to a PVDF membrane (Sigma). The blots were washed with TBST (10 m*M* Tris-HCl, 150 m*M* NaCl, 0.05% Tween-20, pH 8.0), and blocked with Blotto (5% nonfat milk in TBST) at room temperature for 1 h. The blots were incubated in anti-bovine fibronectin polyclonal antibody (Santa Cruz Biotechnology, Santa Cruz, CA) at room temperature for 1 h. After washing with TBST, the blots were incubated in anti-goat immunoglobulin G-horseradish peroxidase-conjugated antibody (Sigma), and then in chemiluminescence reagent (SuperSignal West Dura; Pierce). The relative densities of the protein bands were analyzed with QualityOne (Biorad).

5.2.11 Statistical Analysis

All experiments were conducted at least 3 times. All quantifiable data is reported with the mean and standard deviation. Student T tests were conducted where appropriate to determine significance. Significance was set as a p-value of less than 0.05.

5.3 Results

A number of protocols have been developed to generate osteogenic cells from hESC[4-7]. For our study, we derived an osteogenic population through embryoid body formation and plating in the presence of osteogenic supplements (ascorbic acid, *β*-glycerol phosphate and dexamethasone) and the sequential administration of growth factors (TGF-β1, BMP2, and FGF2) over fifteen days. Another possible approach to generate osteoblasts from hESC is to first generate mesenchymal-like stem cell population and differentiate them toward the osteogenic lineage over a longer time[20, 23, 24]. In Figure 5.1 we compare the osteogenic potential of cells generated from our approach and a published hESC-derived mesenchymal-like stem cell protocol[20]. After two weeks of culture under osteogenic conditions, expression of transcripts for type I collagen and Runx2 was observed in our hESC derived osteogenic progenitors at a level similar to human mesenchymal stem cells (data not shown) and higher than in the hESC-derived mesenchymal-like stem cells (Figure 5.1A). After 3 weeks of osteogenic culture our hESC derived osteogenic progenitors also showed increased mineralization compared to the hESC-derived mesenchymal-like stem cells (Figure 5.1B).

The effects of FGF2 supplementation after BMP-2 supplementation were examined. The osteogenic potential of hESC derived osteogenic progenitors with and without the FGF2 supplementation was studied (Figure 5.1C). The FGF2 supplementation increased the osteocalcin expression of hESC derived osteogenic progenitors on all of our test substrate architectures (NF, solid, and control - 0.1% gelatin-coated tissue culture plastic) compared to hESC derived osteogenic progenitors

which were not exposed to FGF2 supplementation cultured on the same surface. The increased expression of Runx2 on the NF matrix with FGF2 supplementation compared to that without FGF2 was also observed. This indicates that the FGF2 treatment does not hinder the hESC derived osteogenic progenitor cells further differentiation toward the osteblastic lineage.

SEM was used to examine the morphology of the hESC derived osteogenic progenitor cells after 48hrs of osteogenic culture on the thin matrices and films (Figure 5.2). hESC derived osteogenic progenitor cells on the NF matrix were less spread ($1490\pm188\mu m^2$ reported as average cell area± standard deviation) with more processes interacting with the nanofibers on the flat (solid) films ($4891\pm1204\ \mu m^{2*}$, * indicates a p value <0.05 compared to the NF matrix) or control ($2840\pm167\ \mu m^{2*}$). This is consistent with other reports of cellular morphology on NF materials[19, 25-27]. Next osteogenic and neuronal differentiation was examined over time (Figure 5.3). hESC derived osteogenic progenitor cells cultured on the NF matrix expressed higher levels of osteogenic markers (Runx2 and osteocalcin) and reduced level of neuronal marker TUJ1 compared to flat (solid) films and control at all time points. hESC derived osteogenic progenitor cells on the NF matrix expressed increased levels of collagen type I after 1 week of osteogenic culture compared to flat (solid) films. These cells expressed reduced levels of collagen type I at both 2 and 6 weeks compared to hESC derived osteogenic progenitor cells on the flat (solid) film. This change in the relative expression of collagen type I could be due to a more quickly maturing ECM and a reduced need for new collagen type 1 on the NF matrix than on the flat (solid) film. This is supplemented by increased osteocalcin staining (Figure 5.4A) after 2 weeks and increased calcium

(Figure 5.4B) staining after 3 weeks of osteogenic culture of the hESC derived osteogenic progenitor cells on NF matrix compared to the cells grown on the flat (solid) film and control surface.

Differences in integrin expression by cells cultured on NF materials compared to solid materials have been observed previously[8, 25]. The expression of αV, α2, α5, β1, and β3 integrins were examined in the hESC derived osteogenic progenitor cells on the NF matrix and flat (solid) films. After 2 weeks of osteogenic culture, α2 integrin was differently expressed (Figure 5.5A) and when cells were exposed to α2 integrin antibodies decreased Runx2 and osteocalcin expression was observed on both NF matrix and flat (solid) films (Figure 5.5B and 5.5C). As α2 integrin expression is considered necessary for osteogenic differentiation[28, 29], the observed effect on cellular differentiation is not a surprise.

Next, differentiation (Figure 5.6) and histological organization (Figure 5.7) activities were examined on 3-D NF and SW scaffolds. After 4 weeks of culture, hESC derived osteogenic progenitor cells on NF scaffolds were found to express increased levels of Runx2 and reduced levels of TUJ1 compared to SW scaffolds. After 6 weeks of culture hESC derived osteogenic progenitor cells on NF scaffolds were found to express increased levels of collagen type I and osteocalcin compared to SW scaffolds. Cells grown on NF scaffolds may continue to express higher levels of collagen type I at later time points than those on the SW scaffolds due to a insufficient number of cells within the NF scaffold to produce the needed proteins for ECM maturation. Histology of the hESC derived osteogenic progenitor cells on the NF scaffolds shows increased cellular organization and mineralization compared to the SW scaffold (Figure 5.7A) after 6 weeks

of osteogenic culture. The NF scaffold contained increased levels of both collagen (Figure 5.7B) and calcium (Figure 5.7C) compared to the SW scaffold at this time.

Differences in the initial microenvironment created by protein adsorption from the medium could be contributing to the increased differenitation and histological organization of the cells on the scaffolds. Previous studies have found the profile and amount of total protein to differ on NF and solid materials[8, 15]. In this study, the NF scaffolds were found to adsorb significantly more protein from the media than the SW scaffolds (Figure 5.8A). Fibronectin, an important ECM protein during early osteogenesis[30, 31], adsorbed from the media was unable to be detected on either scaffold from a western blot. However, NF scaffolds exposed to pure fetal bovine serum were shown to adsorb more fibronectin than similarly treated solid scaffolds (Figure 5.8B).

5.4 Discussion

hESC represent a potentially unlimited source of cells for tissue engineering applications. However, best practices for their controlled differentiation have yet to be established. In vivo hESC exposed to osteogenic culture conditions prior to implantation selectively differentiated to bone over other mesenchymal lineages (cartilage and fat)[32] indicating that hESC can maintain their induced lineage in vivo.

In this study, growth factors where added sequentially to emulate their varied expression during osteogenesis[33, 34]. Additionally, previous studies with hESC have shown that TGF-β1 promotes mesodermal[35] and chondrogenic[36] differentiation, while BMP-2 increases both chondrogenesis[37] and osteogenesis[17]. FGF2, on the

other hand, increases number of osteogenic precursor cells[38, 39]. Sequential administration of growth factors leads to the development of osteogenic progenitors which have greater osteogenic potential than mesenchymally differentiated hESC (Figure 5.1). The progenitor population was then used to examine the effects of NF architecture in 2-D and 3-D on hESC osteogenic differentiation.

Although FGF2 has been shown to have a negative effect on late osteogenic differentiation and mature osteoblast cell survival[40], in our study the cell population treated with FGF2 had greater osteogenic potential on the materials than hESC derived osteogenic progenitor cells not receiving FGF2 stimulation (Figure 5.1C). This increased osteogenic potential may be due to maintenance of increased proliferative capacity after FGF2 treatment. This increased number of cells could enhance cell-cell interactions or signalling which may promote their increased differentiation. However, given that the objective of this study was to examine the effects of scaffold wall architecture on differentiation and tissue formation, the mechanism by which FGF2 increases the osteogenic potential of the cell population is outside the scope of this study but may be of considerable importance to be investigated in future studies.

Increased expression of many osteogenic markers was observed in hESC derived osteogenic progenitor cells on the NF matrix and scaffold compared to the flat (solid) film and the SW scaffold. However, there was inconsistency between the 2-D and 3-D culture in terms of the long term expression of collagen type I. Changes in cell density or differences in cell interactions between 2-D and 3-D cultures may explain this discrepancy in that numerous cell types have been shown to respond differently to 2-D and 3-D culture[41-43].

Interactions between type I collagen and α2β1 integrin have been linked to the expression of genes associated with the osteogenic phenotype[28, 29]. Increased expression of α2 integrin has been previously observed in neo-natal osteoblasts on NF materials compared to solid materials[25]. In this study, increased expression of the α2 integrin was observed in hESC derived osteogenic progenitor cells grown on the NF matrix compared to hESC derived osteogenic progenitor cells grown on flat (solid) films (Figure 5.3A). This improved integrin expression was then linked to osteogenic differentiation in that decreased expression of osteogenic markers when α2 integrin antibodies were added to the culture (Figure5.3B and 5.3C).

A previous study showed that NF scaffolds adsorbed increased levels of serum proteins in a different profile than SW scaffolds[15]. The profile of the proteins as well as the increased amount of protein adsorbed on the NF materials compared to the SW materials may lead to a preferential niche for osteogenic differentiation of the hESC derived osteogenic progenitor cells. Additionally, the proteins on the NF materials may have a different conformation then those on the solid material allowing them to further stimulate cellular differentiation as nanoscale features have been found to affect the supramolecular organization [44, 45] and activity[46] of adsorbed proteins.

The NF matrix and scaffold architecture itself could also be responsible for the observed differences in differentiation by directly influencing cell behavior. Previous studies showed that osteoblasts on NF scaffolds do not alter their α2β1 integrin expression when collagen fibril formation is blocked[25] and pre-osteoblasts on the NF matrix do not alter their cytoskeleton structure (in terms of stress fiber or focal adhesion

formation) when the NF matrix is modified with gelatin[19], indicating that the NF materials interact with cells in a manor similar to the secreted collagen ECM.

Further refinement of the cellular differentiation process, culture conditions and scaffold design will be necessary to form functional 3-D bone tissue. For instance, it has been suggested that mouse embryonic stem cells require the formation of a cartilage template in order to form bone tissue[47]. This may also be the case for hESC, however further testing will be necessary to determine the optimal strategy to utilize hESC for bone tissue engineering applications. As the NF scaffold contained more osteogenically differentiated cells and more organized tissue than the SW scaffold, the NF scaffold may be important to provide the optimal condition for bone tissue engineering.

5.5 Conclusions

NF architecture in both 2-D and 3-D enhances the osteogenic differentiation of hESC derived osteogenic progenitor cells compared to flat surfaces. In 2-D culture, hESC derived osteogenic progenitor cells grown on the NF matrix are morphologically different compared to cells cultured on flat (solid) films or control. hESC derived osteogenic progenitor cells grown on the NF matrix exhibit increased expression of α2 integrin compared to flat (solid) films, which was linked to the expression of the osteogenic markers Runx2 and osteocalcin. Increased expression of collagen type I, Runx2 and osteocalcin and mineralization of the matrix were observed in hESC derived osteogenic progenitor cells grown on NF matrices and scaffolds compared to hESC derived osteogenic progenitor cells grown on flat (solid) films and SW scaffolds. hESC derived

osteogenic progenitor cells grown on NF scaffolds also produced a more organized tissue containing more calcium and collagen than cells grown on SW scaffolds.

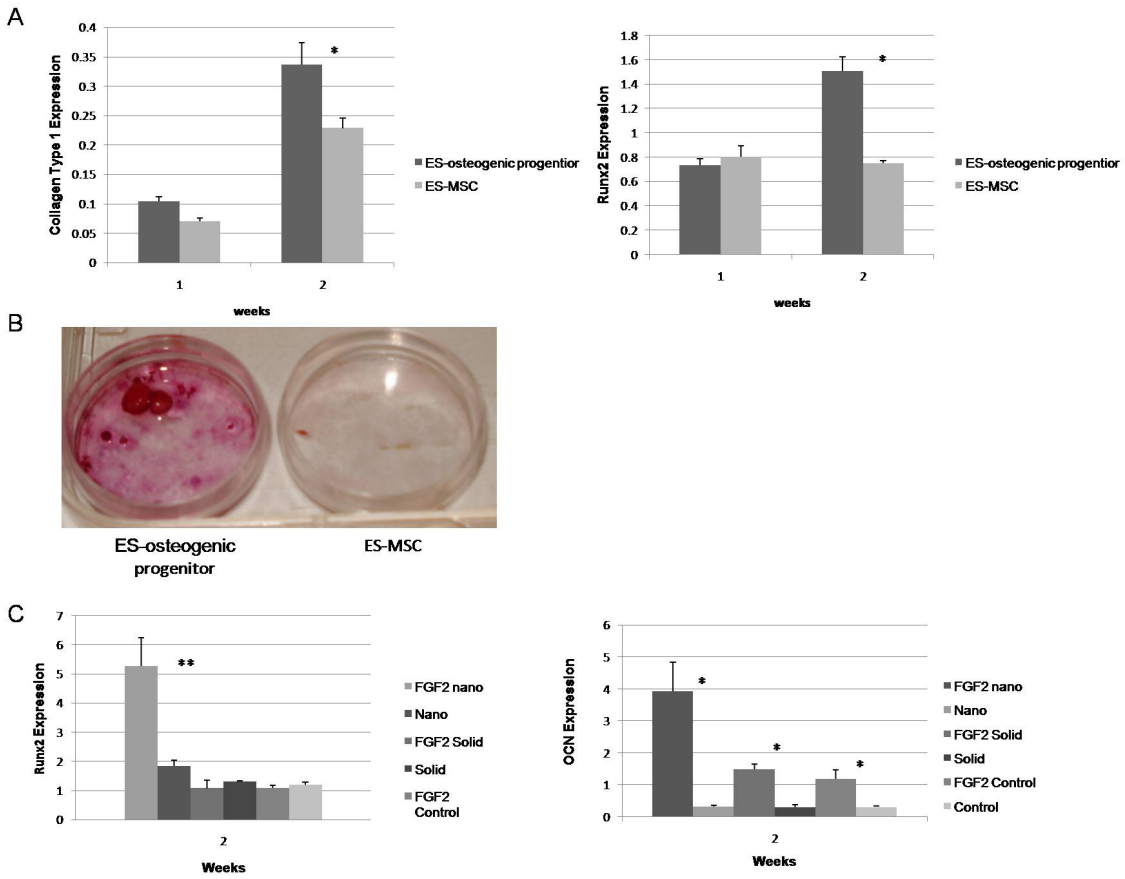

Figure 5.1: Comparison of the osteogenic potential of hESC derived osteogenic progenitor cells and hESC derived mesenchymal cells. (A) Quantitative PCR collagen type 1 and Runx2 after 2 weeks of osteogenic differentiation. Expression levels were normalized to β actin. * denotes p-value <0.05; (B) Alizarin red staining of hESC derived osteogenic progenitor cells and hESC derived mesenchymal cells after 3 weeks of osteogenic differentiation; (C) Quantitative PCR expression of osteogenic markers by hESC derived osteogenic progenitors with and without bFGF supplementation prior to seeding on nanofibrous matrices (nano), flat films (solid) and 0.1% glelatin coated tissue culture plastic (control). Expression levels were normalized to β actin. * denotes p-value <0.05. ** denotes p-value <0.01.

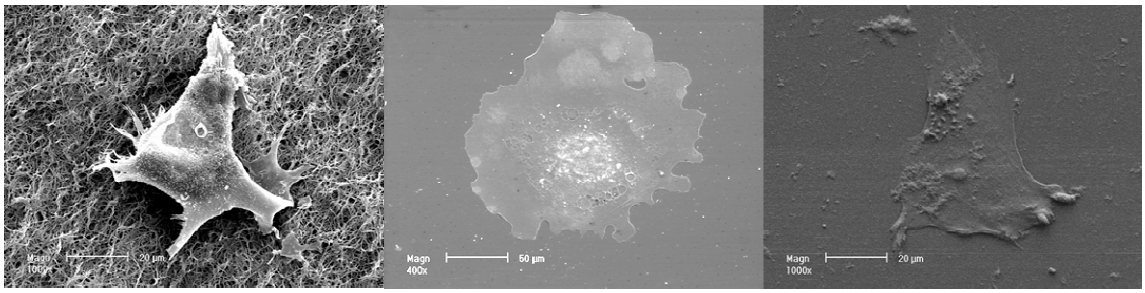

Figure 5.2: SEM micrographs of hESC derived osteo progenitor cells after 48 hrs of culture under osteogenic differentiation conditions on nanofibrous matrix (Nano), flat films (Solid), gelatin coated tissue culture plastic (Control), Scale bar =20μm (Nano & Control), 50 μm (Solid).

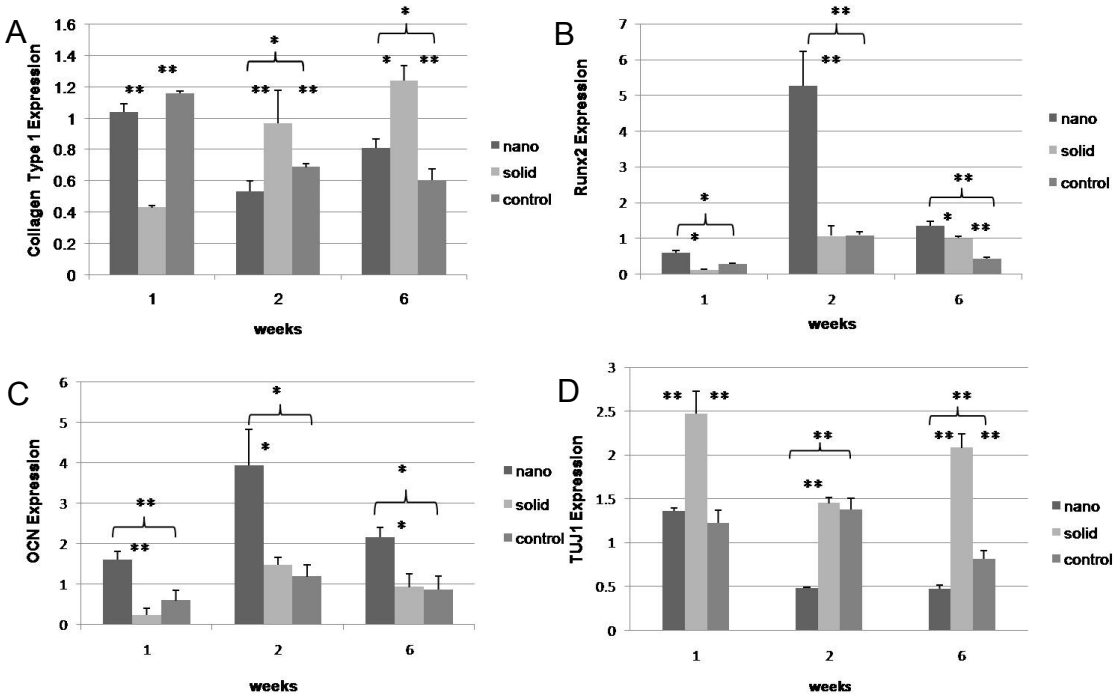

Figure 5.3: Expression of markers of osteogenic and neuronal differentiation over time under osteogenic differentiation conditions on nanofibrous matrices (nano), flat (solid) films (solid) and 0.1% gelatin coated tissue culture plastic (control) using quantitative PCR for (A) Collagen type 1, (B) Runx2, (C) osteocalcin, and (D) TUJ1. * denotes p-value <0.05. ** denotes p-value <0.01

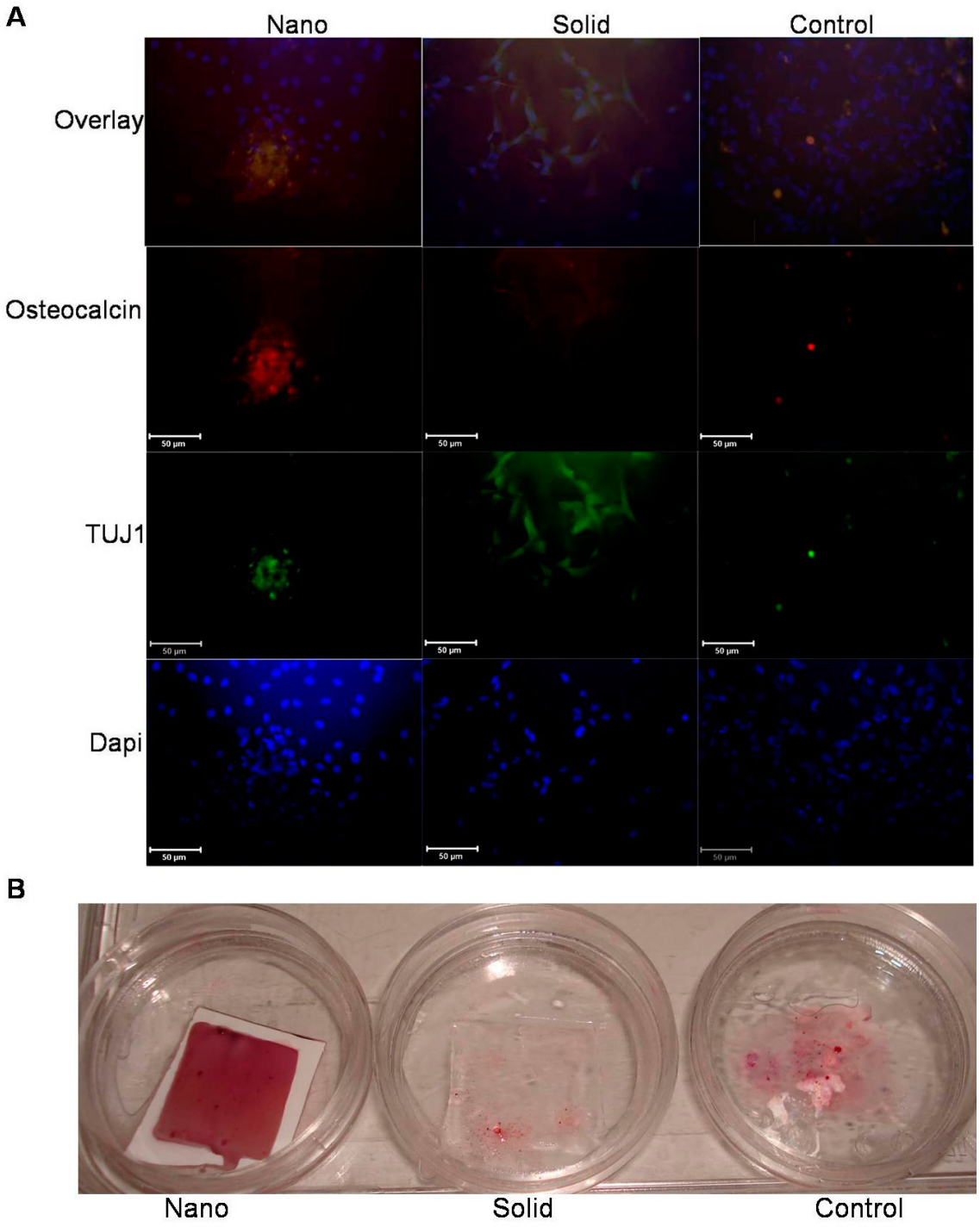

Figure 5.4: (A) Immunofluorescence localization of Neuronal (TUJ1) and late bone differentiation (Osteocalcin) markers after 2 weeks culture under osteogenic differentiation conditions on nanofibrous matrix (Nano), flat films (Solid) and gelatin coated tissue culture plastic (Control). Scale bar =50µm. (B) Calcium staining after 3 weeks under osteogenic differentiation conditions on nanofibrous matrix (Nano), flat films (Solid) and gelatin coated tissue culture plastic (Control).

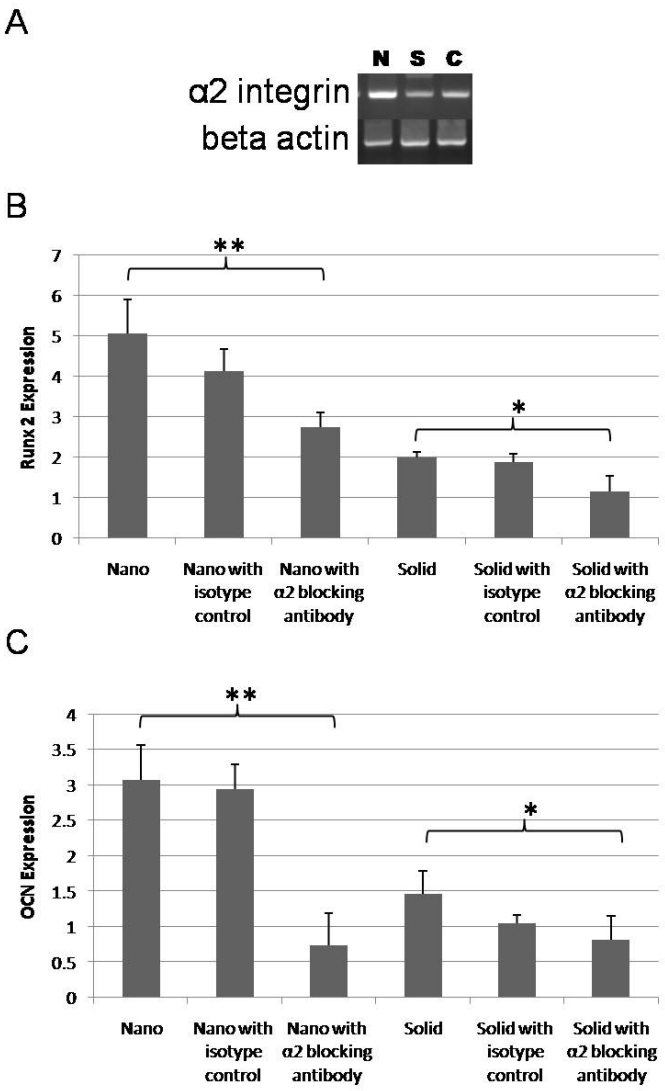

Figure 5.5: Effects of integrin blocking on osteogenic differentiation after 2 weeks of differentiation. (A) PCR of expression of α2 integrin on nanofibrous matrix (N), flat (solid) films (S) and 0.1% gelatin coated tissue culture plastic (C); (B) quantitiative PCR of expression of Runx2 on nanofibrous matrix (Nano), on nanofibrous matrix with control IGG isotype (Nano with isotype control), on nanofibrous matrix with mouse anti-human integrin alpha 2 monoclonal antibody (α2 blocking nano), on flat films (Solid), on flat films with control IGG isotype (solid with isotype control), and on flat films with mouse anti-human integrin alpha 2 monoclonal antibody (α2 blocking solid). * denotes p-value <0.05. ** denotes p-value <0.01. (C) quantitiative PCR of expression of osteocalcin on nanofibrous matrix (Nano), on nanofibrous matrix with control IGG isotype (Nano with isotype control), on nanofibrous matrix with mouse anti-human integrin alpha 2 monoclonal antibody (α2 blocking nano), on flat films (Solid), on flat films with control IGG isotype (solid with isotype control), and on flat films with mouse anti-human integrin alpha 2 monoclonal antibody (α2 blocking solid). * denotes p-value <0.05. ** denotes p-value <0.01.

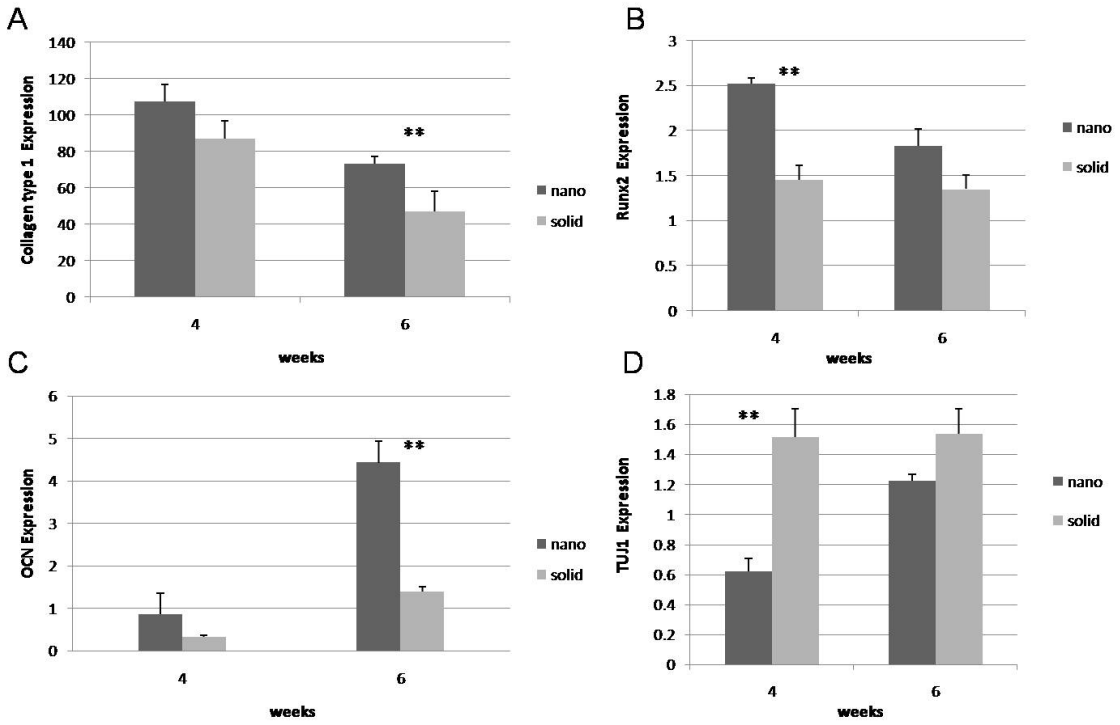

Figure 5.6: Quantitative PCR analysis of (A) Collagen type 1 (B) Runx2 (C) osteocalcin and (D) TUJ1 over time under osteogenic differentiation conditions on nanofibrous scaffolds (nano), and solid-walled scaffolds(solid). ** denotes p-value <0.01.

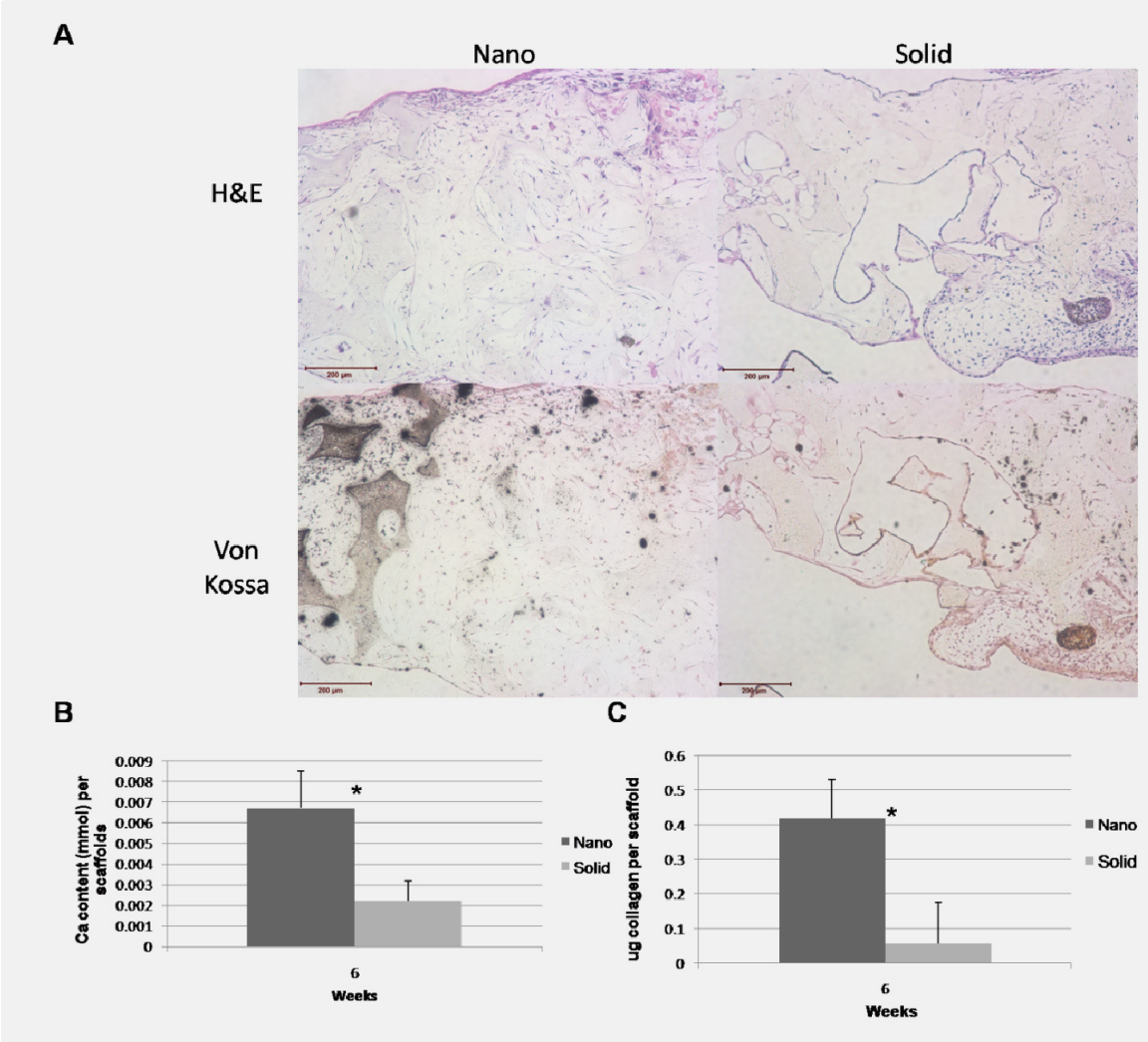

Figure 5.7: (A) Histology organization of cellular (H&E) and calcium (Von Kossa) staining of the scaffolds after 6 weeks of culture on nanofibrous (Nano) and solid-walled (Solid) scaffolds. Scale bar =200μm. (B,C) Quantification of scaffold calcium (B) and collagen (C) content after 6 weeks of osteogenic culture. * denotes a $p<0.05$.

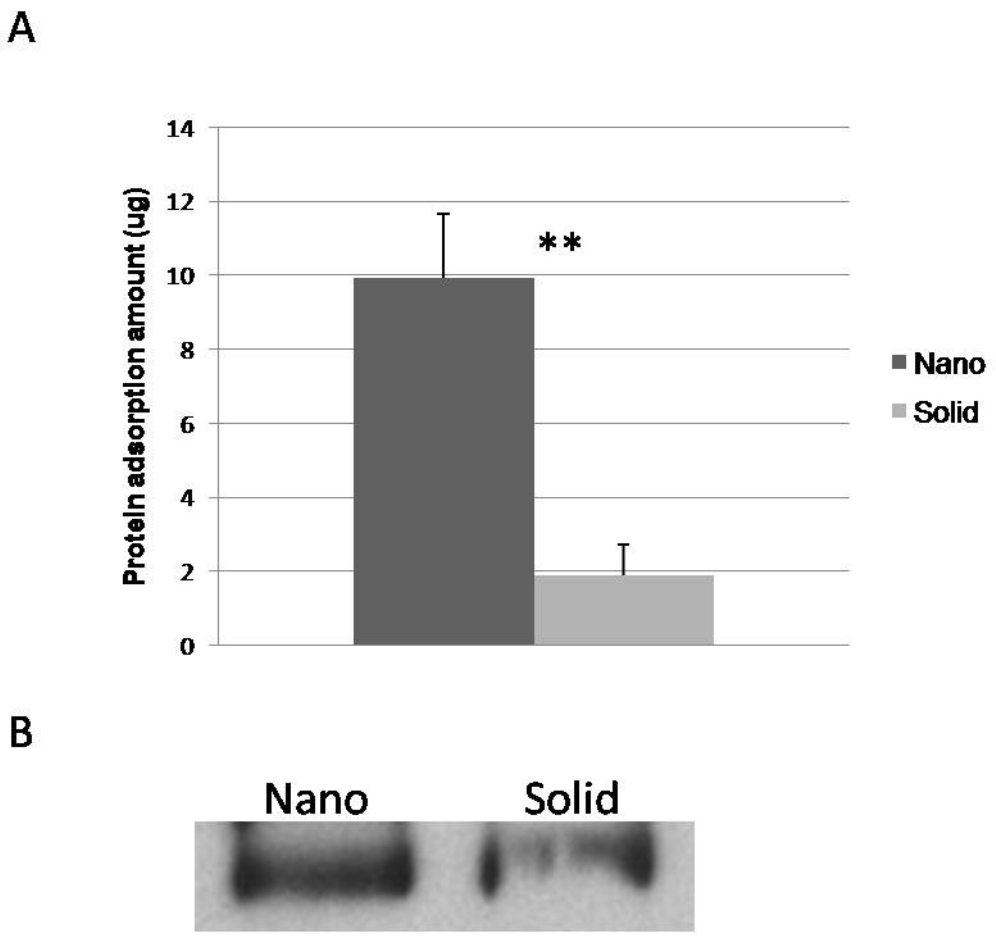

Figure 5.8: Protein adsorption to scaffolds after exposure to medium containing bovine serum protein or fetal bovine serum for 4 hr: (A) Amount of adsorbed proteins (MicroBCA assay) from nanofibrous scaffolds (Nano) and solid-walled scaffolds (Solid) treated with media. ** denotes a p-value < 0.01. (B) western blot of fibronectin extracted from nanofibrous scaffolds (Nano) and solid-walled scaffolds (Solid) cultured in fetal bovine serum for 4hr.

5.6 References

1. Thomson, J.A., J. Itskovitz-Eldor, S.S. Shapiro, M.A. Waknitz, J.J. Swiergiel, V.S. Marshall, and J.M. Jones. Embryonic Stem Cell Lines Derived from Human Blastocysts. Science, 1998. **282**: p. 1145-1147.

2. Fehrer, C. and G. Lepperdinger. Mesenchymal stem cell aging. Exp Gerontol, 2005. **40**: p. 926-930.

3. Muraglia, A., R. Cancedda, and R. Quarto. Clonal mesenchymal progenitors from human bone marrow differentiate in vitro according to a hierarchical model. J Cell Sci, 2000. **113**: p. 1161-1166.

4. Sottile, V., A. Thomson, and J. McWhir. In vitro Osteogenic Differentiaiton of Human ES Cells. Cloning and Stem Cells, 2003. **5**: p. 149-155.

5. Cao, T., B.C. Heng, C.P. Ye, H. Liu, W.S. Toh, P. Robson, P. Li, Y.H. Hong, and L.W. Stanton. Osteogenic differentiation within intact human embryoid bodies result in a marked increased in osteocalcin secretion after 12 days of in vitro culture, and formation of morpholoigcally distinct nodule-like structures. Tissue and Cell, 2005. **37**: p. 325-334.

6. Karp, J.M., L.S. Ferreira, A. Khademhosseini, A.H. Kwon, J. Yeh, and R.S. Langer. Cultivation of human embryonic stem cells without the embroid body step enhances osteogenesis in vitro. Stem Cells, 2006. **24**: p. 835-843.

7. Bielby, R., A. Boccaccini, J. Polak, and L. Buttery. In vitro differentiation and in vivo mineralization of osteogenic cells derived from human embryonic stem cells. Tissue Eng, 2004. **10**: p. 18-25.

8. Smith, L.A., X. Liu, J. Hu, P. Wang, and P.X. Ma. Enhancing Osteogenic Differentiation of Mouse Embryonic Stem Cells by Nanofibers. In preparation.

9. Smith, L.A., X. Liu, and P.X. Ma. Nano-fibrous Scaffolds Enhance Osteogenic Differentiation of Embryonic Stem Cells In preparation.

10. Elsdale, T. and J. Bard. Collagen substrata for studies on cell behavior. J cell biology, 1972. **54**: p. 626-637.

11. Ma, P.X. and R. Zhang. Synthetic nano-scale fibrous extraellular matrix. Biomed Mater Res, 1999. **46**: p. 60-72.

12. Chen, V.J. and P.X. Ma. poly(L-lactic acid) scaffolds with interconnected spherical macropores. Biomaterials, 2004. **25**: p. 2065-2073.

13. Zhang, R. and P.X. Ma. Synthetic nano-fibrillar extracellular matrices with predesigned macroporous architectures. J Biomedi Res, 2000. **52**: p. 430-438.

14. Chen, V.J., L.A. Smith, and P.X. Ma. Bone regeneration on computer-designed nano-fibrous scaffolds. Biomaterials, 2006. **27**: p. 3973-3979.

15. Woo, K.M., V.J. Chen, and P.X. Ma. Nano-fibrous scaffolding architecture selectively enhances protein adsorption contributing to cell attachment. J Biomed Mater Res, 2003. **67A**: p. 531-537.

16. Caspi, O., A. Lesman, Y. Basevitch, A. Gepstein, G. Arbel, I.H. Habib, L. Gepstein, and S. Levenberg. Tissue engineering of vascularized cardiac muscle from human embryonic stem cells. Circ Res, 2007. **100**: p. 263-272.

17. Kim, S., S.S. Kim, S.H. Lee, S.E. Ahn, S.J. Gwak, J.H. Song, B.S. Kim, and H.M. Chung. In vivo bone formation from human embryonic stem cell-derived osteogenic cells in poly(D,L-lactic-co-glycolic acid)/hydroxyapatite composite scaffolds. Biomaterials, 2008. **29**: p. 1043-1053.

18. Levenberg, S., N.F. Huang, E. Lavik, A.B. Rogers, J. Itskovitz-Eldor, and R.S. Langer. Differentiation of human embryonic stem cells on three-dimensional polymer scaffolds. Proc Natl Sci USA, 2003. **100**: p. 12741-12746.

19. Hu, J., X. Liu, and P.X. Ma. Induction of osteoblast differentiation phenotype on poly(L-lactic acid) nanofibrous matrix. Biomaterials, 2008. **29**: p. 3815-3821.

20. Hwang, N.S., S. Varghese, Z. Zhang, and J. Elisseeff. Chondrogenic Differentiation of Human Embryonic Stem Cell-Derived Cells in Arginine-Glycine-Aspartate-Modified Hydrogels. Tissue Eng, 2006. **12**: p. 2695-2706.

21. Woessner, J.F. The Determination of Hydroxyproline in Tissue and Protein Samples Containing Small proportions of this Imino Acid. Arch of Biochem Biophys, 1961. **93**: p. 440-447.

22. Neuman, R. and M. Logan. The Determination of Collagen and Elastin in Tissues. J Biol Chem, 1950 **186**: p. 549-556.

23. Lian, Q., E. Lye, K. Suan Yeo, E. Khia Way Tan, M. Salto-Tellez, T. Liu, N. Palanisamy, R. El Oakley, E. Lee, B. Lim, and S. Lim. Derivation of clinically compliant MSCs from CD105+, CD24- differentiated human ESCs. Stem Cells, 2007. **25**: p. 425-436.

24. Barberi, T., L. Willis, N. Socci, and L. Studer. Derivation of multipotent mesenchymal precursors from human embryonic stem cells. PLoS Med, 2005. **2**: p. e161.

25. Woo, K., J. Jun, V. Chen, J. Seo, J. Baek, H. Ryoo, G. Kim, M. Somerman, and P.X. Ma. Nano-fibrous scaffolding promotes osteoblast differentiation and biomineralization. Biomaterals, 2007. **28**: p. 335-343.

26. Shih, Y.V., C.N. Chen, S.W. Tsai, Y.J. Wang, and O.K. Lee. Growth of Mesenchymal Stem ells on Electrospun Type I collagen Nanofibers. Stem Cells, 2006. **24**: p. 2391-2397.

27. Schindler, M., I. Ahmed, J. Kamal, A. Nur-E-Kamal, T.H. Grafe, H.Y. Chung, and S. Meiners. A synthetic nanofibrillar matrix promotes in vivo-like organization and morphogenesis for cells in culture. Biomaterials, 2005. **26**: p. 5624-5631.

28. Xiao, G., D. Wang, D. Benson, G. Karsenty, and R.T. Franceschi. Role of the a2-Integrin Osteoblast-specific Gene Expression and Activation of the OSF2 Transcription Factor. J Biol Chem, 1998. **273**: p. 32988-32994.

29. Mizuno, M., R. Fujisawa, and Y. Kuboki. Type I collagen-induced osteoblastic differentiation of bone-marrow cells mediated by collagen-alpha2beta1 integrin interaction. J Cell Physiol, 2000. **184**: p. 207-213.

30. Weiss, R. and A. Reddi. Role of Fibronectin in collagenous matrix-induced mesenchymal cell proliferation and differentiation in vivo. Exp Cell Res, 1981. **133**: p. 247-254.

31. Cowles, E., M. DeRome, G. Pastizzo, L. Brailey, and G. Gronowicz. Mineralization and the Expression of the Matrix Proteins During In Vivo Bone Development. Calcif Tissue Int, 1998. **62**: p. 74-82.

32. Tremoleda, J., N. Forsyth, N. Khan, D. Wojtacha, I. Christodoulou, B. Tye, S. Racey, S. Collishaw, V. Sottile, A. Thomson, A. Simpson, B. Noble, and J. McWhir. Bone tissue formation from human embryonic stem cells in vivo. Cloning and Stem Cells, 2008. **10**: p. 119-132.

33. Huang, Z., E.R. Nelson, R. Smith, and S. Goodman. The Sequenital Expression Profiles of Growth Factors from Osteoprogenitors to osteoblasts In Vitro. Tissue Eng, 2007. **13**: p. 2311-2320.

34. Chaudhary, L., A. Hofmeister, and K. Hruska. Differential growth factor control of bone formation through osteoprogenitor differentiation. Bone, 2004. **34**: p. 402-411.

35. Schuldiner, M., O. Yanuka, J. Itskovitz-Eldor, D. Melton, and N. Benvenisty. Effects of eight growth factors on the differentiation of cells derived from human embryonic stem cells. Proc Natl Acad Sci USA, 2000. **97**: p. 11307-11312.

36. Hwang, N.S., S. Varghese, and J. Elisseeff. Derivation of chondrogenically-committed cells from human embryonic cells for cartilage tissue regeneration. PLoS ONE, 2008. **3**: p. e2498.

37. Toh, W.S., Z. Yang, H. Liu, B.C. Heng, E. Lee, and T. Cao. Effects of culture conditions and bone morphogenetic protein 2 on extent of chondrogenesis from human embryonic stem cells. Stem Cells, 2007. **25**: p. 950-960.

38. Debiais, F., M. Hott, A. Graulet, and P. Marie. The effects of fibroblast growth factor-2 on human neonatal calvaria osteoblastic cells are differentiation stage specific. J Bone Miner Res, 1998. **13**: p. 645-654.

39. Martin, I., A. Muraglia, G. Campanile, R. Cancedda, and R. Quarto. Fibroblast Growth Factor-2 Supports ex Vivo Expansion and Maintenance of Osteogenic Prescursors from Humand Bone Marrow. Endocrinology, 1997. **138**: p. 4456-4462.

40. Mansukhani, A., D. Ambrosetti, G. Holmes, L. Cornivelli, and C. Basilico. Sox2 induction by FGF and FGFR2 activating mutations inhibits Wnt signaling and osteoblast differentiation JCB, 2005. **168**: p. 1065-1076.

41. Baharvand, H., S. Hashemi, S. Ashtian, and A. Farrokhi. Differentiation of human embryonic stem cells into hepatocytes in 2D and 3D culture systems in vitro. International Journal of Developmental Biology, 2006. **50**: p. 45-652.

42. Chen, S., R. Revoltella, S. Papini, M. Michelini, W. Fitzgerald, J. Zimmerberg, and L. Margolis. Multilineage differentiation of rhesus monkey embryonic stem cells in three-dimensional culture systems. Stem Cells, 2003. **21**: p. 281-295.

43. Cukierman, E., R. Pankov, D. Stevens, and K. Yamada. Taking cell-matrix adhesions to the third dimension. Science, 2001. **294**: p. 1708-1712.

44. Roach, P., D. Farrar, and C. Perry. Surface Tailoring for Controlled Protein Adsorption: Effect of Topography at the Nanometer Scale and Chemistry. . J Am Chem Soc, 2006. **128**: p. 3939-3945.

45. Denis, F., P. Hanarp, D. Sutherland, J. Gold, C. Mustin, P. Rouxhet, and Y. Dufrene. Protein Adsorption on Moldel Surfaces with Controlled Nanotopography and Chemistry. Langmuir, 2002. **18**: p. 819-828.

46. Sutherland, D., M. Broberg, H. Nygren, and B. Kasemo. Influence of Nanoscale Surface Topography and Chemistry on the Functional Behaviour of an Adsorbed Model Macromolecule. Macromol. Biosci., 2001. **1**: p. 270-273.

47. Jukes, J., S. Both, A. Leusink, L. Sterk, C. van Blitterswijk, and J. de Boer. Endochondral bone tissue engineering using embryonic stem cells. Proc Natl Sci USA, 2008. **105**: p. 6840-6845.

Chapter 6

Conclusion

6.1 Summary

In this thesis, biological effects of synthetic poly(L-lactic acid) nanofibers on the osteogenic differentiation of mouse and human embryonic stem cells were examined. These nanofibers emulate the fibrillar structure of type 1 collagen, which is known to affect cellular behavior.

In the first study, undifferentiated mouse embryonic stem cells were seeded onto thin matrices and films to simulate interactions with the scaffold walls. In these studies, the nanofibrous architecture was found to enhance mesodermal and osteogenic differentiation as well as mineralization while reducing neuronal differentiation compared to flat (solid) films. When the contribution of integrin signaling to this differentiation was examined, it was found that α2 integrin played a significant role in the mesodermal and osteogenic differentiation on both architectures. However, α5 integrin was found to have significant effect on the mesodermal and osteogenic differentiation of the embryonic stem cells cultured on the nanofibrous thin matrices, but not the flat (solid) architecture under the culture conditions and time periods studied. This indicates that the

increased fibronectin adsorption on the nanofibrous material compared to the flat (solid) film may help facilitate the directed differentiation of these cells under the culture conditions and time periods examined.

Next, pre-differentiated mouse embryonic stem cells were seeded on to the nanofibrous thin matrices and flat (solid) films with various biologically active molecules to examine how these cues affect differentiation on the different architectures. The nanofibrous thin matrices were able to support osteogenic differentiation without the addition of any biologically active factors, although the addition of such factors enhanced the differentiation of these cells. The flat (solid) films required the addition of osteogenic supplements and growth factors to achieve osteogenic differentiation.

Differentiation and mineralization was examined on the nanofibrous and solid architecture in two and three dimensional culture in the presence of osteogenic supplements and growth factors. It was found that three dimensional nanofibrous scaffolds increased differentiation compared to two dimensional nanofibrous matrices, either two dimensional flat (solid) films, or three dimensional solid-walled scaffolds. In three dimensional culture, the nanofibrous scaffolds was also found to contain significantly more type 1 collagen and calcium than the solid-walled scaffolds.

Using the knowledge gained from the mouse embryonic stem cell studies, the effects of the nanofibrous architecture on the osteogenic differentiation of human embryonic stem cells were examined. Because of differences in cellular behavior between the mouse and human embryonic stem cells, a new differentiation protocol was developed. The new differentiation protocol was compared to more traditional systems of osteogenic differentiation of human cells and found to provide either better or the

similar differentiation and mineralization. The human embryonic stem cells were then seeded onto the different architectures for two and three dimensional culture. In both cases, the nanofibrous architecture was found to enhance differentiation, extracellular matrix depositions and mineralization.

Overall, this work indicates that poly (L-lactic acid) nanofibers generated by the phase separation technique have the ability to enhance the osteogenic differentiation of embryonic stem cells, a far less committed cell type than had previously been examined on these materials.

6.2 Future Work

There are a number of different avenues that this research could lead to in the future. Continuing the line of research presented in this thesis, the nanofibrous three dimensional culture system or scaffolds seeded with embryonic stem cells could continue to be developed for clinical use. This could entail in vivo studies to ensure that the tissue developed in vitro survives in vivo and incorporates into the native bone. Additionally, studies would be needed to show that the cells have been differentiated sufficiently in vitro that they no longer possess the ability to generate tumors in vivo. After this the in vitro differentiation protocol would have to be revised to eliminate the use of animal products to limit rejection problems during clinical use.

Additionally, the system could be studied in vitro in order to examine the mechanisms underlying the enhancement of the cellular differentiation on the nanofibrous material. In this case, the interplay of integrin signaling through focal adhesion kinase could be studied more in depth along with the role of cytoskeletal

organization on RhoA and Rac1, and the role of cell to cell interactions through such molecules as cadherins, neural adhesion molecule and Notch. Once a better understanding of how the nanofibrous scaffolds enhance cellular differentiation is achieved, it can be determined how to further exploit their desired biological effects in the development of more advanced biomaterials.

The system could also be further developed for use in the study of developmental biology. With further improvement to the differentiation protocol and the materials, the yield of the desired cell type could be increased significantly. The system could then be used to study the human developmental process leading to a better understanding of how the process occurs, what factors affect the development and how to better correct developmental defects in the clinic.

Pure cell systems developed with aid of synthetic nanofibers could also be used in the drug discovery process providing a better model of how potential compounds will behave in the human body than currently used mouse models. A substantial amount of time and money could be saved on new drug development by using these human cells rather than animal models, since drugs advancing to clinical trials will have shown effectiveness in human cells and may have better odds of being effective in humans.

It is important to note that although the generation of bone tissue was the focus of this thesis, the future work directions could be applied to any number of tissue types since embryonic stem cells are able to differentiate into any tissue within the body and type 1 collagen which the synthetic poly (L-latic acid) nanofibers emulate is the base of the extracellular matrix in several other tissues.